MULTI-LEVEL RISK MANAGEMENT OF BUILDING SETTLEMENT INDUCED BY TUNNELLING IN SOFT CLAY

MULTI-LEVEL RISK MANAGEMENT OF BUILDING SETTLEMENT INDUCED BY TUNNELLING IN SOFT CLAY

BY ROHAM AKBARIAN, M.Sc., B.Sc.

A THESIS SUBMITTED TO THE SCHOOL OF GRADUATE STUDIES IN PARTIAL FULFILMENT OF THE REQUIREMENTS FOR THE DEGREE OF

MASTER OF APPLIED SCIENCE

Descriptive note

MASTER OF APPLIED SCIENCE (2019) McMaster University

(Civil Engineering) Hamilton, Ontario

TITLE: Multi-Level Risk Management of Building Settlement Induced by Tunnelling in Soft Clay

AUTHOR: Roham Akbarian

M.Sc. (Politecnico di Milano, Milan, Italy)

B.Sc. (University of Tehran, Tehran, Iran)

SUPERVISOR: Dr. Peijun Guo

NUMBER OF PAGES: CL, 150

Lay Abstract

The aim of this study is to provide a multi-level risk management (RM) framework to address and quantify the risk of surface building settlement induced by tunnelling in soft clay in urbanized areas. The focused is placed on quantifying the risk of tunnel-induced settlement of existing buildings, by taking into account multiple uncertainty levels. The framework addresses the tunnel-induced settlement risk, both during the construction of the tunnel as well as after its completion, for buildings with shallow and deep foundations. It offers different classes of assessment to quantify the risk, according to the structure's current condition and with respect to specific limit-state functions designated for each class. The proposed framework was implemented in an example to demonstrate the procedure and outcomes.

Abstract

Tunnelling in urban areas is one of the most challenging engineering activities, as it has relatively high "risk" due to various uncertainties and the intensity of the possible consequences. Numerous studies have been conducted to address the tunnelling risk, by mainly focusing on the "identification" of the causes and how to control or mitigate the risks. However, limited work has been done on how to quantify the risk by considering the multi-level uncertainties encountered in different phases of the project. The primary objective of this work is to develop a multi-scale risk management (RM) framework to address and quantify the risk of ground surface settlement, induced by tunnelling, in soft clay in urbanized areas. The specific focus is placed on quantifying the risk of tunnel-induced settlement for existing buildings, by taking into account multiple uncertainty levels (*e.g.* uncertainties of parameters, uncertainties of models, *etc.*). The framework addresses the tunnel-induced settlement risk, both during the construction of the tunnel as well as after its completion, for buildings with shallow and deep foundations. It offers different classes of assessment to quantify the risk, according to the structure's current condition and the corresponding limit-state function, that is designated to each class. The RM framework is aligned with ISO 31000 risk management act, consisting of "risk identification", "risk analysis" and "risk evaluation". Risk identification includes studies on tunnelling technical reports, field observations, *etc.*, in order to identify the causes of short-term and long-term tunnelling-induced settlement. The risk analysis involves a series of fault tree, event tree and consequence tree analyses to estimate the likelihood of the ground subsidence and subsequent events. For risk evaluation, different probabilistic methods (*e.g.* first-order reliability method, second-order reliability method and Monte Carlo sampling) are utilized to estimate the risk of surface buildings with shallow and deep foundations. The framework has been implemented in an example problem, to demonstrate the procedure and to address the main influential parameters in each class of assessment using the alpha importance measure. Rt risk tool has been utilized to perform reliability calculations and FORM has been used as the primary method due to its valuable balance between computational cost and accuracy. The outcomes of this RM framework are risk registers and colour-coded risk maps including the exceedance probability of a predefined settlement threshold for each building in the affected area. This framework receives technical data and provides risk-based information for higher-level managers and decision-makers to prioritize their actions and allocate their resources in the most effective way.

***Key words**: multi-level risk management (RM) framework, soft clay, tunnelling-induced settlement, probabilistic risk assessment (PRA), Rt risk tool*

Acknowledgement

I would like to express my sincere gratitude to a number of people who provided exceptional support for my graduate studies. First and foremost, my gratefulness goes to my supervisor, Professor Peijun Guo, for his endless support and inspiration. I also would like to thank other professors and staff at Department of Civil Engineering with whom I have had the chance to meet during the classes or seminars. Their knowledge and advices are always appreciated.

I would like to extend thanks to my fellow officemates whom I have learned a lot from, and they were great people to work with. Especially, I would like to thank Amir Arsalan Jameei for hours of productive discussion.

Last but not least, my unbound gratefulness goes to my mother and my sister for their wholehearted supports from miles away during all these years in Canada and Italy and my invaluable friends for their sincere support and kindness.

Table of Contents

Lay Abstract iv

Abstract v

Acknowledgement vii

Table of Contents viii

List of Figures xi

List of Tables xiv

List of Abbreviations xv

List of Symbols xviii

Chapter 1. Introduction 1

1.1 Scope of this research 2

1.2 Thesis outline 2

Chapter 2. Literature review 4

2.1 Historical advancement in tunnel engineering 4

2.2 Significance of ground investigation 5

2.2.1 Challenges and uncertainties in ground investigation 6

2.2.1.1 Geological uncertainties 6

2.2.1.2 Groundwater (Geomorphological) uncertainties 7

2.2.1.3 Uncertainties of soil mechanical properties 7

2.2.1.4 Uncertainties regarding soil classification 8

2.2.2 Shield Tunnelling and Tunnel Boring Machines (TBM) 9

2.2.3 Slurry TBMs versus EPB TBMs 11

2.3 Ground loss and ground movement during tunnelling 13

2.3.1 Green field settlement 13

2.3.2 Pile settlements 17

2.3.2.1 Concept of the design charts 17

2.3.2.2 Procedure to use the design charts 18

2.4 Long-term (consolidation) settlement in soft clays 19

2.4.1 Quantifying ground movements due to consolidation settlements 22

2.4.2 Formulation for long-term settlement by Laver et al. (2016) 23

2.5 Uncertainty, risk and reliability 24

2.5.1 Risk definition 24

2.5.2 Uncertainty types 27
2.5.2.1 Aleatory uncertainty 27
2.5.2.2 Epistemic uncertainty 27
2.5.3 Sources of uncertainty 27
2.5.4 Uncertainty description 27
2.5.5 Risk analysis 28
2.5.5.1 Influence diagram 29
2.5.5.2 Event tree diagram 29
2.5.5.3 Fault tree diagram 30
2.5.6 Risk evaluation 32
2.5.7 Tools for reliability analysis 36
2.5.7.1 Analysis of function 36
2.5.7.2 Probability transformation 38
2.5.8 Reliability methods 42
2.5.8.1 First order second moment – FOSM 42
2.5.8.2 First order reliability method – FORM 44
2.5.8.3 Second order reliability method – SORM 48
2.5.8.4 Sampling methods 48

2.6 Developing flowcharts 48

2.7 Necessity of a more rigorous risk management framework 48

Chapter 3. Methodology and analysis 51

3.1 Statement of the problem and the general framework 51

3.2 Risk management framework during construction (short-term) 53

3.2.1 Risk identification 53
Settlement above and ahead of the face 54
Settlement along the shield 54
Settlement at the shield tail 55
Settlement caused by lining deformation 55
Other potential risks 55
3.2.2 Risk analysis 56
3.2.2.1 Fault tree analysis: short-term 56
3.2.2.2 Building database 61
3.2.2.3 Buildings with shallow foundations 64
3.2.2.4 Buildings with deep foundations 69
Risk evaluation flowchart (short-term) 71
3.2.3 Risk evaluation 74
3.2.3.1 Buildings with shallow foundations 74
3.2.3.2 Buildings with deep foundations 79
3.2.4 Updated building database and risk register 81

3.3 Risk management framework during operation (long-term) 83
3.3.1 Risk identification 83
3.3.2 Risk analysis for long-term settlement 84
3.3.2.1 Influence diagram analysis 84
3.3.2.2 Fault tree analysis 86
3.3.2.3 Event tree analysis 88
3.3.2.4 Consequence tree analysis 90
3.3.3 Risk evaluation 92
3.4 Limitations of the proposed risk evaluation methodologies 96
3.5 Outcomes of the RM analyses 97
3.5.1 Updating building (structure) database 97
3.5.2 Developing the risk map 98
Chapter 4. Implementation of the multi-class risk analysis 101
4.1 Example of short-term risk management 102
4.1.1 Risk analysis 102
4.1.1.1 Fault tree analysis 102
4.1.2 Risk evaluation 105
4.1.2.1 SSRABS3: Settlement risk evaluation for Class 3 buildings 105
4.1.2.2 SSRABS2: Settlement risk evaluation for Class 2 buildings 109
4.1.2.3 SSRABD2: Settlement risk evaluation of Class 2 buildings 111
4.1.2.4 Utilizing other reliability methods 113
4.2 Example of long-term risk management 114
4.2.1 Risk analysis 114
4.2.1.1 Fault tree analysis 115
4.2.1.2 Event tree analysis 117
4.2.1.3 Consequence tree analysis 118
4.2.2 Risk evaluation 118
4.2.2.1 LSRAC2: Long-term settlement risk evaluation for Class 2 buildings 118
4.3 Total settlement risk analysis (TSRA) 122
4.4 The effect of introducing parameters' correlation 124
Chapter 5. Conclusion and future work 125
References 132
Appendix I: Design charts for short and long piles 142

List of Figures

Figure 1. Different tunnelling methods 1

Figure 2. Relationship between cost of change and knowledge during a project (Project Management Institute, 2008) 5

Figure 3. Approximate correlations of soil types and permeability (after Schmidt 1974) 8

Figure 4. Slurry TBM (Herrenknecht Inc.) 12

Figure 5. EPB TBM (Herrenknecht Inc.) 12

Figure 6. Gap parameter and its components (after Lee et al. 1992) 16

Figure 7. Short pile and long pile definitions (after Loganathan, 2011) 17

Figure 8. ISO risk management act (2009) 26

Figure 9. Schematic view of an influence diagram 29

Figure 10. Schematic view of an event tree 29

Figure 11. Example of a fault tree 30

Figure 12. Basic reliability problem (Becker, 1996) 34

Figure 13. Geometrical representation of β and probability of failure in standard normal space 35

Figure 14. Second convergence criterion for FORM (after Haukaas, 2018) 46

Figure 15. Risk management; A multi-disciplinary act 50

Figure 16. The proposed risk management capabilities 52

Figure 17. General risk management procedure for tunnelling 52

Figure 18. Sources of ground movement in shield tunnelling (after Tamagnini et al., 2005) 53

Figure 19. Overcutting at curve 54

Figure 20. Groundwater drawdown 56

Figure 21. Fault tree analysis: short-term – straight section 57

Figure 22. Fault tree analysis: short-term – curved section 58

Figure 23. Schematic projection of the tunnel on the urban city map 59

Figure 24. Tunnel's influential zones and their dimensions: Zone 1 (Loganathan 2011), Zone 2 (after Bowles, 1996) and Zone 3 (after Peck, 1969) 60

Figure 25. Tunnel influential zones: completed - Zone 2 (after Bowles, 1996) and Zone 3 (after Peck, 1969) 61

Figure 26. Map of building classes 63
Figure 27. Hogging-sagging zones 67
Figure 28. Risk management framework for short-term settlement risk 73
Figure 29. Model for Class 3 reliability analysis of shallow foundations 74
Figure 30. Model for Class 2 reliability analysis of shallow foundations 76
Figure 31. Model for Class 1 reliability analysis of shallow foundations 78
Figure 32. Model for Class 2 reliability analysis of deep foundations 80
Figure 33. Influence diagram of long-term tunnel settlement 85
Figure 34. Fault tree analysis for long-term settlement 87
Figure 35. Event tree analysis for long-term settlement 89
Figure 36. Consequence tree analysis for long-term settlement 91
Figure 37. Model for Class 2 reliability analysis for long-term settlement 94
Figure 38. Risk management framework for long-term settlement risk 95
Figure 39. Risk map – an example 99
Figure 40. The settlement condition of tunnel and the critical areas – an example 100
Figure 41. Short-term fault tree for straight section - solved example 103
Figure 42. Short-term fault tree for curve section - solved example 105
Figure 43. SSRABS3 - Rt risk tool model 106
Figure 44. SSRABS2 - Rt risk tool model 110
Figure 45. Bending stress, lateral deflection and pile settlement models - Rt risk tool 111
Figure 46. Long-term fault tree analysis - solved example 116
Figure 47. Long-term event tree analysis - solved example 119
Figure 48. Long-term consequence tree analysis - solved example 120
Figure 49. Long-term (left) and total settlement (right) risk evaluation model - Rt risk tool 123
Figure 50. Future work: software's capabilities 131
Figure 51. Design charts (short pile) (after Loganathan 2011) 143
Figure 52.Undrained shear strength correction factor (short pile) (after Loganathan 2011) 144

Figure 53. Correction factor for pile length to centreline depth (short pile) (after Loganathan 2011) 145

Figure 54. Pile's diameter correction factor (short pile) (after Loganathan 2011) 146

Figure 55. Design charts (long pile) (after Loganathan 2011) 147

Figure 56. Undrained shear strength correction factor (long pile) (after Loganathan 2011) 148

Figure 57. Correction factor for pile length to centreline depth (long pile) (after Loganathan 2011) 149

Figure 58. Pile's diameter correction factor (long pile) (after Loganathan 2011) 150

List of Tables

Table 1. Tunnelman's ground classification for soils 10

Table 2. Fault tree's symbol description 31

Table 3. Flowchart indicators 49

Table 4. Building database 62

Table 5. CIRIA damage classification (CIRIA PR30, 1996) 66

Table 6. Damage classification by $\varepsilon crit$, (after Boscardin & Cording, 1989) 69

Table 7. List of parameters in Class 3 reliability analysis for shallow foundations 75

Table 8. List of parameters in Class 2 reliability analysis for shallow foundations 77

Table 9. List of parameters in Class 1 reliability analysis for buildings with shallow foundations. 79

Table 10. List of parameters in Class 2 reliability analysis for deep foundations 80

Table 11. Risk register 82

Table 12. List of parameters in Class 2 reliability analysis for long-term settlement risk assessment 93

Table 13. Updated building database 97

Table 14. Short-term analysis: base faults of a straight section 102

Table 15. List of parameters and their values in SSRABS3 107

Table 16. SSRABS3 – alpha importance measure 108

Table 17. List of parameters and their values in SSRABS2 109

Table 18. SSRABS2 - alpha importance measure 110

Table 19. List of parameters and their values in SSRABD2 112

Table 20. SSRABD2 – alpha importance measure 113

Table 21. Long-term analysis: sub-main faults 117

Table 22. Class 2 assessment parameters – long-term settlement risk assessment 121

Table 23. Total settlement – alpha importance measure 122

List of Abbreviations

Abbreviation	Description
ANN	artificial neural network
BD1	Class 1 building with a deep foundation
BD2	Class 2 building with a deep foundation
BD3	Class 3 building with a deep foundation
BS1	Class 1 building with a shallow foundation
BS2	Class 2 building with a shallow foundation
BS3	Class 3 building with a shallow foundation
EPB	earth-pressure balance tunnel boring machine
ESR	effective stiffness ratio
FD	finite difference
FE	finite element
FEM	finite element method
FORM	first-order reliability method
FOSM	first-order second-moment
ISO	international organization of standardization
ITA	international tunnel association
LL	liquid limit
LR	logistic regression
LSD	limit state design

LSRAC1	long-term settlement risk analysis for Class 1 buildings
LSRAC2	long-term settlement risk analysis for Class 2 buildings
MECE	mutually exclusive and collectively exhaustive event
MVFOSM	mean-value first-order second-moment
PI	plasticity index
PRA	probabilistic risk assessment
RM	risk management
SORM	second-order reliability method
SRA	settlement risk analysis
SRM	short-term risk map
SSRABD1	short-term settlement risk analysis for Class 1 buildings with deep foundations
SSRABD2	short-term settlement risk analysis for Class 2 and Class3 buildings with deep foundations
SSRABS1	short-term settlement risk analysis for Class 1 buildings with shallow foundations
SSRABS2	short-term settlement risk analysis for Class 2 buildings with shallow foundations
SSRABS3	short-term settlement risk analysis for Class 3 buildings with shallow foundations
TBM	tunnel boring machine
TSRA	total settlement risk analysis
TZ1	tunnelling affected Zone 1
TZ2	tunnelling affected Zone 2

TZ3	tunnelling affected Zone 3
USCS	unified soil classification system
WSD	working stress design

List of Symbols

Symbol	Description
Δ_{hor}	the horizontal movement
$\Delta_{s/h}$	the maximum relative settlement
∇_g	the gradient of the limit-state function g
$+P_b$	the tunnelling-induced compressive axial force of the pile in the “base” case
$+P_{max}$	the compressive axial force of the pile
$-P_b$	the tunnelling-induced tensile axial force of the pile in the “base” case
$-P_{max}$	the tensile axial force of the pile
a_{hd}	the depth factor
A_i	the ith action
A_{RS}	the coefficient of time factor
B_{RS}	the power of time factor
$B_{s/h}$	the length of the building interacting with horizontal movement
$B\upsilon$	the building’s Poisson’s ratio
C_{clay}	the clay cover depth
c_f	the cost of failure
C_u	the undrained shear strength
d_m	the step direction
D_X	the diagonal matrix
DS	the dimensionless surface settlement

$f_R(r)$	the marginal probability distribution functions
$F_R(r)$	the cumulative probability distribution functions
G_p	the physical gap parameter
H_{cmax}	the maximum horizontal displacement
$I_{s/h}$	the moment of inertia of the equivalent beam
$J_{y,x}$	the Jacobian matrix of random variables x and y
$k^{+P}_{L_p/H}$	the correction factor for ratio of pile length to the tunnel axis level for compressive axial force
$k^{-P}_{L_p/H}$	the correction factor for ratio of pile length to the tunnel axis level for tensile axial force
$k^{M}_{L_p/H}$	the correction factor for ratio of pile length to the tunnel axis level for bending moment
$k^{\rho}_{L_p/H}$	the correction factor for ratio of pile length to the tunnel axis level for bending moment
K_0	the coefficient of effective earth pressure at-rest
k_1	the soil's volume ratio of nonuniform axial intrusion to uniform axial intrusion
$k_{concrete}$	the permeability of the concrete segment
k^{+P}_{cu}	the correction factor for undrained shear strength for compressive axial force
k^{-P}_{cu}	the correction factor for undrained shear strength for tensile axial force
k^{M}_{cu}	the correction factor for undrained shear strength for bending moment
k^{ρ}_{cu}	the correction factor for undrained shear strength for lateral deflection
k^{+P}_{d}	the correction factor of pile diameter for compressive axial force
k^{-P}_{d}	the correction factor of pile diameter for tensile axial force

k_d^M	the correction factor of pile diameter for bending moment
k_d^ρ	the correction factor of pile diameter for lateral deflection
k_h	the horizontal permeability
k_{joint}	the permeability of the broken watertight
$k_{t\text{-}equ}$	the equivalent permeability of tunnel
k_v	the vertical permeability of soil
L_c	the depth of tunnel axis below water table
L_R	the ratio between equivalent ground loss and ground loss of the base case
$L_{s/h}$	the length of sagging/hogging zone
$\tilde{\mathbf{L}}$	the lower-triangular Cholesky decomposition
M_b	the tunnelling-induced bending moment of the pile in the “base” case
M_{design}	the design bending moment
$M_{induced}$	the tunnel-induced bending moment of piles
M_{max}	the maximum induced bending moment
NS_i	the nondimensional settlement value for fully impermeable lining
m_x	the vector of the means of random variable x
n	the number of joints/segments of a tunnel ring, total number of experiments
n_E	the number of experiments with e as outcome
P_{design}	the design axial force of piles
p_f	the probability of failure
P_i	the tunnel supporting pressure

$P_v^{'}$	the vertical effective stress at tunnel springlines
P_w	the pore water pressure
R_{xx}	the correlation matrix
S_{cmax}	the maximum consolidation settlement above the tunnel centreline
s_j	the watertight joint aperture
s_m	the step size
$S_c(x)$	the consolidation settlement at horizontal distance x
$t_{s/h}$	the furthest distance from natural axis to the edge
U_{3D}^*	the face pressure release parameter
$U_{z=0}$	the immediate settlement at $z = 0$
y^*	the design point
γ_w	the unit weight of water
δ_x	the maximum axial intrusion at the tunnel face
ε_0, V_L	the average ground loss
ε_b	the bending strain of building's equivalent simple beam
ε_d	the diagonal strain of building's equivalent simple beam
ε_F	the ground loss ratio
ε_h	the horizontal strain of building's equivalent simple beam
θ_i	the consequence of the action A_i
μ_g	the mean of the limit-state function g
μ_R	the mean of the resistance function R

μ_S	the mean of the demand function S
ν_{design}	the design settlement of the pile
ν_{max}	the head settlement pf the pile
ν_w	the kinematic viscosity of water
ρ_b	the tunnelling-induced lateral deflection of the pile in the “base” case
ρ_{design}	the design lateral deflection of the pile
ρ_{max}	the lateral deflection of the pile
$\sigma_{allowable}$	the allowable stress
σ_g	the standard deviation of the limit-state function g
σ_R	the standard deviation of R
$\Sigma_{R,S}$	the covariance matrix of R and S
σ_S	the standard deviation S
σ_s	the surcharge
υ	the soil’s undrained Poisson’s ratio
BE	the building’s Young’s modulus (Young's modulus of the equivalent beam)
Cov[]	the covariance operator
D	the tunnel’s diameter
E	the soil’s undrained modulus
E[]	the expected value operator
g	the total gap parameter, limit-state function, gravitational accelaration of earth
G	the shear modulus, limit-state function

$g(x)$	the limit-state function
H	the tunnel depth to the centreline
BH	the building's height (or height of the equivalent beam)
i	the transverse settlement trough width parameter
L	the pile's length
N	the tunnel stability parameter
$P(A\|B)$	the probability of A given B
$P(E)$	the probability of happening of event e
R	the radius of the tunnel, resistance function
RP	the dimensionless displacement factor
S	demand function
t	the consolidation time
t_p	the tunnel perimeter
$T\sigma_y/T\varepsilon_y$	the tunnel's yield stress/strain
TE	the tunnel Young's modulus
$T\nu$	the tunnel Poisson's ratio
x	the horizontal distance from the tunnel axis
Z	the section modulus
Z	the depth below the ground surface
α	the alpha vector
β	the reliability index

Δ	the thickness of the tailpiece, the maximum relative settlement at the considered area
ζ	the clearance required for the erection of the lining
ϕ	the cumulative probability distribution in standard normal space, the internal friction angle of the soil
ω	the workmanship parameter

Chapter 1. Introduction

Tunnels and tunnelling practice have come a long way in history. They have always been a vital component of civilization from their early purposes as "qanat" (*i.e.* aqueduct) about 3000 years ago until now as major components in various engineering practices such as mining, underground structures, transportation engineering, *etc*.

Many densely populated and highly developing cities are located on delta regions with alluvial soft ground soils, *e.g.* Shanghai, Cairo, Mexico City and Amsterdam. These soft grounds, particularly soft clays, require specific strategies and equipment for tunnel construction. The control of long-term post-construction deformation of the tunnels is also challenging.

Tunnel excavation can be performed using different methods (*e.g.* drill and blast, sequential tunnelling, mechanized tunnelling using boom-type extractors, full-face excavators, *etc.*) that are applicable under certain conditions depending on the ground and groundwater conditions, depth, dimensions and geometry (see Figure 1).

Sandvik Inc.	Sandvik Inc.	Herrenknecht Inc.
Jumbo drill machine	Roadheader	TBM
(drill and blast method)	(boom-type excavator)	(full-face excavator)

Figure 1. Different tunnelling methods

In addition to the excavation method, the nature of the practice, working environment, complexity and uncertainty of ground conditions and material (soil or rock) properties all contributes to difficulties encountered in a project. Nowadays, rapid urbanization and fast-growing underground development offer even an extended challenge in design, construction and management of such facilities. Additionally, tunnelling under urbanized areas is becoming more demanding due to the disastrous consequences in case of failure and the domino effect that may be triggered by failure in ground control or

excessive settlement of the ground induced by tunnelling. Consequently, it is mandatory that the designer, the contractor and the owner perform necessary risk analyses to assure the required level of reliability.

1.1 Scope of this research

The aim of this work is to quantitively evaluate the associated risk of ground settlement induced by tunnelling in soft clay. Owing to the high compressibility, low permeability and low shear strength of soft clay, the short-term and long-term settlements induced by tunnelling may have significant influence on existing surface buildings, or even cause disastrous consequences. The framework addresses and quantifies the risk of tunnelling, considering the effect of multi-level uncertainties both in the short term and the long term. The risk analyses conducted in this study are mainly oriented toward the significance of the tunnelling-induced settlement of the surface structures. It also provides the required data to conduct a risk-informed decision-making. This research attempts to develop an approach that can be used to prioritize the resources to mitigate the problem in a cost-effective and timely manner.

1.2 Thesis outline

This thesis is organized in five chapters. Chapter 1 is an introduction on risks in tunnels (or generally, underground structures) and the importance of quantifying the risks by providing an overview about the associated challenges, as well as the general configuration of this thesis.

Chapter 2 provides a review on the fundamentals of tunnelling in soft clays as well as the concept of risk management (RM) and reliability analysis. It reviews the significance of ground investigation, the fundamental knowledge of tunnelling and the main factors that should be considered during the design and construction of a tunnel in soft ground. The comprehensive literature review covers the studies that have been conducted to evaluate tunnelling-induced settlement, both in the short and long term. The essential concepts and tools for RM are then introduced and explained in-detail, followed by a concise introduction to probabilistic risk analysis (PRA), which is used in this study to analyze the associated risk together with the reliability methods. In addition, the

generalized frameworks of ground risk analysis, their components and their deficiencies to quantify the settlement risk are discussed.

Chapter 3 deals with the methodologies and risk analyses. A unique strategy for RM is introduced, in which different methods are used to deal with the risk of short-term and long-term settlements. Each methodology is then subcategorized into three fundamental sections: risk identification, risk analysis and risk evaluation. Risk identification encapsulates all the pertinent geohazards and causes of the ground settlement due to tunnelling. Risk analysis performs PRA to evaluate the likelihood of an unfavourable event and the possible scenarios for the aftermath of the event. Risk evaluation contains the fundamental analysis to determine the settlement risk, in the form of exceedance probability of a designated settlement threshold, based on predefined limit-state functions. These risk evaluations are conducted using different classes of assessment, which are proposed based on the foundation type and "building score" value describing the vulnerability of the structure located above the tunnel to settlement. Both the short-term and long-term assessments enable the analyst to perform the "total" settlement risk evaluation, based on the immediate and delayed settlements and to evaluate the ultimate risk, associated with surface and subsurface settlements in the form of probabilities.

Chapter 4 demonstrates the implementation of the framework in the form of a solved example. The example covers both short-term and long-term assessments, each containing the result of risk analyses and risk evaluations. The risk analyses are performed in the form of fault trees, event tree and consequence tree. The risk evaluations are performed by using reliability methods *e.g.* first-order reliability method (FORM) and second-order reliability method (SORM). The aim of this chapter is not to exhibit the results of the application of the proposed framework to a real case study, but to demonstrate the sequence and outcomes of the analyses. The input data are reasonable values, selected as an example, to show the RM procedure.

Final remarks and conclusions are provided in Chapter 5 as a recap on the proposed frameworks, the results and the final comments. A brief note on the future extensions of this work is also provided.

Chapter 2. Literature review

2.1 Historical advancement in tunnel engineering

Tunnel engineering is much more than digging a hole into the ground. In addition to just providing a passage, a modern tunnel usually needs to meet other vital requirements such as ventilation, illumination, power and water supply, surveillance and control, drainage, *etc*. Various techniques for tunnel excavation have been used in engineering to meet different ground conditions, restrictions, influential factors, multi-scale uncertainties and purposes.

Depending on the purpose of a tunnel, different criteria must be satisfied when designing a tunnel. The shape and size of the design cross-section are usually first determined in terms of the purpose of the tunnel (railway tunnel, road tunnel, water tunnel, pressure tunnel, *etc.*). The dimension of a tunnel is also affected by the geotechnical and geological conditions of the ground. Other factors such as clearance, alignment, grades and allowable gradient of profile have some influence on the selection of the dimension and shape of a tunnel.

The Thames Tunnel, which passes underneath the Thames River and is known as the first successful tunnelling project in soft ground, was completed in 1843. Sir Marc Isambard Brunel co-designed the tunnel and introduced the concept of shield tunnelling, which is considered as a turning point in the history of tunnelling in difficult ground. In this method, the face of the tunnel is divided into three floors with twelve cells, each was a working space for workers to dig the ground. The face was first supported by poling boards, which were then removed with the face behind the board being excavated. At the same time, the shield was pushed forward using hydraulic jacks. The shield was 7 m high and 12 m wide and the progress rate was 3-5 metre per week (Harding, 1981).

This significant breakthrough, however, suffered from continuous problem of flooding, which led to disastrous consequences. Later on, James Greathead (1886) resolved the issue with the aid of compressed air. The application of the compressed air in shield tunnelling was a major step forward, which led to the remarkable increase of shield tunnelling all around the world. Different types of shield tunnelling techniques are now used in various circumstances.

2.2 Significance of ground investigation

Site exploration and geotechnical investigation are important for the design, construction and prediction of long-term performance of underground structures. The cost of the project is also significantly affected by geotechnical site exploration, which may have significant influence on the determination of the tunnel alignment and depth. The price for ground investigation should be considered as an investment rather than a cost since adequate ground investigation provides additional data, which reduces the probability of confronting unexpected ground conditions, or generally construction risk, when the cost of any change would be significantly higher than that during feasibility and design phases (see Figure 2).

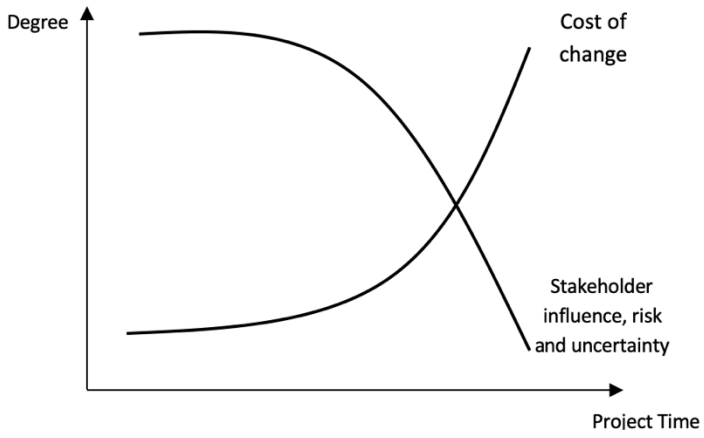

Figure 2. Relationship between cost of change and knowledge during a project (Project Management Institute, 2008)

Geological and geotechnical investigations are important in design and construction of underground structures. Detailed ground investigation decreases the level of soil's uncertainties in design phase. Moreover, it reduces the probability of encountering unexpected conditions. These unexpected ground conditions may need extra attention, funding and, most importantly, may cause delay in project completion. This delay could be the onset of all big disputes when the project is not progressing according to the plan. It has been observed that projects with more comprehensive ground investigations mostly have less cost overruns and fewer disputes (Bickel *et al.,* 1996).

Another reason for the significance of ground investigation is that for a tunnel, ground acts both as load and support to the tunnel. Moreover, underground construction projects are primarily geotechnical engineering related. The nature of ground changes,

either horizontally or vertically, and even the timing of the construction affects the ground behaviour. Therefore, geotechnical explorations are important in all project phases from pre-feasibility studies to closure. Not only are they able to provide the required knowledge of regional and local geology and hydrogeology, they also bring valuable information about the characteristics of surrounding materials and specific design parameters.

It should be noted that the utmost benefits of ground investigation are to minimize the uncertainties related to the ground condition, predicting how the ground and groundwater affect the behaviour of structures during and after construction. This helps the bidders to provide a definitive design condition, a geotechnical basis for the bid, with "changed condition" being fairly determined (Bickel *et. al.* 1996).

"The degree of exploration required to establish the most economical and expeditious design and construction program is in no way related to the funds available for the work!" as clearly stated by Harvey W. Parker in Tunnel Engineering Handbook (1996). In other words, even though the funding controls the project in many different perspectives, it does not determine the required work. It is extremely risky to start the design and construction based on insufficient data. To acquire a general overview about the site, municipality and adjacent projects' documents provide rich knowledge of the area.

It is absolutely beneficial to contribute a proper amount of time to this phase before moving on to the field investigation since a comprehensive knowledge achieved from the literature enables the field investigator to perform the exploration in the most optimum way. It is also worth to mention that each project is unique and has its own limitations, which is the reason to perform exclusive project-oriented investigations for supplementary data.

2.2.1 Challenges and uncertainties in ground investigation

2.2.1.1 Geological uncertainties

There are numerous uncertainties in the ground. Soil properties may vary with time, weather conditions and groundwater conditions and location. Spatial variability is one of the remarkable sources of uncertainty that may lead to differential settlement of the

tunnel. For instance, uncertainties regarding soil strata and the geometry of the adjacent soil layers with respect to each other. In addition, the geological and geotechnical condition exposed during excavation may be different from exploration stratigraphy mapping, achieved by site investigation. These geological uncertainties are considered as one of the risk sources in underground engineering.

2.2.1.2 Groundwater (Geomorphological) uncertainties

Another source of uncertainty is groundwater. It is the most troublesome parameter to foresee and to deal with, during tunnelling projects. For instance, groundwater may fluctuate periodically due to natural reasons *e.g.* seasonal variations or from human activities (groundwater pumping and dewatering). Uncertainties of groundwater tends to have a significant influence on the evaluation of soil properties and the groundwater pressure that plays a key role in the ground deformation and the failure of the excavation.

2.2.1.3 Uncertainties of soil mechanical properties

In addition to the above-mentioned factors, uncertainty can also be found in the characterization of soil mechanical properties. For example, the properties of soft clay such as permeability, compressibility and shear strength are affected by various factors including stress level, stress state, stress history, void ratio and internal structure or fabric. Examples of the uncertainties related to the mechanical properties of soil are:

1) Spatial variability of soil owing to its heterogeneity including density, water condition, composition, *etc.*
2) The difference in the rate of loading between the lab tests and the in-situ situation: the rate of loading in the lab tends to exceed field loading rate after excavation, which results in different material properties and performances.
3) The other parameter that control the ground deformation and settlement is permeability, which is difficult to measure and highly sensitive to disturbance. Also, horizontal permeability is sometimes ten times higher than vertical permeability (Bickel *et al.* 1996).
4) Soil disturbance is another extremely important factor especially for soft ground. This disturbance leads to lower strength and permeability.

5) It is also worthwhile to mention that some soft rocks and soils tend to deteriorate when exposed either to water or air. This should be taken into account and the sample should be protected during delivery to the lab.

2.2.1.4 Uncertainties regarding soil classification

Soil classification is an important task during ground investigation. For instance, unified soil classification system (USCS) is primarily based on the grain size distribution. For fine-grained soils, the classification is based on the liquid limit (LL) and the plasticity index (PI). It is also possible to descriptively know the relative density, based on the SPT value which is used to estimate the coarse-grained soil mass strength. For fine-grained soils, the strength is attainable by performing undrained shear strength tests, either in-situ or in lab. Schmidt (1974) proposed a correlation between soil type and permeability (Figure 3).

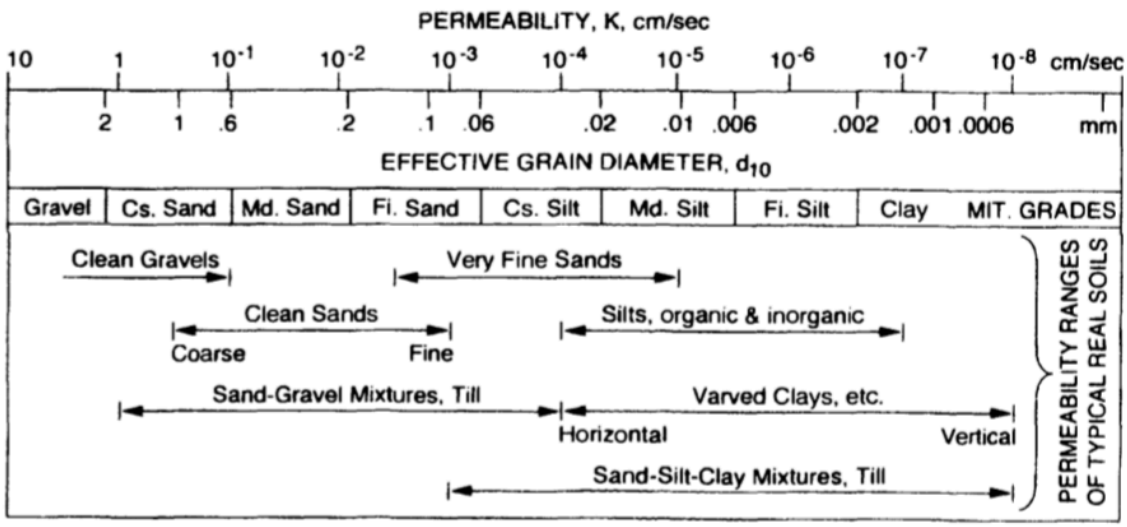

Figure 3. Approximate correlations of soil types and permeability (after Schmidt 1974)

In engineering practice, various methods have been used to estimate the mechanical properties of soils, such as laboratory tests, in-situ tests and empirical methods based on the physical properties of soils. For example, the shear strength of clay can be estimated from the CPT test, liquid limit and plasticity index, various laboratory tests (triaxial, direct shear), *etc.* These different methods all introduced uncertainties with regard to soil properties.

The other classification, which is more practical in tunnelling, is based on ground behaviour. "Tunnelman's ground classification system", which is still in-use today, was proposed by Heuer (1974). Table 1 shows the Heuer's descriptions. Deere *et al.* (1969) proposed classification, which correlates USCS soil classification to Heuer's tunnelman's ground classification.

There is a general relationship between the strength of fine-grained soil and its behaviour. Shield tunnelling can be related to the simple overload ratio, which is the ratio between net overburden pressure at springlines and undrained shear strength of clay.

In general, the construction of a tunnel has four stages (Bickel *et al.,* 1996):

- Excavation
- Primary stabilization
- Secondary (final) stabilization
- Provision of supplementary services (ventilation, illumination, *etc.*)

The approach for tunnel excavation depends on numerous factors, in which the ground condition, purpose of the tunnel and the permitted level of ground disturbance are the most important ones. In soft ground, mechanized tunnelling using TBMs is the most commonly used in engineering practice.

2.2.2 Shield Tunnelling and Tunnel Boring Machines (TBM)

Shield tunnelling is a construction approach for tunnels in weak or soft ground when the work area needs continual stabilization. The shield acts as a shelter for personnel and equipment by providing a reaction force to retain the ground. If the excavation face has enough self-support time, the work is done using an open face shield. If the excavation face cannot maintain stability without support, which usually occurs in soft ground, closed-face excavation has to be carried out.

A TBM is an advanced, multifunctional piece of machinery in tunnel construction, which has accelerated the tunnelling industry and has allowed many previously "impossible" or

Classification		Behaviour	Typical soil types
Firm		Heading can be advanced without initial support, and final lining can be constructed before ground starts to move.	Loess above water table, hard clay, marl, cement sand and gravel when not highly overstressed
Ravelling	Slow ravelling	Chunks or flakes of material begin to drop out of the arch or walls sometime after the ground has been exposed, due to loosening or to overstress and "brittle" fracture (ground separates or breaks along distinct surfaces, opposed to squeezing ground). In fast ravelling ground, the process starts within a few minutes, otherwise the ground is slow ravelling.	Residual soils or sand with small amounts of binder may be fast raveling below the water tale, slow raveling above. Stiff fissured clays may be slow or fast raveling depending upon degree of overstress
	Fast ravelling		
Squeezing		Ground squeezes or extrudes plastically into tunnel, without visible fracturing or loss of continuity, and without perceptible increase in water content. Ductile, plastic yield and flow due to overstress.	Ground with low frictional strength. Rate of squeeze depends on degree of overstress. Occurs at shallow to medium depth in clay of very soft to medium consistency. Stiff to hard clay under high cover may move in combination of raveling at execution surface and squeezing at depth behind surface.
Running	Cohesive-running	Granular materials without cohesion are unstable at a slope greater than their angle of repose. When exposed at steeper slopes they run like granulated sugar or dune sand until the slope flattens to the angle of repose.	Clean, dry granular materials, apparent cohesion in moist sand, of weak cementation in any granular soil. May allow the material to stand for a brief period of raveling before it breaks down and runs. Such behaviour is cohesive-running.
	running		
Flowing		A mixture of soil and water flows into the tunnel like a viscous fluid. The material can enter the tunnel from the invert as well as from the face. crown, and walls, and can flow for great distances, completely filling the tunnel in some cases.	Below the water table in silt, sand, or gravel without enough clay content to give significant cohesion and plasticity. May also occur in highly sensitive clay when such material is disturbed.
Swelling		Ground absorbs water, increases in volume, and expands slowly into the tunnel.	Highly over-consolidated clay with plasticity index in excess of about 30, generally containing significant percentages of Montmorillonite.

Table 1. Tunnelman's ground classification for soils (after Heuer, 1974)

"economically-infeasible" projects to be completed. TBM can be used for tunnel construction in many ground conditions. These full-face excavators provide us with the main steps of tunnelling, namely excavation, muck removal, ground stabilization and maintenance. However, they only produce circular cross sections. In general, TBMs can be classified into three groups: open TBMs, single-shield TBMs and double-shield TBMs. For the purpose of excavation in soft clay, the second type is most suitable. In this type of TBM, the advance of the machine and lining installment are not coincident. The thrust is provided by hydraulic jacks that lean on the last ring of the linings. After the jacks reach their limit of extension, the excavation is stopped, and jacks are depressed and provide the space for the erector to install the segment. Based on how the face pressure is provided to keep the surface stability, single-shield TBMs can be further classified as slurry TBMs and Earth-Pressure Balance (EPB) TBMs.

2.2.3 Slurry TBMs versus EPB TBMs

Greathead (1886) proposed the application of compressed air in shield tunnelling to tackle the problem of groundwater flooding during the construction of London Underground. This method was very helpful and a starting point for the construction of more shield-driven tunnels; however, it turns out that it has some disadvantageous performance and safety issues. For instance, the air permeability of the ground should be sufficiently low. Otherwise, no pore air pressure is generated. Another issue with high volume of compressed air is a potential fire and blast threat, especially in a closed area of a chamber where the consequence would be catastrophic. An alternative approach is to use bentonite slurry instead of the compressed air. In this way, the excavation face is supported by the pumped slurry which forms a filter cake at the interface of the tunnel and the excavation face to compensate the earth and water pressures.

Since the tunnel is being excavated, the mixture of soil and bentonite slurry has to be transported out of the tunnel. The slurry can be circulated throughout the circuit from the face, up to the slurry plant where the muck is separated from the bentonite and the filtered bentonite is reinjected into the circuit. Slurry TBMs can be used for tunnel construction in a vast range of soil types from soft clays to rocks. Figure 4 shows a slurry TBM.

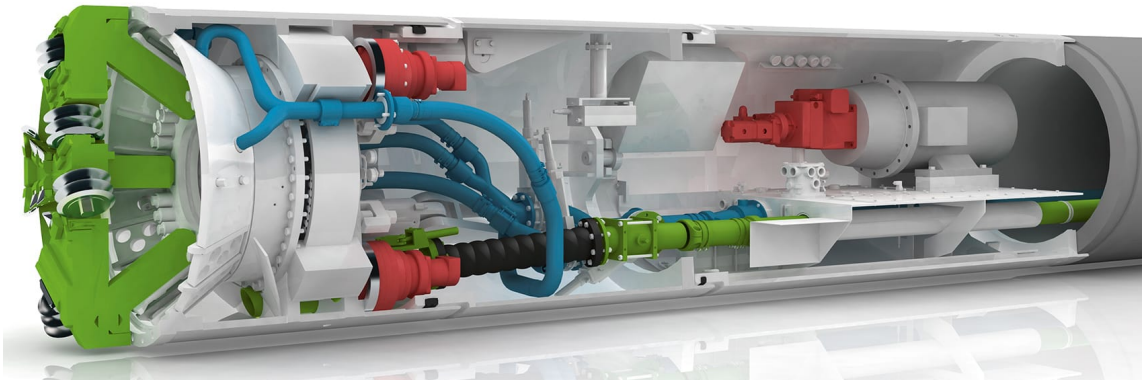

Figure 4. Slurry TBM (Herrenknecht Inc.)

The main disadvantage of slurry TBMs is the need for a slurry plant and continuous slurry circulation. Construction of a tunnel under a densely populated area may not allow a contractor to have a slurry plant on the ground surface. The EPB TBMs solved this problem by using the excavated materials to compensate the ground pressure. This innovative method can be used in soft ground soils with low permeability (*e.g.* clay, silt and loam). The speed of screw conveyor and the advancement rate of the TBM regulate the pressure condition. EPB TBMs are used for tunnelling in urbanized area due to their minimized volume loss and disturbance of the ground soil, as well as no interruption on the ground surface. A schematic photo of EPB TBM is provided in Figure 5.

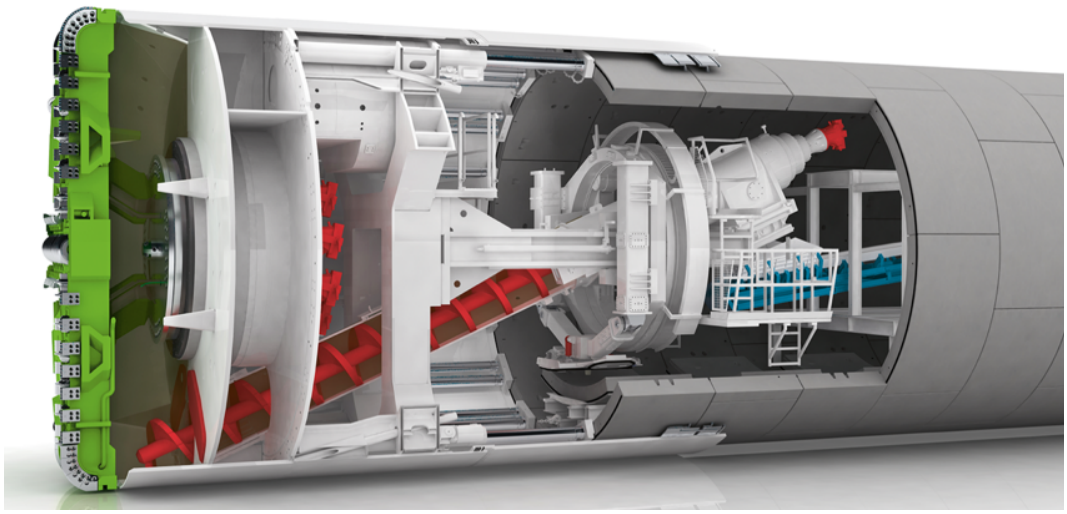

Figure 5. EPB TBM (Herrenknecht Inc.)

2.3 Ground loss and ground movement during tunnelling

2.3.1 Green field settlement

Numerous investigations have been performed to assess and mitigate the associated risk of settlement induced by tunnelling, including the ground movement during the boring action. The fundamental concept of "ground loss" is the controlling factor for ground movement, which is defined as the volume of the material that has been excavated excessively to the actual design volume. This ground loss may be at the face, around the shield or tails of the TBMs or at the curvatures.

The average ground loss ε_0 is defined as:

$$\varepsilon_0 = \frac{\pi\left(R + \frac{g}{2}\right)^2 - \pi R^2}{\pi R^2} * 100\% \approx \frac{g}{R} * 100\% \qquad \textit{(Eq. 2-1)}$$

where g = the total gap parameter, and R = the radius of the tunnel.

Starting from early 50's, studies have been carried out to estimate the ground movement either empirically (*e.g.* Martos, 1958; Peck, 1969; Schmidt, 1969; Attewell and Farmer, 1974; Atkinson and Potts, 1977; Attawell and Woodman, 1982; Mair 1983; Herzog, 1985; Vermeer and Bonnier, 1991; New and O'Reilly, 1991; and Macklin, 1999), analytically (*e.g.* Sagaseta, 1987; Lo *et al.,* 1984; Verruijt and Booker, 1996; Loganathan and Poulos, 1998; Chi *et al.,* 2001; Bobet, 2001; Chou and Bobet, 2002; and Park, 2005; or numerically using Finite Element (FE) or Finite Difference (FD) methods (*e.g.* Rowe *et al.,* 1983; Lee *et al.,* 1992; Gioda and Swoboda, 1999; Addenbrooke and Potts, 2001; Vermeer *et al.,* 2003; Melis *et al.,* 2002; Mroueh and Shahrour, 2002;; Ocak, 2009; Ercelebi *et al.,* 2011; Hosseini *et al.,* 2012; and Mathew and Lehane, 2013). Recently, much research has been conducted based on the application of novel computational algorithms such as artificial neural network (ANN) and support vector machines to estimate ground movement; see *e.g.,* Shi *et al.* (1998), Suwansawat (2002), Suwansawat and Einstein (2006), Neaupane and Adhikari (2006), Santos Ovì dio and Celestino Tarcìsio (2008), Yao *et al*. (2010), Ocak and Seker (2013). Empirical methods, which are the most used in practice, are mainly based on the assumptions of Martos (1958) that the shape of the transverse settlement trough above a mining drift can be approximated by a Gaussian curve. Peck (1969) and Schmidt (1969) investigated numerous case studies and

proposed that the Gaussian curve is also valid for shallow tunnels in soils. The Peck's formula is:

$$S_x = S_{max}.\exp\left(-\frac{x^2}{2i^2}\right) \qquad \textit{(Eq. 2-2)}$$

where x = horizontal distance from the tunnel centreline,

i = horizontal distance from the tunnel centreline to the point of inflection on the surface settlement trough, and

S_{max} = the maximum settlement which happens above the centreline.

It can be shown that approximating the longitudinal settlement trough using the cumulative probability distribution curve is reasonable, but it is only valid for tunnels in clays (Mair *et al.*, 1997).

Loganathan and Poulos (1998) proposed analytical calculations for ground settlement, based on the equivalent ground loss ε_0. In this approach, the ground settlement was formulated based on the gap parameter g, representing the component of volume loss, introduced by Lee *et al.* (1992):

$$g = G_p + U_{3D}^* + \omega \qquad \textit{(Eq. 2-3)}$$

in which G_p is the physical gap between shield and lining outer diameters. When a tunnel advances in perfect alignment with full support at the face, the total gap g is identical to the physical gap G_p:

$$G_p = 2\Delta + \zeta \qquad \text{In case of no grouting} \qquad \textit{(Eq. 2-4)}$$

$$G_p = (7-10)\% * (2\Delta + \zeta) \qquad \text{Considering grout shrinkage (Park, 2005)} \qquad \textit{(Eq. 2-5)}$$

where Δ is the thickness of the tailpiece and ζ is the clearance required for the erection of the lining.

Defining parameters describing the effect of the face pressure release U_{3D}^* and over-excavation (workmanship) ω, U_{3D}^* is 3D elastoplastic deformation at the tunnel face.

When EPB TBMs are utilized, U_{3D}^{*} can be considered to be negligible; *i.e.* $U_{3D}^{*} = 0$. For any other construction method:

$$U_{3D}^{*} = k_1 \frac{\delta_x}{2} \qquad \textit{(Eq. 2-6)}$$

$$k_1 = \frac{\text{Volume of nonuniform axial intrusion across the tunnel face determined by 3D analysis}}{\text{Volume assuming uniform axial intrusion}} \qquad \textit{(Eq. 2-7)}$$

where δ_x is maximum axial intrusion at the tunnel face (Lee *et al.,* 1992). According to Lee, during design, $k_1 = 1$ is reasonable and Eq. (2-6) is simplified to:

$$U_{3D}^{*} = \frac{\delta_x}{2} \qquad \textit{(Eq. 2-8)}$$

The displacement δ_x can be related to a dimensionless factor Ω:

$$\Omega = \frac{\delta_x E}{R P_0} \qquad \textit{(Eq. 2-9)}$$

where P_0 is the total stress removal at the tunnel face, defined as:

$$P_0 = (K_0' P_v' + P_w) - P_i \qquad \textit{(Eq. 2-10)}$$

where K_0' = the effective earth pressure coefficient at rest,

E = undrained Young's modulus at tunnel springlines,

P_v' = vertical effective stress at tunnel springlines,

P_w = pore water pressure at tunnel springline, and

P_i = the tunnel supporting pressure. If the tunnel is fully excavated $P_i = 0$, the presence of the air at the surface cause $P_i > 0$.

Another component of the gap parameter g is the workmanship parameter ω, as illustrated in Figure 6. The workmanship parameter ω considers the over-excavations happens because of deviations from the design advancement line. It is the common practice to advance the shield at a slightly upward pitch relative to the actual design grade to avoid the problem of diving (Lee *et al.* 1992). This leads to the overcutting near the crown of the tunnel. In addition to this, yawing produces additional loss due to the

movement of the shield from side to side or at curves. This is highly dependent on the skilfulness of the operator and it is hard to address prior to the construction.

In order to define the workmanship parameter ω, we first define ω^* as

$$\omega^* = \min\left\{0.6G_p, \frac{1}{3}U_i\right\} \qquad \textit{(Eq. 2-11)}$$

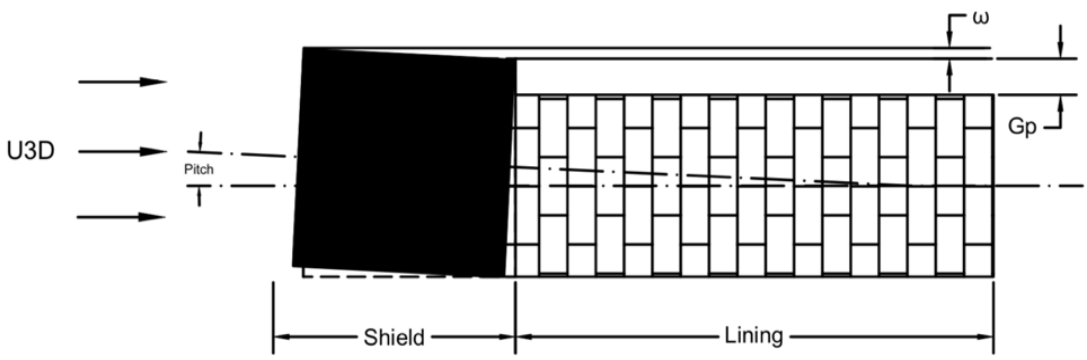

Figure 6. Gap parameter and its components (after Lee et al. 1992)

in which U_i, the elasto-plastic plane strain displacement at tunnel crown, is determined as:

$$\frac{U_i}{R} = 1 - \left\{\frac{1}{1 + \frac{2(1+\nu)C_u}{E}\left[\exp\left(\frac{N-1}{2}\right)\right]^2}\right\}^{\frac{1}{2}} \qquad \textit{(Eq. 2-12)}$$

where C_u is the undrained shear strength, E and υ are undrained Young's modulus and undrained Poisson's ratio of the soil, respectively. N is the stability parameter; According to Broms and Bennermark (1967), to have stable tunnel face, the range for stability number for shallow tunnels in soft clay must be between 0 and 6. N is determined as:

$$N = \frac{\sigma_s + \gamma H - P_i}{C_u} \qquad \textit{(Eq. 2-13)}$$

where σ_s = total surcharge acting on the ground surface,

γ = the unit weight of soil,

H = tunnel depth to the centreline,

P_i = face support pressure applied at tunnel face,

C_u = soil's undrained shear strength.

ω also considers the radial ground loss due to overcutting bead. If there is no overcutting bead, then $\omega = \omega^*$. Otherwise, if the bead spans the upper 180° of the hood, then $\omega = \omega^* + 1 * (\text{bead thickness})$ and if bead covers the full circumference, $\omega = \omega^* + 2 * (\text{bead thickness})$. A schematic view of the gap parameter and its components has been shown in Figure 6.

2.3.2 Pile settlements

2.3.2.1 Concept of the design charts

The concept of design charts for pile settlements induced by tunnelling is firstly introduced by Loganathan (2011). These design charts are established via a series of numerical analysis using GEPAN which is a boundary-element program developed by Xu and Poulos (1999). The program is based on elastic continuum analysis. Two series of design charts are developed based on the length of the pile: short piles are the ones where length of pile L is smaller than the depth of the tunnel axis H and long pile are the ones with their lengths L greater than H (see Figure 7).

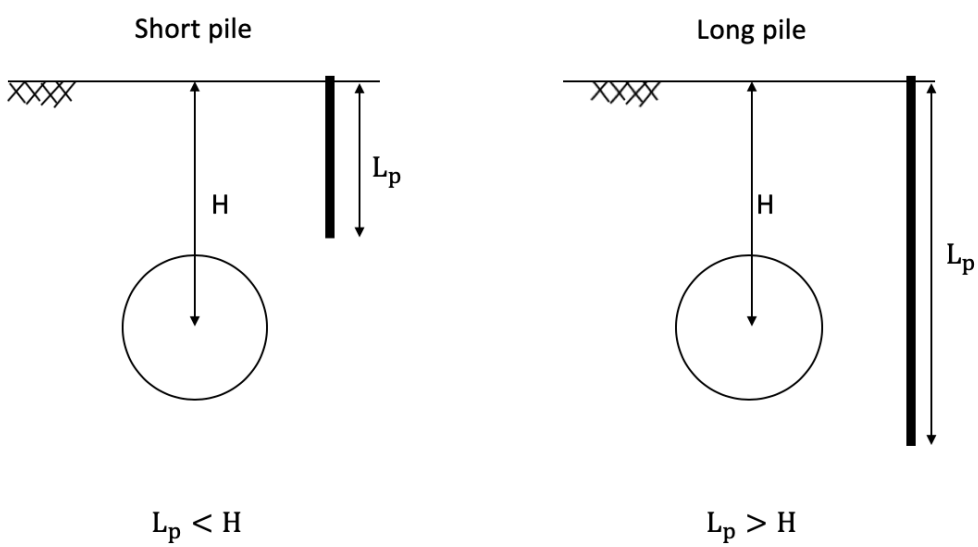

Figure 7. Short pile and long pile definitions (after Loganathan, 2011)

Based on a series of parametric analyses, the maximum forces and deformation of a pile under different conditions are expressed as:

$$M_{max} = M_b k_{cu}^{M} k_d^{M} k_{L_p/H}^{M}$$
$$\rho_{max} = \rho_b k_{cu}^{\rho} k_d^{\rho} k_{L_p/H}^{\rho} \qquad \textit{(Eq. 2-14)}$$

And axial response:

$$+P_{max} = +P_b k_{cu}^{+P} k_d^{+P} k_{L_p/H}^{+P}$$
$$-P_{max} = -P_b k_{cu}^{-P} k_d^{-P} k_{L_p/H}^{-P} \qquad \textit{(Eq. 2-15)}$$
$$\nu_{max} = \nu_b k_{cu}^{\nu} k_d^{\nu} k_{L_p/H}^{\nu}$$

where M_{max}, ρ_{max}, $+P_{max}$, $-P_{max}$ and ν_{max} are maximum pile's induced bending moment, lateral deflection, compressive axial force, tensile axial force and head settlement, respectively. k_{cu} is the correction factor for undrained shear strength, k_d is the correction factor of pile diameter and $k_{L_p/H}$ is the correction factor for ratio of pile length to the tunnel axis level. The design charts are provided in Appendix I.

Design charts are developed based on the "base" case with the following characteristics:

- Tunnel excavated in homogeneous clay,
- The undrained shear strength is 60 kPa,
- Tunnel outer diameter $D_{out} = 6$ m,
- Tunnel cover (depth to centreline) $H = 20$ m,
- Pile diameter $D_{Pile} = 0.5$ m,
- Pile length $L_{Pile} = 15$ m for short piles and $L_{Pile} = 25$ m,
- Young's modulus of the pile is 30 GPa,
- Ground loss is 1 percent.

2.3.2.2 Procedure to use the design charts

The procedure of the calculation of the values of pile's induced stress, bending moment and head settlement is outlined as following:

1. Find the equivalent average ground loss ε_0,

2. Find the ground loss ratio ε_F:

$$\varepsilon_F = R^2 \varepsilon_0 \qquad \textit{(Eq. 2-16)}$$

   in which R is the tunnel radius.
3. Find the ratio between the equivalent ground loss and the ground loss of the base case:

$$L_R = \frac{\varepsilon_F}{\varepsilon_{FB}} \qquad \textit{(Eq. 2-17)}$$

4. Find the raw base values based on the horizontal distance between pile and tunnel centrelines,
5. Multiply the raw values by L_R to find the base values,
6. Find the base correction factors based on shear strength of the soil, pile's diameter and pile length ratio (consulting the design charts),
7. Multiplication of the correction factors by the base values to calculate the axial and lateral responses (stresses and deformations)

The above procedure leads to results of the induced lateral and axial stresses and deformations. Then by knowing the design values, the total stress and settlements are achievable.

2.4 Long-term (consolidation) settlement in soft clays

As previously mentioned, consolidation settlement is a major contributor to the total settlement of a tunnel in soft grounds. Soft, water-retaining grounds with very low permeability are most susceptible to consolidation settlement. Tunnel construction, including grouting and the changes in groundwater table, tend to induce excess pore water pressure in the soil. The dissipation of the excess pore pressure leads to an increase in effective stress hence settlement.

In contrast to extensive literature dealing with short-term or immediate settlement, the studies on causes, behaviour and quantifying the long-term movements of tunnels in soft ground are limited.

Schmidt (1989) stated that the so-called "delayed settlement" is due to at least three

different mechanisms namely pore pressure reduction due to radial plastic displacement, pore pressure generation due to excess face support and the role of tunnel as a drain. He then performed a series of analysis to quantify the pore pressure change which is considered as the key element to calculate the consolidation settlement.

O'Reilly *et al.* (1991) conducted an analysis based on the monitoring records of the Grimsby tunnel for eleven years. They also provided an FE analysis which confirmed their observations. Samarasekera *et al.* (1992) performed a series of analysis on pore water pressure change around the tunnel and addressed the influence of depth, cover to depth ratio and soil properties on settlement. The pore pressure behaviour is modeled via an uncoupled consolidation analysis and solved by finite element method (FEM). They also considered the effect of the support by introducing effective stiffness ratio (ESR).

Yi *et al.* (1993) performed a coupled viscoplastic consolidation analysis to address the time-dependent ground deformation with strain-hardening behaviour of the soil by conducting triaxial creep test. Mair *et al.* (1993) explained the settlement of the tunnels in clay using plasticity solutions and compared the proposed solution with field measurements. Based on their study, subsurface vertical and horizontal deformations as well as pore pressure changes can be addressed by considering a plane-strain situation perpendicular to the tunnel axis and assuming soil to be elastic perfectly-plastic. Shirlaw *et al.* (1994) conducted a review work, explaining the pore pressure variation immediately after excavation and in long term, in different case studies. They also proposed mechanisms of pore pressure variation: mechanism 1 is due to the seepage into the tunnel, mechanism 2 is the result of having face pressure lower than overburden pressure and mechanism 3, is when the face pressure is greater than the overburden pressure. They also stated that 30% to 90% of the total settlement is contributed by consolidation settlement, which in many cases, also causes a widened settlement trough (with respect to immediate settlement).

Bowers *et al.* (1996) conducted a series of 3-year measurements on Heathrow express trial tunnel and observed that the Gaussian curve, which reasonably fits the immediate settlement trough, shows some dissimilarities for long-term settlement, especially at the flanks. They proposed an empirical formula for settlement trough of a tunnel which was excavated in London clay and left unsupported for two years. The effect of the

consolidation settlement on the overlying structures was also mentioned and the fact that damage to the structures is not because of the displacement, but rather to angular distortion and tensile ground strain. It is also worth mentioning that the shape of the settlement trough does not greatly change the tensile ground strain. However, the widening of the trough slightly increased the affected area.

Komiya *et al.* (2001) conducted an analysis dealing with the effect of grouting on soil consolidation in shield tunnelling by performing field measurements, lab tests and numerical analyses. A comparison was made between compaction tail void grouting and grout jacking. They found that, although grout jacking produces a greater heave against the settlement, in the long term, it experiences larger consolidation settlements due to the dissipation of excess pore water pressure generated during the jacking as well as grout shrinkage. The lab test results disclosed that even slightly overconsolidated clays show better grouting efficiency comparing to normally consolidated clays, with the efficiency directly proportional to the grout volume. FE modeling of the lab tests acknowledged that the amount and extent of generated excess pore water pressure during grouting control the long-term grout efficiency.

Shen *et al.* (2014) conducted a study on long-term behaviour of the Shanghai subway tunnels, bored in the alluvial soft clays of the Yangtze river. Their field monitoring data depicted a continuous differential settlement, which reached to more than 200 mm in some areas along the tunnel. It was observed that the differential settlement was more severe at tunnel-station connections, below the river, at cross passages and at the soil layer boundaries. This differential settlement was the major cause of the longitudinal settlement pattern of the tunnel and, according to the authors, was mainly controlled by the step between the rings and their relative movements rather than the bending or deformation of the lining. Based on the observations, most of the tunnel's lining were deformed into a horizontal ellipse. This deformation worsened the groundwater infiltration and caused more consolidation settlements endangering the serviceability of the tunnel. Their analyses also stated that during the early operational years, the cyclic loading of the trains remarkably contributed to the total consolidation settlements.

Soga *et al.* (2017) described the behaviour of a single tunnel, a twin tunnel and cross passages in soft clays, as well as the possible mechanisms for settlement based on the drainage conditions and compressibility of the soil. The soil-lining permeability difference and its effect on the consolidation mechanism was discussed. A method for

evaluating the long-term settlement was also reviewed which was based on the work of Wongsaroj *et al.* (2013) and Laver *et al.* (2016). This is further addressed in the next section.

Di *et al.* (2019) conducted a series of analysis targeting susceptive positions for differential settlement in Yangtze area, China. Five metro lines were analyzed including 67 tunnel-station connections, 55 cross-passages, 4 wells and 3 U-shaped grooves. The results showed that the differential settlements of almost 85% of tunnel stations were less than that of the adjacent tunnels. Moreover, the settlements of 73% of the crossing passages were found to be more than the ones on the side of each tunnel. Track slab deformation was pervasive as a result of this uneven settlements.

2.4.1 Quantifying ground movements due to consolidation settlements

Mair and Taylor (1997) stated that the increase in differential settlement induced by consolidation was small, implying that additional building damage compared with what occurred during the tunnel excavation was negligible. However, later studies (Mair *et al.*, 2003; Farrell *et al.,* 2014) disclosed that the value of the differential settlement, induced by consolidation, was a function of time. If the observation were to last sufficiently long, the settlement could have reached a critical value; *e.g.* a noticeable fraction of short-term settlement or even greater than it. Hence, quantifying the long-term settlement is important for the prediction of soil behaviour, tunnel settlement, as well as possible damage and risk.

Despite the fact that numerous studies have been conducted for the consolidation settlement in clayey soil, limited work has been performed to quantify the magnitude and extent of it. Exclusively, a series of studies have been performed on the London stiff clay to provide a method to evaluate the ground movements over time. With the aid of parametric FE analysis, Wongsaroj *et al.* (2013) evaluated the magnitude and extent of long-term ground movements in both transient and steady states. They proposed a normalized dimensionless maximum surface settlement NS plotted against the dimensionless relative permeability RP for different cover to depth ratios and horizontal to vertical permeability ratios. Laver *et al.* (2016) extended the Wongsaroj *et al.* (2013) study to quantify both vertical settlement and horizontal deformation induced by consolidation as well as the peak horizontal strain, which is a crucial component for the evaluation of damage to the surface buildings (Burland, 1995). This method adopted a

new permeability index based on a more realistic definition of seepage toward the tunnel and provided equations rather than graphical tools.

Although the formulation of Laver *et al.* (2016) is versatile, its applicability is questioned since the proposed formulation is based on a parametric FE analysis using data collected from overconsolidated London clay. Nevertheless, the formulation may still be practical to evaluate the time-dependent behaviour of the soft clay as long as the effect of the OCR and the variation of stress level are properly addressed.

2.4.2 Formulation for long-term settlement by Laver *et al.* (2016)

The consolidation settlement formula proposed by Laver *et al.* (2016) is based on the assumptions that the seepage occurs radially toward the tunnel and the consolidating layer lies between $2.5\mathrm{D}$ (D being tunnel's diameter) from the tunnel centreline. The formulation by Laver *et al.* (2016) provided the vertical settlement and horizontal ground displacement as:

- Transverse profile for settlement:

$$S_c(x) = \frac{\alpha}{\alpha - 1 + \exp \mu \left(\frac{x}{K_L Z_0}\right)^2} S_{cmax} \qquad \textit{(Eq. 2-18)}$$

- horizontal displacement:

$$H_c(x) = \frac{3a_{hd}^2 x}{|x|^3 + 2a_{hd}^3} H_{cmax} \qquad \textit{(Eq. 2-19)}$$

in which, S_{cmax} = the maximum consolidation settlement,

H_{cmax} = the maximum horizontal displacement,

x = the horizontal distance from the tunnel axis,

$\alpha = e^{\mu} \frac{2\mu - 1}{2\mu - 1} + 1$,

$$\mu = \begin{cases} -0.004 & RP < 0.1 \\ 0.1 & RP \geq 0.1 \end{cases}$$

RP = dimensionless displacement factor,

$K_L = 0.8 - 6V_L$ where V_L is volume loss.

2.5 Uncertainty, risk and reliability

2.5.1 Risk definition

Uncertainty, risk and reliability are terms that are used in everyday life when dealing with lack of "sureness." However, the definition of "risk" from scientific point of view is more complicated. This section first provides a concise explanation about the meaning of these terminologies, then the frameworks and tools are introduced, which basically form the pillars of an RM plan. The intention of this part of the thesis is to introduce the major topics in RM, even to readers who are new to the field.

The word "risk" has numerous meanings. In everyday life, one may define it as the possibility of suffering of harm and danger (Webster Dictionary). In engineering practice, it has more specific and sophisticated meanings. The international organization of standardization (ISO), in its risk management vocabulary (2009), defines risk as the effects of uncertainties on system's objectives. In the context of engineering practice, risk is defined as a function of the probability of occurrence and the consequence of it:

$$\text{Risk} = \text{R}(\text{Probability}, \text{Consequence}) \qquad \textit{(Eq. 2-20)}$$

This definition can be specified in a more technical way as:

$$\text{Risk} = \text{R}(\text{Hazard}, \text{Volnurability}, \text{Exposure}) \qquad \textit{(Eq. 2-21)}$$

This definition technically states that the consequence of a potentially hazardous happening is basically due to the vulnerability of the system to that specific hazard as well as the degree of exposure or "closeness" of the vulnerable asset. The fundamental parameters of this definition (hazard, vulnerability, exposure) are key players in decision-making process which is one of the outputs of the RM analysis.

Risk management is defined as a set of coordinated activities to direct and control a system with regard to risk (ISO, 2009). RM can be applied to an entire system, to all of its areas and levels, at any time, as well as to specific functions, projects and activities.

Casagrande (1965) used the word "calculated risk" in his Terzaghi's lecture, in which he introduced the following procedure to identify and deal with risk:

Step 1: Appraise the probable ranges for all pertinent quantities involved in the solution, by using imperfect knowledge, accompanied by judgment and experience,

Step 2: Select a suitable margin of safety, or degree of risk, by considering socio-economic consequences that result from failure.

Some years later, another remarkable geotechnical engineer, Robert Whitman, during his Terzaghi's lecture in 1984, recapped the probabilistic approaches and the reliability concept to evaluate the so-called "calculated risk". These clues were then followed by many researchers all around the world for many different problems of geotechnical engineering; *e.g.* dams, dikes, foundations, *etc.*

To properly perform an RM plan, it is more suitable to define the sequence of activities in the form of a framework that contains the components and the workflow of each step. Exclusively in geotechnical engineering, in addition to ISO 31000 (ISO, 2009), which is shown in Figure 8, one may refer to Swedish geotechnical society risk management cycle (SGF, 2017), international tunnel association (ITA) guidelines for tunnelling risk management (Eskesen *et. al.*, 2004), GeoQ risk management approach (Staveren, 2006), China's RM standards on tunnels and underground structures (Hu *et. al.*, 2014), Zhang *et. al.* (2015), Qian *et al.* (2016), *etc.* All these approaches share the same fundamental bases, which include:

1. Risk identification
2. Risk analysis
3. Risk evaluation
4. Risk monitoring and communication

In particular, Steps 1 to 3 are referred to as "risk assessment", which are performed in chronological order. This is because no risk analysis can be conducted before risk identification is fully carried out and no risk evaluation should be done before risk analysis is completed.

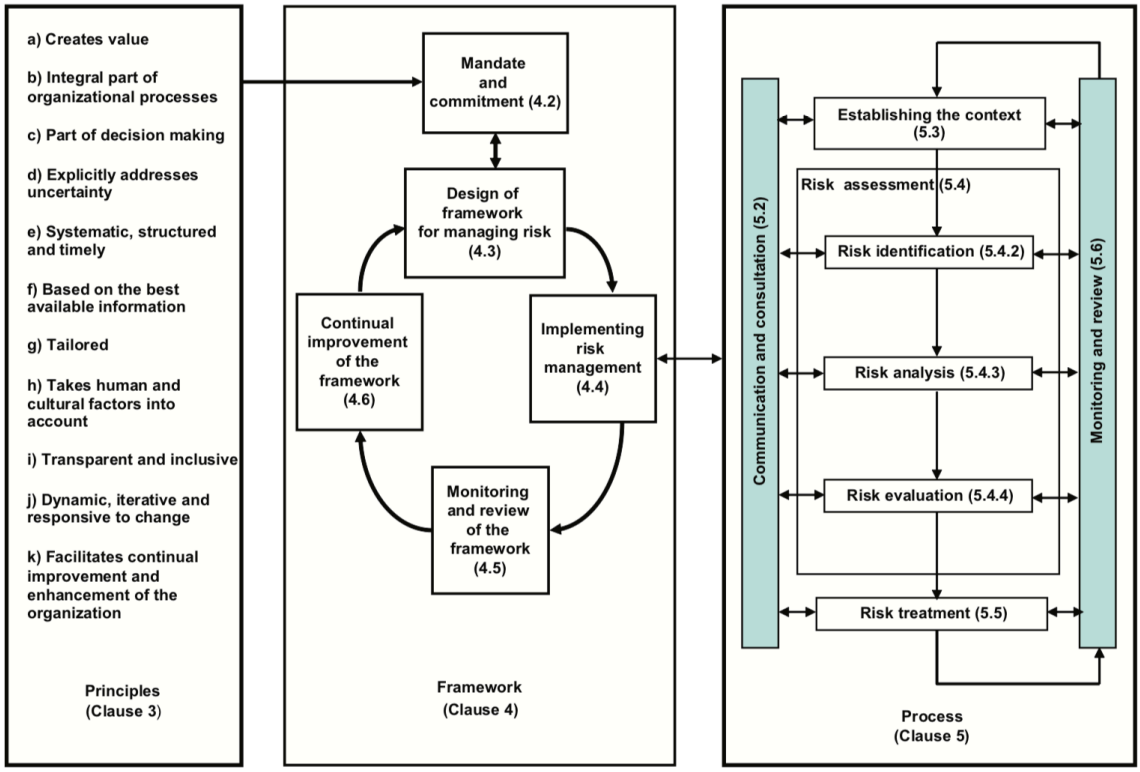

Figure 8. ISO risk management act (2009)

Risk identification is a critical step in RM. In fact, failure to properly recognize the risk may lead to overlooking of it in the further procedures. There are a number of powerful tools to identify risk. First and foremost, literature review and previous experience provide rich sources of information at low cost. Using risk registers, checklists, interviews and questionnaires have been proven to be helpful. Field investigation is another tool, which is relatively costly but sometimes necessary, since not all the required data are always available through review.

Duddeck (1996) classified underground risk into five groups: geo-related risks, functional risks, contractual risks, environmental risks and financial risks. For more information on other groups, one may refer to the rich literature in these areas (*e.g.* Essex, 2007).

Risk identification does not only consider the sources of potential hazard instead, it considers any source of uncertainty that must be addressed, given that lack of certainty

is the reason of any risk analysis. Even though, controversy is still ongoing on the definition and categorization of uncertainty, they are generally in two types.

2.5.2 Uncertainty types

2.5.2.1 Aleatory uncertainty

Aleatory uncertainty is not controllable. This type of uncertainty was first discussed by Pascal via the "Pascal demon" as an intrinsic part in the nature of a phenomenon which is not separable. For instance, German scientist Heisenberg (1927) proposed the well-known Heisenberg's uncertainty principle, which states that the position and momentum of a particle cannot be exactly measured at the same time, even theoretically. In fact, the more accurately the position is measured, the less accurate is the estimate of the velocity. This is not because of lack of knowledge, but an inherent characteristic of the phenomenon. This type of uncertainty is not reducible throughout the RM and by mitigation measures.

2.5.2.2 Epistemic uncertainty

Epistemic uncertainty is basically the realization of our knowledge about a phenomenon. This uncertainty can be diminished by data acquisition, quality control and even simply repetition.

2.5.3 Sources of uncertainty

Uncertainty may come from various sources. Inherent uncertainty is aleatory and is an intrinsic feature of a phenomenon. Statistical uncertainty is another source which is due to lack of data. Model uncertainty, which is due to the failure in properly defining the influential parameters, could be aleatory or epistemic. For example, a model that is known to be simplified and can be improved is epistemic. On the other hand, the "unknown unknowns" that are neither known nor simplified, are aleatory. Measurement uncertainties and human errors are also two main sources of epistemic uncertainty.

2.5.4 Uncertainty description

There are three main approaches to describe uncertainty suitable for specific tasks. The primary approach is to use probability, which is known as "probabilistic methods". There are two schools of thoughts in probability namely Frequentist and Bayesian. Frequentist

school considers probability as frequency of happening when the experiments are repeated for a sufficiently large number of times:

$$P(E) = \lim_{n \to \infty} \frac{n_E}{n} \qquad \textit{(Eq. 2-22)}$$

in which n_E is the number of experiments with E as outcome and n is the total number of the experiments. Supporters of Frequentist school is sometimes called as classical statisticians. The Bayesian school, on the other hand, explicates the probability as degree-of-belief. The probability is defined as the extent of the belief of occurrence of a phenomenon. This school of thought is based on the well-known Bayes' theorem:

$$P(A|B) = \frac{P(B|A)}{P(B)} P(A) \qquad \textit{(Eq. 2-23)}$$

$P(A|B)$ or "posterior" is achieved by knowing the marginal probability of A, $P(A)$ or "prior", the conditional probability of B given A, $P(B|A)$ or "likelihood", and the marginal probability of B, $P(B)$ known as "normalization".

2.5.5 Risk analysis

Risk analysis is one of the three pillars of risk assessment. The two terms, risk analysis and risk assessment, are sometimes used interchangeably. However, from ISO's standpoint, risk assessment has a broader meaning and includes risk identification, risk analysis and risk evaluation.

Risk assessment, in its general form, is categorized in "qualitative" and "quantitative" risk assessments. Qualitative risk assessment describes the risk sources, evaluation methods and mitigation measures in a descriptive manner. This method has its own benefits, *e.g.* agility and ease; however, it is sometimes highly biased and subjective to the knowledge of the analyst, perception of the phenomenon and lack of flexibility (ISO, 2009).

Quantitative risk assessment addresses the problem with a more precise and reliable language especially for engineers. Various tools have been developed for quantitative description of each step of RM (*i*.e. identification, analysis and evaluation).

After identification, another set of tools are available to perform the analysis namely fault trees, event trees and influence diagrams are among the most used ones. A short description of these tools is presented in the subsection that follows.

2.5.5.1 Influence diagram

An influence diagram, as it is schematically shown in Figure 9, is basically a representation of all (or at least all that the analyst is aware of) influential agents acting on a system where arrows show the influence direction. This graph represents the interconnectivity of parameters and models in the form of a network. It is highly informative and simple to use.

Figure 9. Schematic view of an influence diagram

2.5.5.2 Event tree diagram

Event tree diagrams depict the sequence of happenings one after another. Technically, they demonstrate the what/if scenarios graphically. In addition to visualization, this tool enables us to calculate the probability of domino (cascading) consequences from an initial event. Event tree diagrams are mostly used for defining failure scenarios with their probability of occurrence in pre-event risk analysis. A schematic view of an event tree is shown in Figure 10.

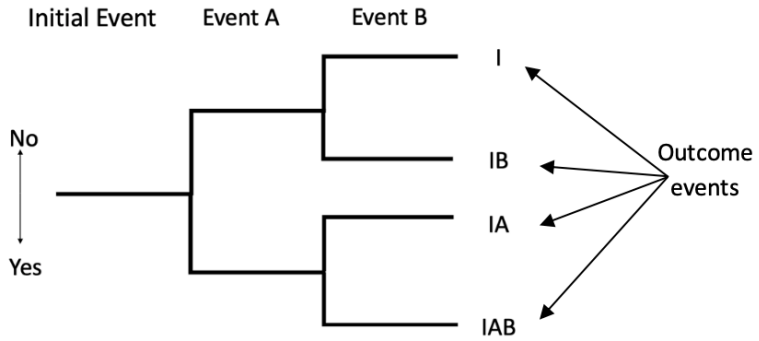

Figure 10. Schematic view of an event tree

2.5.5.3 Fault tree diagram

Fault tree diagram is a more sophisticated tool that uses Boolean logic to recognize the causes of failure of a component or a system. This top-down analysis enables us to appraise the probability of failure of a top event by knowing the probability of failure of a series of sub events. Fault tree and event tree are mostly used in a complementary manner.

Fault tree analysis, however, is mostly carried out to see the cause or causes of the failure. It was firstly utilized in aerospace engineering to evaluate the risk of failure of a shuttle, and also in the design of nuclear power plants. The concept was later extended to many engineering fields. Figure 11 shows a sample of a fault tree.

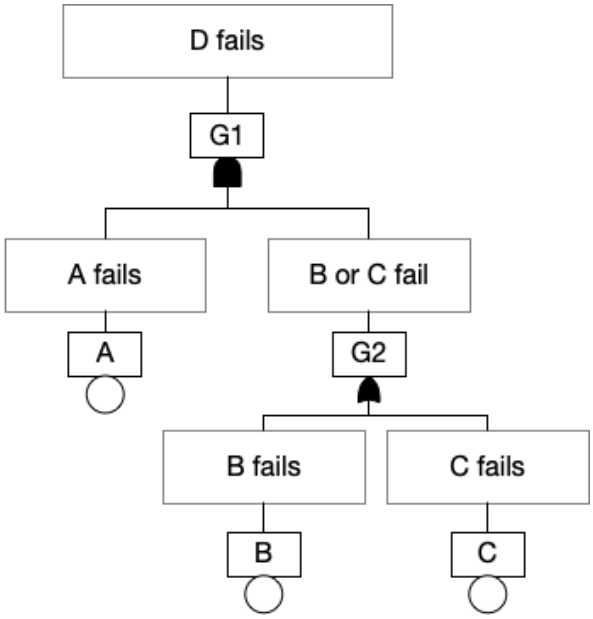

Figure 11. Example of a fault tree

Fault tree analysis follows a bottom-up calculation. In Figure 11, component G2 fails when either component B or component C fail. Component G1 fails when G2 and A fails simultaneously. In designing fault tree diagrams, a series of symbols are utilized to represent the relationship between the events. These symbols are classified in three categories of primary event symbols, gate symbols and transfer symbols, which are listed in Table 2 (Stamatelatos, 2002).

Symbol	Description	Symbol	Description
Primary event symbols			
	BASIC EVENT - A basic initiating fault requiring no further development	n	**COMBINATION -** Output fault occurs if n of the input faults occur
	CONDITIONING EVENT - Specific conditions or restrictions that apply to any logic gate (used primarily with PRIORITY, AND and INHIBIT gates)		**EXCLUSIVE OR -** Output fault occurs if exactly one of the input faults occurs
	UNDEVELOPED EVENT - An event which is not further developed either because it is of insufficient consequence or because information is unavailable		**PRIORITY AND -** Output fault occurs if all of the input faults occur in a specific sequence (the sequence is represented by a CONDITIONING EVENT drawn to the right of the gate)
	HOUSE EVENT - An event which is normally expected to occur		**INHIBIT -** Output fault occurs if the (single) input fault occurs in the presence of an enabling condition (the enabling condition is represented by a CONDTIONING EVENT drawn to the right of the gate)
Gate symbols		**Transfer symbols**	
	AND - Output fault occurs if all of the input faults occur		**TRANSFER IN -** Indicates that the tree is developed further at the occurrence of the corresponding TRANSFER OUT (*e.g.* on another page)
	OR - Output fault occurs if a least one of the input faults occurs		**TRANSFER OUT -** Indicates that this portion of the tree must be attached at the corresponding TRANSFER IN

Table 2. Fault tree's symbol description (Stamatelatos, 2002)

With the help of fault tree analysis, it is possible to realize the sequence of events that leads to failure. In more technical language, a series of basic events is recognized. If they all occur, the top event will occur. This set of basic events is called a "cut set". A minimal cut set or a minimal failure set is a smallest set of basic events. It should be noted that if one event is dismissed from a minimal cut set, the failure of top event will not occur.

2.5.6 Risk evaluation

In the context of the reliability analysis in engineering, the general definition of risk (Eq. 2-21) is redefined as:

$$\mathrm{Risk} = \mathrm{p_f} * \mathrm{c_f} \qquad \textit{(Eq. 2-24)}$$

where $\mathrm{p_f}$ is probability of failure and $\mathrm{c_f}$ is the cost of failure. This formulation is the basis of the risk-based decision making which will be discussed further in this chapter.

If risk is presented by a probability of failure, reliability would be the complement of the probability of failure:

$$\mathrm{Reliability} = 1 - \mathrm{p_f} \qquad \textit{(Eq. 2-25)}$$

The problem of finding $\mathrm{p_f}$ is called a "reliability problem". Two major factors in a reliability problem are random variables and the limit-state function. Random variables are variables whose outcomes are corresponding to a random phenomenon. Mathematically, a random variable is a function from a sample space to real numbers $(f: S \rightarrow \mathbb{R})$. Sample space is the domain that contains all possible events.

For civil engineers, limit-state functions are not alien. In fact, they are used in everyday civil engineering designs, but those were not in-common back in 70's or earlier when the designs were all based on the working stress design (WSD) method. In WSD, all the uncertainties are taken into account only by having a lump safety factor value. In early 80's, WSD was gradually replaced by limit state design (LSD), in which limit-state functions are used to define the thresholds of failure and different factors are considered for both load and resistance.

The limit-state surface partitions the joint probability distribution of the random variables into safe and unsafe zones:

$$\begin{aligned} g(\mathbf{x}) &< 0 && \text{Failure} \\ g(\mathbf{x}) &> 0 && \text{Safe} \\ g(\mathbf{x}) &= 0 && \text{Limit-state} \end{aligned} \qquad \textit{(Eq. 2-26)}$$

where the limit-state function is denoted by g and $\mathbf{x}$ is the vector of the random variables. The "basic" reliability problem or the fundamental problem in reliability is defined by the following limit-state function:

$$g = R - S \qquad \textit{(Eq. 2-27)}$$

in which R is resistance random variable and S is the random variable which represents demand or load. If S exceeds R, failure occurs, and the probability of identifying this occurrence is the goal of the reliability analysis. Considering resistance and load are statically independent, we have:

$$p_f = \iint_{R<s} f_R(r) f_s(s)\, dr ds = \int_0^{\infty} \int_0^{s} f_R(r) f_s(s)\, dr ds = \int_0^{\infty} F_R(s) f_s(s)\, ds \qquad \textit{(Eq. 2-28)}$$

where $f_R(r)$ and $F_R(r)$ are marginal and cumulative probability distribution functions of resistance, respectively, and $f_s(s)$ is probability distribution function for demand (since they are independent, their joint probability distribution function is equal to the product of their marginal probability distribution functions). Figure 12 shows the marginal probability distribution of resistance and demand and the shared area between them. It should be noted that this area is not equal to the probability of failure.

Now, consider a case where both R and S have normal probability distribution. In this case, g also follows normal distribution because it is a linear function of normally distributed variables. Therefore:

$$\mu_g = \mu_R - \mu_S \qquad \textit{(Eq. 2-29)}$$

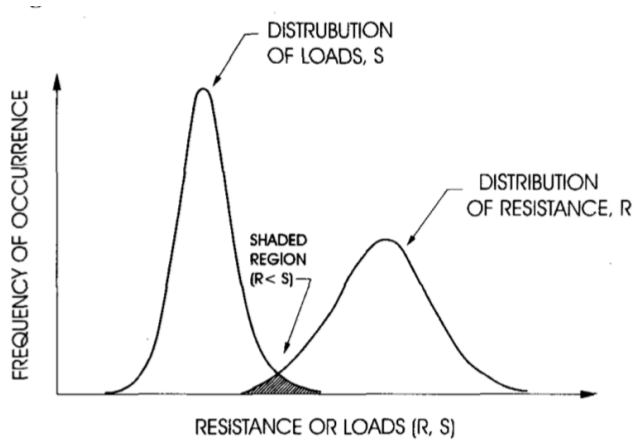

Figure 12. Basic reliability problem (Becker, 1996)

where μ_R is the mean of the resistance and μ_S is the mean of the demand. The variance of a linear function g is:

$$\sigma_g^2 = \nabla_g^T \boldsymbol{\Sigma}_{R,S} \nabla_g = \begin{pmatrix} 1 \\ -1 \end{pmatrix}^T \begin{pmatrix} \sigma_R^2 & 0 \\ 0 & \sigma_s^2 \end{pmatrix} \begin{pmatrix} 1 \\ -1 \end{pmatrix} = \sigma_R^2 + \sigma_S^2 \qquad \textit{(Eq. 2-30)}$$

As mentioned before, g has normal distribution. Therefore, the standardized form of the function g (*i.e.* $\frac{g-\mu_g}{\sigma_g}$) has standard normal distribution. Its cumulative distribution function CDF can be written as:

$$p_f = P(g \leq 0) = \phi\left(\frac{g - \mu_g}{\sigma_g}\right) \qquad \textit{(Eq. 2-31)}$$

Having $g = 0$ for the limit-state function, Eq. (2-31) can be re-written as:

$$p_f = \phi\left(\frac{-\mu_g}{\sigma_g}\right) = \phi(-\beta) \qquad \textit{(Eq. 2-32)}$$

The mean to standard deviation ratio is called reliability index β, which is the distance, in the form of number of standard deviations, from the mean. In the standard normal space, which is the suitable space for reliability analysis, the variables are normalized so that their mean value is zero and standard deviation is unit. This means that the mean in

standard normal space is always located at the origin. As a result, the distance between the origin and the limit-state function depicts β.

Figure 13 represents the concept of limit-state function in three dimensions. The joint probability distribution is depicted in grey and the limit-state function distinguishes the safe and unsafe areas. In Figure 13, it is assumed that the limit-state function is a function of two random variables X_1 and X_2. Therefore, the limit-state function can be depicted by a curve, located on the X_1-X_2 plane. The geometrical interpretation of β is also shown in Figure 13. The determination of the probability of failure requires solving the multiple integral of Eq. (2-28) and finding the cumulative probability of the failure region. However, this multivariate integration cannot be solved analytically most of the time. Reliability methods, which will be mentioned in the following sections, provide an approximation to this integral. It is worth mentioning that the problems with only one limit-state function are called "component reliability analysis" and problems with more than one limit-state function are called "system reliability analysis".

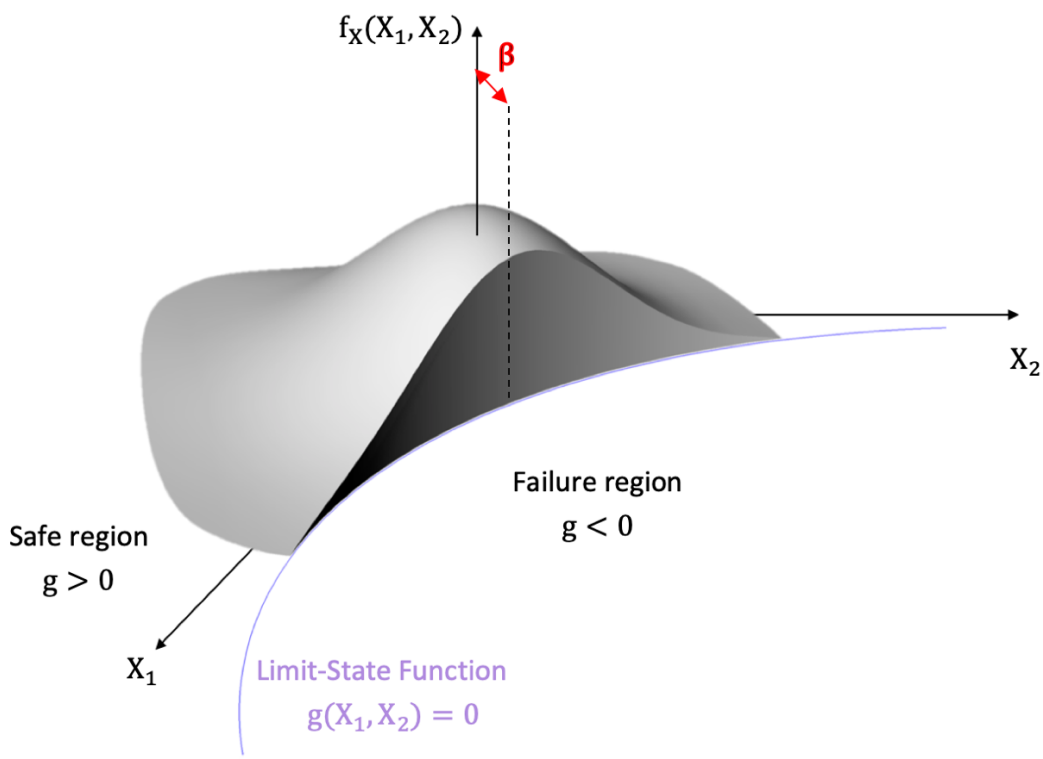

Figure 13. Geometrical representation of β and probability of failure in standard normal space

2.5.7 Tools for reliability analysis

2.5.7.1 Analysis of function

The ultimate goal of reliability analysis is to find the probability of failure based on a limit-state function, which is a function of random variables. In other words, a limit-state function is a dependent variable of a functional form of independent variable(s). Analysis of function is used in the cases where this functional form is known.

The data quality of random variables is not always the same. In some cases, only the second-moment information (*i.e.* mean, standard deviation and correlation coefficients) is available. There are other cases, in which we have better data quality, where the entire probability distribution of random variables is available. Analysis of function is used in both of these cases to provide statistical data about the dependent random variable.

Supposing that only the second-moment information of random variables is available, and the limit-state function is linear, we have:

$$\mathrm{y}_1 = \mathrm{h}(\mathbf{x}) = \mathrm{a} + \mathbf{b}^{\mathrm{T}}\mathbf{x} \qquad \textit{(Eq. 2-33)}$$

The mean of the function is then:

$$\mu_{\mathrm{y}_1} = \mathrm{E}[\mathrm{h}(\mathbf{x})] = \mathrm{E}[\mathrm{a} + \mathbf{b}^{\mathrm{T}}\mathbf{x}] = \mathrm{E}[\mathrm{a}] + \mathrm{E}[\mathbf{b}^{\mathrm{T}}\mathbf{x}] = \mathrm{a} + \mathbf{b}^{\mathrm{T}}\mathbf{m}_{\mathbf{x}} \qquad \textit{(Eq. 2-34)}$$

where $\mathbf{m}_{\mathbf{x}}$ is the vector of the means. Eq. (2-34) states that the mean of the linear function is achieved simply by plugging the mean of the random variables into the function. The variance is determined as:

$$\begin{aligned} \sigma_{\mathrm{Y}_1}^2 &= \mathrm{E}\left[\left(\mathrm{Y}_1 - \mu_{\mathrm{Y}_1}\right)^2\right] \\ &= \mathrm{E}\left[\left((\mathrm{a} + \mathbf{b}^{\mathrm{T}}\mathbf{x}) - (\mathrm{a} + \mathbf{b}^{\mathrm{T}}\mathbf{m}_{\mathbf{x}})\right)^2\right] \\ &= \mathrm{E}[(\mathbf{b}^{\mathrm{T}}\mathbf{x} - \mathbf{b}^{\mathrm{T}}\mathbf{m}_{\mathbf{x}})^2] \\ &= \mathbf{b}^{\mathrm{T}}\boldsymbol{\Sigma}_{\mathbf{xx}}\mathbf{b} \end{aligned} \qquad \textit{(Eq. 2-35)}$$

Considering another function $y_2 = c + \mathbf{d}^T\mathbf{x}$, the covariance between two linear functions is:

$$\mathrm{Cov}[y_1, y_2] = E\left[\left(y_1 - \mu_{Y_1}\right)\left(y_2 - \mu_{Y_2}\right)\right] = \mathbf{b}^T\boldsymbol{\Sigma}_{\mathbf{xx}}\mathbf{d} \qquad \textit{(Eq. 2-36)}$$

The calculations of second-moment information are extendable to non-linear functions. However, depending on the complexity of the function, analytical expressions may not be easily derived. Taylor's expansion can be utilized to approximate the function about the mean value, as:

$$y = h(\mathbf{x}) \approx \mathbf{h}(\mathbf{m_x}) + \nabla h(\mathbf{m_x})^T(\mathbf{x} - \mathbf{m_x}) \qquad \textit{(Eq. 2-37)}$$

in which, $\nabla h(\mathbf{m}_x)^T$ is the gradient vector of the function, evaluated at the mean. It follows that:

$$\begin{aligned} \mu_y &= h(\mathbf{m_x}) \\ \sigma_y^2 &= \nabla h(\mathbf{m_x})^T\boldsymbol{\Sigma}_{\mathbf{xx}}\nabla h(\mathbf{m_x}) \\ \mathrm{Cov}[y_1, y_2] &= \nabla h_1(\mathbf{m_x})^T\boldsymbol{\Sigma}_{\mathbf{xx}}\nabla h_2(\mathbf{m_x}) \end{aligned} \qquad \textit{(Eq. 2-38)}$$

Now, rather than knowing the second-moment data, when the whole probability distributions are given, we must determine the distribution of the function. Again, we assume that y is a function of x:

$$y = h(x) \qquad \textit{(Eq. 2-39)}$$

when considering h as a monotonically increasing function, the inverse of the function can be expressed as:

$$x = h^{-1}(y) \qquad \textit{(Eq. 2-40)}$$

The so-called "probability preserving equation" is then:

$$F_Y(y) = F_X(x) = F_X\left(h^{-1}(y)\right) \qquad \textit{(Eq. 2-41)}$$

The concept of "probability preserving equation" can be explained in term of the uncertainties. Since the function is monotonically increasing, for a specific outcome y, there is only one outcome of x. Therefore, they show the same uncertainty, and as a result, the same probability.

Knowing that probability distribution function PDF is the derivative of cumulative distribution function CDF with respect to the random variable:

$$f_Y(y) = \frac{dF_Y(y)}{dy} = \frac{dF_X(x)}{dy} = \frac{dF_X\left(h^{-1}(y)\right)}{dy} \qquad \textit{(Eq. 2-42)}$$

Using the chain rule, one has

$$f_Y(y) = \frac{dF_Y(y)}{dy} = \frac{dF_X(x)}{dy} = \frac{dx}{dy}\frac{dF_X(x)}{dx} = \frac{dx}{dy}f_X(x) \qquad \textit{(Eq. 2-43)}$$

In multi-variate cases, similar to the cases of having second-moment data, the analytical expression for y may not be always achievable. However, using probability preserving equation we have:

$$f_Y(y_1, y_2, \dots, y_n)dy_1 dy_2 \dots dy_n = f_X(x_1, x_2, \dots, x_n)dx_1 dx_2 \dots dx_n \qquad \textit{(Eq. 2-44)}$$

This can be re-written in the form of the Jacobian determinant as:

$$f_Y(y_1, y_2, \dots, y_n) = f_X(x_1, x_2, \dots, x_n)\left|\det\left(\mathbf{J}_{\mathbf{y},\mathbf{x}}\right)\right|^{-1} \qquad \textit{(Eq. 2-45)}$$

2.5.7.2 Probability transformation

As discussed previously, when the information of independent random variables is known as well as the functional form, the distribution or the second-moment information can be calculated using "analysis of function". There are also cases where the information of the dependent and independent random variables is given but the functional form is to be determined. For these cases, "probability transformation" is used.

In reliability analysis, it is mostly desired to first transform all the variables to standard normal space in which the calculations are performed. Standard normal space has some specific characteristics, *e.g.* rotational and radial symmetry, as well as exponential decay of the probability density function from the mean.

First, the transformation of a single random variable is performed. Since CDFs are given, by using probability preserving equation, we have

$$\begin{gathered} F_Y(y) = F_X(x) \\ x = F_X^{-1}\big(F_Y(y)\big) \end{gathered} \qquad \textit{(Eq. 2-46)}$$

Therefore,

$$x = F^{-1}\big(\phi(y)\big) \qquad \textit{(Eq. 2-47)}$$

Let's examine a linear function of random variables:

$$\mathbf{y} = \mathbf{a} + \mathbf{B}\mathbf{x} \qquad \textit{(Eq. 2-48)}$$

in which the vector $\mathbf{a}$ and the square matrix $\mathbf{B}$ are unknowns. Considering the zero mean and unit standard deviation for standard normal space, the "analysis of function" yields

$$\begin{cases} \mathbf{m_y} = \mathbf{a} + \mathbf{B}\mathbf{m_x} = \mathbf{0} \\ \mathbf{\Sigma_{yy}} = \mathbf{B}\mathbf{\Sigma_{xx}}\mathbf{B}^{\mathrm{T}} = \mathbf{I} \end{cases} \qquad \textit{(Eq. 2-49)}$$

Multiplying the second equation by $\mathbf{B}^{-1}$ from left and $(\mathbf{B}^{-1})^{\mathrm{T}}$ from right leads to following expression:

$$\mathbf{\Sigma_{xx}} = \mathbf{B}^{-1}(\mathbf{B}^{-1})^{\mathrm{T}} \qquad \textit{(Eq. 2-50)}$$

Therefore, the unknown matrix $\mathbf{B}^{-1}$ decomposes $\mathbf{\Sigma_{xx}}$ into a matrix multiplied by its transpose. This mathematical procedure is known as Cholesky decomposition, which can be alternatively expressed as:

$$\mathbf{\Sigma_{xx}} = \widetilde{\mathbf{L}}\widetilde{\mathbf{L}}^{\mathrm{T}} \qquad \textit{(Eq. 2-51)}$$

where $\widetilde{\mathbf{L}}$ represents the lower-triangular Cholesky decomposition of the covariance matrix, with

$$\mathbf{B} = \widetilde{\mathbf{L}}^{-1} \qquad \textit{(Eq. 2-52)}$$

Therefore, according to Eq. (2-49), $\mathbf{a}$ is determined as:

$$\mathbf{a} + \widetilde{\mathbf{L}}^{-1}\mathbf{m_x} = \mathbf{0} \rightarrow \mathbf{a} = -\widetilde{\mathbf{L}}^{-1}\mathbf{m_x} \qquad \textit{(Eq. 2-53)}$$

Now, by knowing $\mathbf{a}$ and $\mathbf{B}$**,** the functional form of $\mathbf{y}$ is explicitly expressed as:

$$\mathbf{y} = -\widetilde{\mathbf{L}}^{-1}\mathbf{m_x} + \widetilde{\mathbf{L}}^{-1}\mathbf{x} \qquad \textit{(Eq. 2-54)}$$

It would be easier to perform the Cholesky decomposition on the dimensionless correlation matrix rather than the covariance matrix:

$$\mathbf{\Sigma_{xx}} = \mathbf{D}_{\mathrm{x}}\mathbf{R}_{\mathrm{xx}}\mathbf{D}_{\mathrm{x}} = \mathbf{D}_{\mathrm{x}}\mathbf{L}\mathbf{L}^{\mathrm{T}}\mathbf{D}_{\mathrm{x}} \qquad \textit{(Eq. 2-55)}$$

where $\mathbf{D}_{\mathrm{X}}$ is the diagonal matrix with standard deviations on its main diagonal. The lower-triangular matrix is shown here with $\mathbf{L}$. As a result, the functional form of $\mathbf{y}$ becomes:

$$\mathbf{y} = \mathbf{L}^{-1}\mathbf{D}_{\mathbf{x}}^{-1}(\mathbf{x} - \mathbf{m_x}) \Leftrightarrow \mathbf{x} = \mathbf{m_x} + \mathbf{L}\mathbf{D_x}\mathbf{y} \qquad \textit{(Eq. 2-56)}$$

Previous calculations are extendable to the cases where the whole probability distribution of random variables is known.

We further assume that the variables are uncorrelated; *i.e.*, the joint probability distribution is equal to the product of the marginal probability distributions. For the ith random variable, the probability preserving equation is applicable for each random variable at a time; *i.e.,*

$$\mathrm{F_i}(\mathrm{x_i}) = \phi(\mathrm{y_i}) \Leftrightarrow \mathrm{y_i} = \phi^{-1}(\mathrm{F_i}(\mathrm{x_i})) \Leftrightarrow \mathrm{x_i} = \mathrm{F_i}^{-1}(\phi(\mathrm{y_i})) \qquad \textit{(Eq. 2-57)}$$

The Jacobian matrix for the above transformation is the derivation of the $\mathrm{F_i}$ with respect to $\mathrm{x_i}$, which is the ith random variable:

$$\frac{\partial}{\partial x_i}\left(F_i(x_i) = \phi(y_i)\right) \rightarrow f_i(x_i) = \frac{\partial}{\partial x_i}\phi(y_i) = \frac{\partial y_i}{\partial x_i}\frac{\partial}{\partial y_i}\phi(y_i) = \frac{\partial y_i}{\partial x_i}\varphi(y_i) \qquad \textit{(Eq. 2-58)}$$

A number of probabilistic methods requires both limit-state functions and their gradient. The Jacobian matrix is therefore defined as:

$$\frac{\partial y_i}{\partial x_i} = \frac{f_i(x_i)}{\varphi(y_i)} \qquad \textit{(Eq. 2-59)}$$

So far, we have seen the transformation of random variables with arbitrary distribution into random variables with zero mean and unit standard deviation, regardless of their correlations. If independent random variables, x_i, are correlated, the corresponding transformed variables, z_i, are also correlated.

$$z_i = \phi^{-1}(F_i(x_i)) \qquad \textit{(Eq. 2-60)}$$

To facilitate problem solving, Nataf (1962) assumed that variables are jointly normal. Under this assumption, Liu and Der Kiureghian (1986) gave the following relation between the correlation coefficient ρ_{x_i,x_j} and ρ_{z_i,z_j}:

$$\rho_{x_i,x_j} = \int_{-\infty}^{+\infty}\int_{-\infty}^{+\infty}\left(\frac{x_i - \mu_i}{\sigma_i}\right)\left(\frac{x_j - \mu_j}{\sigma_j}\right)\varphi_2(z_i, z_j, \rho_{z_i,z_j,}) \qquad \textit{(Eq. 2-61)}$$

where

$$x_i = F_i^{-1}(\phi(z_i))$$
$$x_j = F_j^{-1}(\phi(z_j))$$

with φ_2 being the bivariate standard normal distribution function:

$$\varphi_2\left(z_i, z_j, \rho_{z_i,z_j}\right) = \frac{1}{2\pi\sqrt{1-\rho_{x_i,x_j}^2}}\exp\left(-\frac{z_i^2 + z_j^2 - 2\rho_{z_i,z_j}z_iz_j}{2\left(1-\rho_{z_i,z_j}^2\right)}\right) \qquad \textit{(Eq. 2-62)}$$

The Nataf's joint distribution model is valid under the conditions that the CDF are strictly increasing and the correlation matrix of $\mathbf{x}$ and $\mathbf{z}$ are positive definite. The difficulty with solving Eq. (2-62) is that it has to be solved for each pair of random variables.

Up to this point, we have transformed the random variables $\mathbf{x}$ into random variables $\mathbf{z}$, which have zero mean and unit standard deviation, however, they are still correlated. At the end, we can transform these correlated random variables, z_i, to the desired uncorrelated random variables y_i, as

$$\mathbf{y} = \mathbf{B}\mathbf{z}$$
$$\boldsymbol{\Sigma}_{\mathbf{yy}} = \mathbf{B}\boldsymbol{\Sigma}_{\mathbf{zz}}\mathbf{B}^{\mathrm{T}} = \mathbf{I} \quad \rightarrow \quad \boldsymbol{\Sigma}_{\mathbf{zz}} = \mathbf{B}^{-1}(\mathbf{B}^{-1})^{\mathrm{T}} \qquad \textit{(Eq. 2-63)}$$

The covariance matrix can be written in the form of correlation matrix:

$$\boldsymbol{\Sigma}_{\mathbf{zz}} = \mathbf{D}_{\mathbf{z}}\mathbf{R}_{\mathbf{zz}}\mathbf{D}_{\mathbf{z}} \qquad \textit{(Eq. 2-64)}$$

Recalling $\mathbf{D}_{\mathbf{z}} = \mathbf{I}$, the correlation matrix and correlation matrix are the same:

$$\boldsymbol{\Sigma}_{\mathbf{zz}} = \mathbf{R}_{\mathbf{zz}} \qquad \textit{(Eq. 2-65)}$$

follows that

$$\rightarrow \mathbf{R}_{\mathbf{zz}} = \mathbf{B}^{-1}(\mathbf{B}^{-1})^{\mathrm{T}}$$
$$\rightarrow \mathbf{B} = \mathbf{L}^{-1}$$
$$\rightarrow \mathbf{y} = \mathbf{L}^{-1}\mathbf{z} \qquad \textit{(Eq. 2-66)}$$

The Jacobian matrix of Nataf transformation is finally given as

$$\mathbf{J}_{\mathbf{y},\mathbf{x}} = \frac{\partial \mathbf{y}}{\partial \mathbf{x}} = \frac{\partial \mathbf{y}}{\partial \mathbf{z}}\frac{\partial \mathbf{z}}{\partial \mathbf{x}} = \mathbf{L}^{-1}\left[\frac{f_i(x_i)}{\varphi(z_i)}\right] = \mathbf{L}^{-1}[\frac{f_i(x_i)}{\varphi(y_i)}] \qquad \textit{(Eq. 2-67)}$$

2.5.8 Reliability methods

2.5.8.1 First order second moment – FOSM

Analysis of function and probability transformation are two main tools used in various reliability methods. The first method to mention here is “first-order, second-moment”, which is abbreviated as “FOSM”. It is also called “mean-value, first-order, second-moment” or “MVFOSM”. “First-order second-moment” method is called “second-

moment" since in this case, the only available data about the random variable is the second-moment data (mean, standard deviation and correlation coefficients). This method only uses μ_g and σ_g to evaluate the reliability index, which is the ratio between mean and standard deviation of the limit-state function.
Let us examine a general linear limit-state function with following form:

$$g(\mathbf{x}) = a + \mathbf{b}^T\mathbf{x} \qquad \textit{(Eq. 2-68)}$$

To standardize the variables, $\mathbf{x}$ is substituted by $\mathbf{m_x} + \mathbf{LD_xy}$ as discussed in section 2.5.7.2, which leads to:

$$G(\mathbf{y}) = a + \mathbf{b}^T\mathbf{m}_x + \mathbf{b}^T\mathbf{D_xLy} \qquad \textit{(Eq. 2-69)}$$

or

$$G(\mathbf{y}) = c + \mathbf{d}^T\mathbf{y} \qquad \textit{(Eq. 2-70)}$$

in which $c = a + \mathbf{b}^T\mathbf{m_x}$ and $\mathbf{d}^T = \mathbf{b}^T\mathbf{D_xLy}$.

The reliability index β is then:

$$\beta = \frac{\mu_G}{\sigma_G} = \frac{c}{\sqrt{\mathbf{d}^T\mathbf{Id}}} = \frac{c}{\|\mathbf{d}\|} \qquad \textit{(Eq. 2-71)}$$

This method yields the reliability index, but it does not provide the failure probability except for the cases where the limit-state function is linear, and the random variables are normally distributed. For this special case, the failure probability is determined as:

$$p_f = P(G \leq 0) = \phi\left(\frac{0 - \mu_G}{\sigma_G}\right) = \phi(-\beta) \qquad \textit{(Eq. 2-72)}$$

For linear limit-state functions, both the values of mean and standard deviations and the reliability index are exact. In the case of non-linear limit-state functions, the first order approximation is evaluated at mean. This approximation is the cause of one of the main drawbacks of FOSM, known as "invariance problem". In this problem, two mathematically equivalent limit-state surfaces generate different results. This is because although these two functions share the same plane (or hyperplane) at the intersection,

they behave differently outside that intersection and lead to different results when the approximation is performed about each function's mean. One remedy to this problem is to perform the first order approximation at the limit-state which is shared between these two functions rather than the to do it at the mean. This is known as "first-order reliability analysis" or "FORM" which will be discussed next. Other pitfalls of FOSM include inaccuracies of linearly approximating a non-linear function and dismissing the probability distribution information.

2.5.8.2 First order reliability method – FORM

FORM analysis tackles the invariance problem and considers the distribution-type information with a higher computational cost and the possibility of non-convergence. This method still performs a first order approximation.

As mentioned previously, FORM approximates a function at a point on the limit-state surface rather than about the function's mean. This point is called the "design point" and its characteristic is actually encapsulated in the standard normal space. The joint PDF of an uncorrelated standard normal random variable is

$$\varphi(\mathbf{y}) = \frac{1}{\sqrt{(2\pi)^{n}}} \exp\left(-\frac{1}{2}\mathbf{y}^{T}\mathbf{y}\right) \qquad \textit{(Eq. 2-73)}$$

in which n is the number of random variables. It follows the probability density outside of a plane (hyperplane)

$$p_f = \phi(-\beta) \qquad \textit{(Eq. 2-74)}$$

As it has been mentioned, a PDF in standard normal space has rotational symmetry and decays in tangential and radial directions (see Figure 13). As a result, the closest point on the limit-state function to the origin is the point with highest probability density. The limit-state function is denoted by $g(\mathbf{x})$ in the original space, and by $G(\mathbf{y})$ in standard normal space (Haukaas, 2018):

$$G(\mathbf{y}) \approx G(\mathbf{y}^{*}) + \nabla G(\mathbf{y}^{*})^{T}(\mathbf{y} - \mathbf{y}^{*}) \qquad \textit{(Eq. 2-75)}$$

in which, $\mathrm{G}(\mathbf{y}^*)$ is zero since the design point is located on the limit-state function. In FORM analysis, it is typical to introduce a unit vector defined as

$$\boldsymbol{\alpha} = -\frac{\nabla \mathrm{G}(\mathbf{y})}{\|\nabla \mathrm{G}(\mathbf{y})\|} \qquad \textit{(Eq. 2-76)}$$

Substituting Eq. (2-76) into Eq. (2-75), we have:

$$\mathrm{G} \approx -\|\nabla \mathrm{G}(\mathbf{y}^*)\|\boldsymbol{\alpha}^{\mathrm{T}}(\mathbf{y} - \mathbf{y}^*) = -\|\nabla \mathrm{G}(\mathbf{y}^*)\|(\boldsymbol{\alpha}^{\mathrm{T}}\mathbf{y} - \boldsymbol{\alpha}^{\mathrm{T}}\mathbf{y}^*) \qquad \textit{(Eq. 2-77)}$$

Since $\boldsymbol{\alpha}$ is a unit vector, $\boldsymbol{\alpha}^{\mathrm{T}}\mathbf{y}^*$ equals to the length of $\mathbf{y}^*$, which is the distance from the origin to the design point, known as β, therefore

$$\mathrm{G} \approx \|\nabla \mathrm{G}(\mathbf{y}^*)\|(\beta - \boldsymbol{\alpha}^{\mathrm{T}}\mathbf{y}) \qquad \textit{(Eq. 2-78)}$$

Consequently, the FORM problem can be re-written in the form of an optimization problem:

$$\mathbf{y}^* = \mathrm{argmin}\{\|\mathbf{y}\| \mid \mathrm{G}(\mathbf{y}) = 0\} \qquad \textit{(Eq. 2-79)}$$

where argmin denotes the argument of the minimum of the function G.

Convergence criteria

The following recursive formulation can be used to find the design point, $\mathbf{y}^*$:

$$\mathbf{y}_{\mathrm{m}+1} = \mathbf{y}_{\mathrm{m}} + \mathrm{s}_{\mathrm{m}}\mathbf{d}_{\mathrm{m}} \qquad \textit{(Eq. 2-80)}$$

in which, s_{m} is the step size and $\mathbf{d}_{\mathrm{m}}$ is the step direction. The search starts at the origin and stops when convergency criteria are satisfied. The first criterion is that the trial point, y_{m}, must be close to the limit-state surface, such that:

$$\left|\frac{\mathrm{G}(\mathbf{y}_{\mathrm{m}})}{\mathrm{G}_0}\right| \leq \mathrm{e}_1 \qquad \textit{(Eq. 2-81)}$$

where G_0 is a scaling factor which is typically selected as the value of starting point of the search *e.g.* origin of the standard normal space and e_1 is usually selected around 0.001. The second criterion assures that the design point is the closest point to the origin. In other words, the gradient of the limit-state function must be parallel to the position vector of the design point (see Figure 14). This means:

$$\|\mathbf{y}_m - (\boldsymbol{\alpha}_m^T \mathbf{y}_m)\boldsymbol{\alpha}_m\| \leq e_2 \qquad \textit{(Eq. 2-82)}$$

in which, e_2 is usually selected around 0.001.

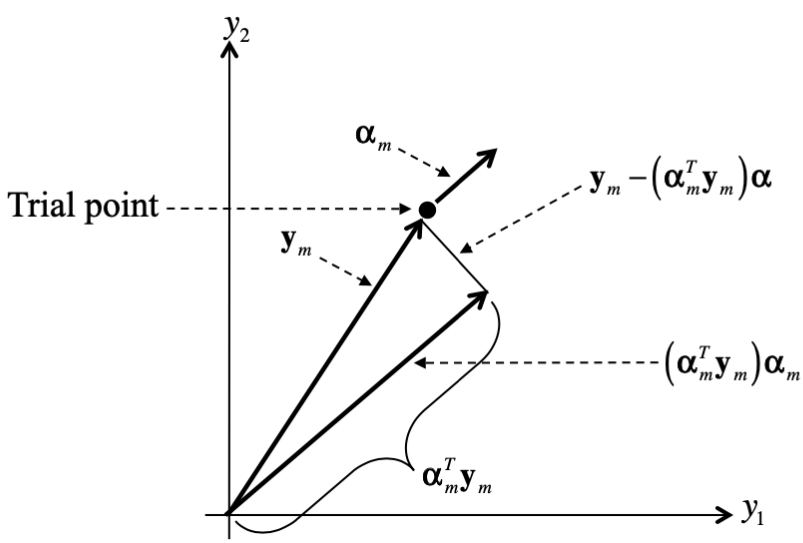

Figure 14. Second convergence criterion for FORM (after Haukaas, 2018)

iHLRF algorithm

The history of research in developing an algorithm to find the design point $\mathbf{y}^*$, goes back to 1970 (Hasofer and Lind, 1974; Rackwitz and Fiessler, 1978). Zhang and Der Kiureghian (1997) developed the following recursive algorithm to find $\mathbf{y}^*$.

Let us consider the case of a non-linear function of two random variables $G(X_1, X_2)$, which is a surface in the standard normal space, with its intersection with X_1-X_2 plane being a non-linear limit-state function, $G(X_1, X_2) = 0$. The surface $G(X_1, X_2)$ can be approximated by a plane at a trial point $\mathbf{y}_m$:

$$G(\mathbf{y}) \approx G(\mathbf{y_m}) + \nabla G(\mathbf{y_m})^T(\mathbf{y} - \mathbf{y_m}) \qquad \textit{(Eq. 2-83)}$$

The intersection of the approximated plane with X_1-X_2 plane generates a linear limit-state function on X_1-X_2 plane such that:

$$G(\mathbf{y_m}) + \nabla G(\mathbf{y_m})^T(\mathbf{y} - \mathbf{y_m}) = 0 \qquad \textit{(Eq. 2-84)}$$

From geometry, the distance from the origin to the closest point on the limit-state function is equal to the function value at the origin divided by the norm of the gradient vector; *i.e.*,

$$\Delta = \frac{G(\mathbf{0})}{\|\nabla G(\mathbf{y}_m)\|} = \frac{G(\mathbf{y}_m) - \nabla G(\mathbf{y}_m)^T y_m}{\|\nabla G(\mathbf{y}_m)\|} = \frac{G(\mathbf{y}_m)}{\|\nabla G(\mathbf{y}_m)\|} + \boldsymbol{\alpha}^T \mathbf{y}_m \qquad \textit{(Eq. 2-85)}$$

By multiplying Δ by alpha vector, the starting point for the next iteration is achieved:

$$\mathbf{y}_{m+1} = -\Delta \frac{\nabla G(\mathbf{y}_m)}{\|\nabla G(\mathbf{y}_m)\|} = \Delta . \boldsymbol{\alpha} \qquad \textit{(Eq. 2-86)}$$

This recursive procedure continues until all convergence criteria are satisfied.

Importance vector

One of the most remarkable outcomes of reliability analysis is the importance vector, which makes it possible to rank the random variables based on their importance. This has outmost importance, especially in multi-model reliability analysis when the influence of one major player may be overlooked due to the complexity of the system. This also provides an idea about the sensitivity of the results with respect to different parameters. It can be shown that the unit vector $\boldsymbol{\alpha}$**,** defined in Eq. (2-76), can be used as importance measure for a linearized limit-state function G.
Recalling Eq. (2-83), the variance of $G(\mathbf{y})$ is:

$$\mathrm{Var}[G(\mathbf{y})] = \nabla G^T \nabla G \qquad \textit{(Eq. 2-87)}$$

Substituting Eq. (2-76) in Eq. (2-87), we have:

$$\mathrm{Var}[\mathrm{G}(\mathbf{y})] = \nabla\mathrm{G}^{\mathrm{T}}\nabla\mathrm{G} = (-\|\nabla\mathrm{G}\|.\boldsymbol{\alpha})^{\mathrm{T}}(-\|\nabla\mathrm{G}\|.\boldsymbol{\alpha}) = \|\nabla\mathrm{G}\|^2(\alpha_1^2 + \cdots + \alpha_{\mathrm{n}}^2) \qquad \textit{(Eq. 2-88)}$$

in which n is the number of random variables. Eq. (2-88) shows the direct contributions of the components of alpha vector to the total variance. The higher the absolute value of the random variable α_i, the more important random variable $\mathrm{y_i}$. If α_{i} is positive, the random variable $\mathrm{y_i}$ acts as a load. Otherwise, the random variable acts as a resistance.

2.5.8.3 Second order reliability method – SORM

SORM is similar to FORM, except that the approximation is extended to a second-order expansion that provides better accuracy but requires more computational efforts.

2.5.8.4 Sampling methods

As another group of reliability methods, sampling methods evaluate the limit-state function many times and then approximates the value of the failure probability. Two common sampling methods are mean-centred Monte Carlo and adaptive sampling. Another appealing method is importance sampling. It provides accurate and robust estimate of the failure probability with fewer samples which considerably reduces the processing time and computational cost.

2.6 Developing flowcharts

A flowchart is a visual tool utilized to exhibit the sequence of actions from start to end. It is commonly used in algorithm development in many fields of engineering and management. It is advantageous to also concisely introduce the typical signs used in a flowchart to better interpret the procedure. These signs are provided in Table 3.

2.7 Necessity of a more rigorous risk management framework

Different RM frameworks have been introduced in this chapter. Each of them has its own strength; however, they all addressed ground risk in a general way using general guidelines. In addition, different types of uncertainties (*e.g.* soil's spatial uncertainties, uncertainties regarding soil's engineering properties, *etc.*) and their importance has

Sign	Description	Sign	Description
	Start/End: indicates the start or termination of work flow.		**Data:** any type of input/output data
	Process: indicates a specific function is being done in this step		**Sub-rutine:** indicates a predefined process
	Decision: indicates a condition between two or more paths		**Document:** representation of a document, report, *etc*.

Table 3. Flowchart indicators

been mentioned in this chapter which requires exclusive attention to be managed. Therefore, a more specialized framework is required to address and quantify the associated risk of settlement induced by tunnelling. That framework should incorporate different levels of uncertainty by providing different strategies to deal with them.

To develop such a framework, many different disciplines and principles must be met with their objectives satisfied. This is the reason why risk management is a multi-disciplinary act. It is a tool that should be delicately fitted into the destination field and carefully carried out.

RM is a multi-façade and multi-level activity. Risk, as a lack of certainty, can be addressed on the probability of the collapse of a tunnel's lining, which is considered as a large-scale problem with catastrophic consequences, to the probability of malfunctioning of the grout pump. The level of these two hazards are not the same; as well as their consequences. The uncertainties that are intrinsic parts of our knowledge about geomaterial are present at different levels, *e.g.* in parameters, in models and in our construction. These uncertainties also propagate due to the interconnections and analysis sequence. With the virtue of reliability analysis, we are able to direct these uncertainties. It has to be noted that it is a proper strategy to divide the problem into more detailed subsections and define different classes of evaluation to properly tackle the uncertainties in each scale with a proper approach.

Another point to mention here is that RM is a dynamic, goal-oriented activity. Although the ultimate target of the RM is to manage the associated risks and sort them based on their importance, it is also significant to realize which specific risk is our priority. Therefore, it is absolutely essential to first introduce the problem and risk causes.

RM for metro tunnels may be seen as a hub, linking different engineering disciplines from geotechnical engineering, geology and hydrogeology to urban planning, management, finance and law (see, Figure 15). In this research, a new framework is proposed to deal with risk in metro lines based on different levels of available data. The details of each part of the framework and their corresponding classes are thoroughly discussed in the following chapter. It should be noted, however, that the current research will only address the risk from geotechnical engineering and geoscience point of view. It will blend the geotechnical engineering concept with concept of reliability to facilitate and promote the act of correct decision-making. This is the core concept of the so called "risk-based" decision making.

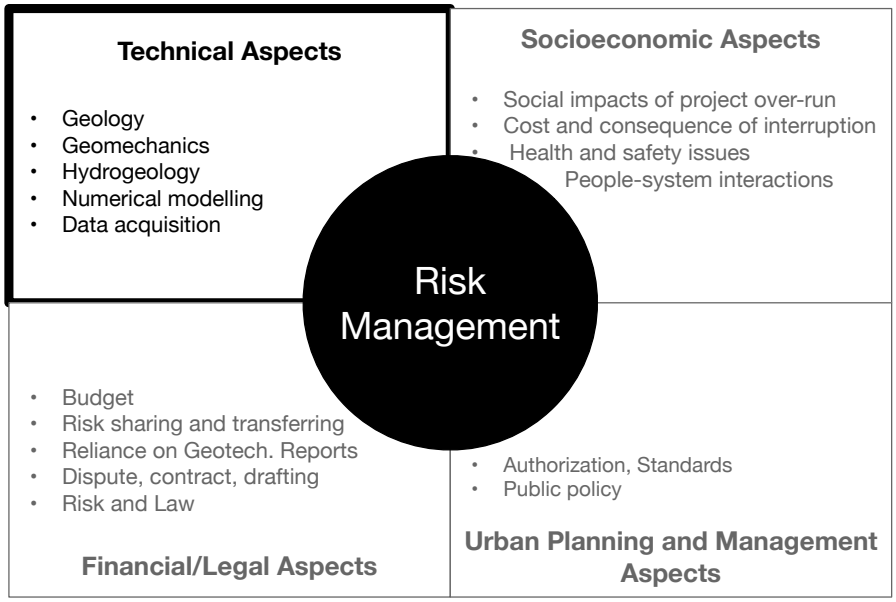

Figure 15. Risk management; A multi-disciplinary act

Chapter 3. Methodology and analysis

3.1 Statement of the problem and the general framework

One of the major concerns of tunnelling in populated, urbanized areas is the risk of ground loss, settlement and damage to the surface buildings. This problem is even more critical when the tunnel is passing under historical, preserved buildings or monuments which are highly sensitive to differential settlements. This chapter focuses on the identification of hazards with their causes associated with tunnel constructed by shield TBM.

The purpose of this study is to provide a more rigorous RM framework to be used in underground projects with the main focus of addressing and quantifying the risk related to tunnel-induced surface settlement, particularly for metro tunnels under urban areas in soft clays. This framework may be used as a guidance for similar projects and for the development of software, based on the proposed procedure to perform risk and reliability analyses as well as the decision-making process.

A number of frameworks has been developed to evaluate the risk of settlement in soft clay (*e.g.* Leca and New, 2007; Huang *et al.*, 2015; Qian *et al.* 2016). These frameworks mainly addressed the risk in a general qualitative way and did not provide step-by-step strategies to quantify the tunnelling risk, especially the ground surface settlement risk. The proposed framework in this research is able to quantify the tunnel-induced settlement risk, both in short term and long term, for surface structures. The proposed framework considers multi-level uncertainties encountered in different phases of the project (*e.g.* uncertainties regarding soil's engineering properties, soil's spatial variability, *etc.*). The proposed framework addresses three main concerns regarding the risk of tunnelling-induced settlement: the causes of settlement, the likelihood of the settlement and the possible consequences. Risk identification is performed to identify the main hazards. Risk analysis is performed, by means of the analyses of fault tree, event tree and consequence tree, in order to estimate the likelihood of the ground subsidence. Risk evaluation is conducted to evaluate the risk of exceeding a predefined settlement threshold, for buildings with shallow and deep foundations, using reliability analysis. The detrimental effect of the settlement on the surface buildings is related to the vulnerability of a building and the distance of the building from the tunnel (an indicator of exposure). Therefore, it is beneficial to classify the building and to establish

a building database, as well as different risk evaluation classes, to estimate the risk of the surface settlement for different building classes (see Figure 16).

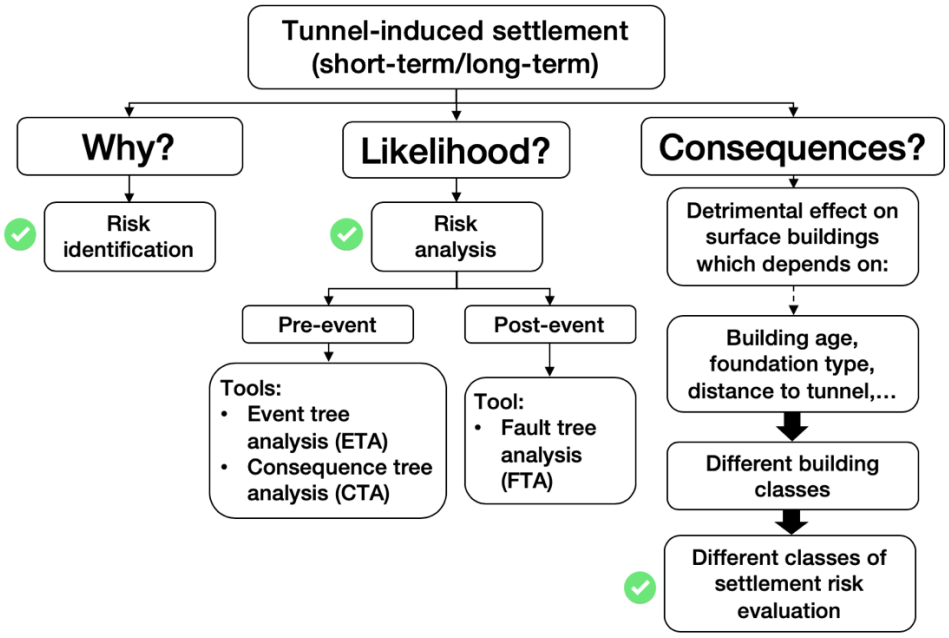

Figure 16. The proposed risk management capabilities

The proposed framework is aligned with ISO 31000 (ISO, 2009), containing risk identification, risk analysis and risk evaluation as parts of risk assessment. The core of this process is the development and continuous updating of building (structure) database, as well as framing a risk register as the outcome of the whole act, which is vital for proper risk communication. The general procedure is shown in Figure 17.

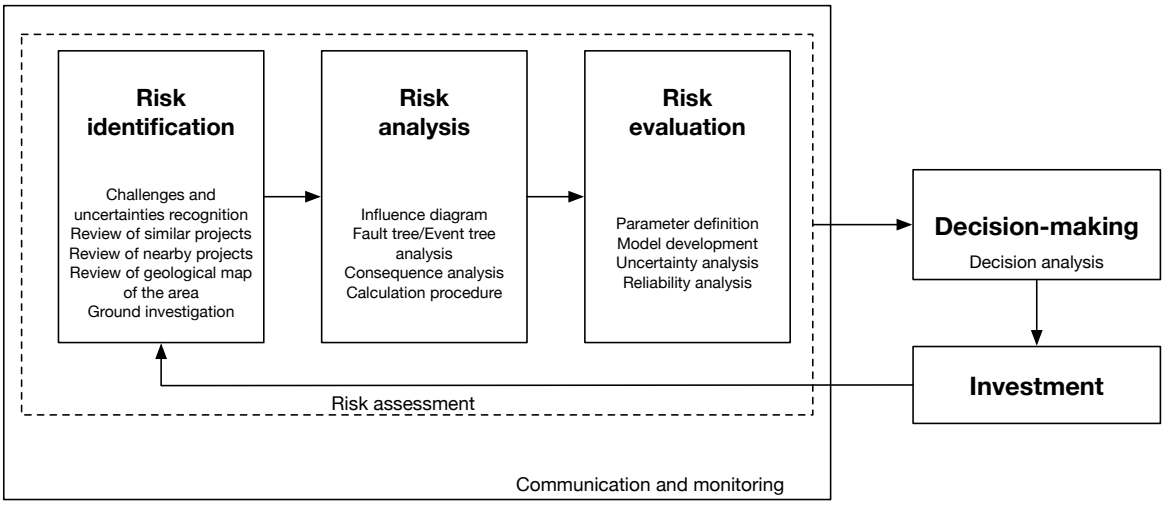

Figure 17. General risk management procedure for tunnelling

The framework consists of two main parts: short-term RM and long-term RM. The short-term RM addresses various risks associated with mechanized tunnelling in soft clay during the design and construction stage of the tunnel, while the long-term RM tackles the associated risks after completion of the construction project.

3.2 Risk management framework during construction (short-term)

3.2.1 Risk identification

During tunnel construction, one of the main concerns of the contractor is how to control ground movement to minimize the potential damage to ground buildings. Ground loss is the main character controlling the risk of surface and subsurface settlements as well as damage to the buildings during the construction of the tunnel. Many studies discussed the causes of ground movement induced by tunnel excavation, *e.g.* Mair and Taylor (1997), Leca and New (2007) and Loganathan (2011). The settlement induced by shield tunnelling mainly occurs ahead of the face, along the shield, and at the shield tail (see Figure 18). Deformation of tunnel lining may also induce ground settlement.

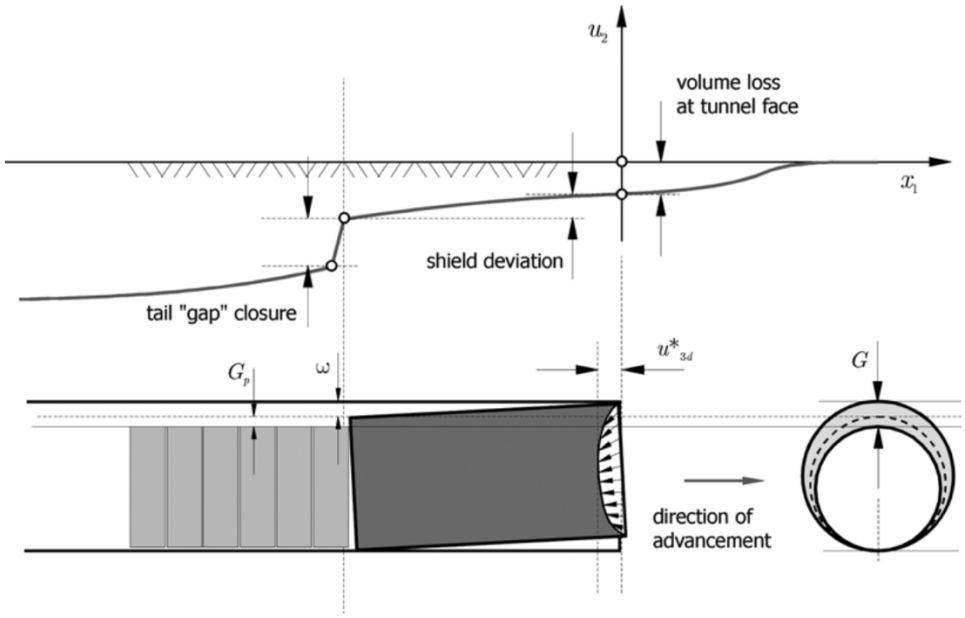

Figure 18. Sources of ground movement in shield tunnelling (after Tamagnini et al., 2005)

Settlement above and ahead of the face

This settlement is due to the ground movement ahead of the face as well as the ground displacement above the shield toward the face. The face support from the TBM and ground and groundwater conditions have remarkable effects on the magnitude of the displacement.

Settlement along the shield

The ground settlement along the body of the shield is generally small. Nevertheless, there are situations when a noticeable settlement is possible due to the following reasons:

1. Over-excavation around the shield: in the process of tunnel construction using TBM, slight over-excavation facilitates the movement of the shield by reducing earth resistance on the shield induced by shield-soil interaction. Some modern TBMs have tapered shield with slightly smaller radius at tail. Some TBMs have tapered shield and overcutting bead simultaneously.
2. In some situations, there are inevitable deviations from the designed advancing line due to unforeseen challenges and difficulties. This is often observed for boring at curves where the dimension and rigidity of the shields leads to an overcutting, as depicted in Figure 19, particularly at curves of small radius.

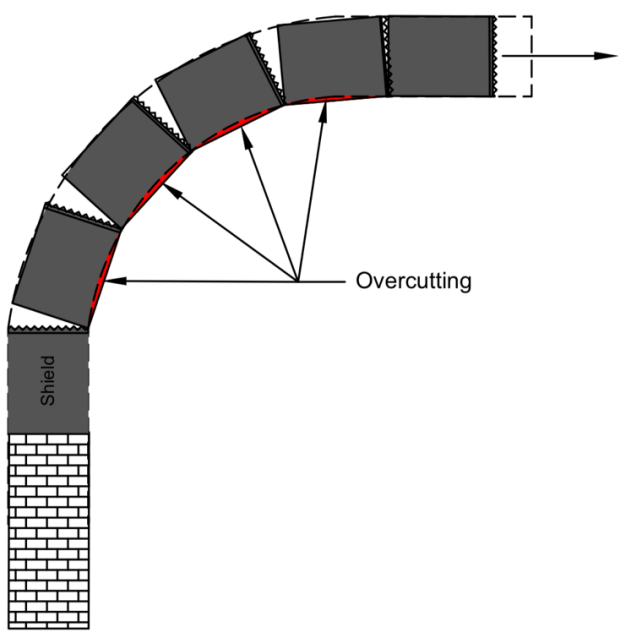

Figure 19. Overcutting at curve

Settlement at the shield tail

The gap develops at the end of the shield between the shield and soil. This gap is usually termed as "tail loss". Owing to the uneven outer diameters of shield and lining, the soil tends to move to fill this void if there is insufficient support expansion, failure or delay to grout or combination of these factors.

Grouting is a powerful tool to control shield and tail ground losses. However, for tunnelling in soft grounds, due to low strength and high deformability of the soil, grouting must be performed in a timely manner. After completion of grouting, deterioration and shrinkage of the grout may reduce the effectiveness of the grout over time. Experiments show that 7 to 10 percent reduction of thickness in cement-soil mix (Ingles, 1972), while a shrinkage of 7 to 8 percent is typical for cement paste with a water/cement ratio of 0.4 (Lagerbald *et al.*, 2010). In addition to effect of the volume shrinkage of grout, the long-term effect of grouting is primarily induced by dissipation of excess pore water pressure induced by grouting. In particular, the grouting process induces excess pore water pressure in soil around the grouted areas. This excess pore water pressure dissipates with long time, which may lead to differential settlement. This effect is more severe in locations where a large amount of grouting is performed, *e.g.* at curves.

Settlement caused by lining deformation

The liners are subject to longitudinal forces, exerted by shield's hydraulic jacks and radial forces from ground soil around the tunnel. These forces cause deformation of the liner, which further results in a variation of stresses in the soil and eventually ground settlement. Similar to tail loss, grouting is the primary and most effective measure to control the ground settlement due to lining deformation. Lining deformation is less critical during construction. However, it is remarkably critical during operation phase and plays a key role in term of the long-term behaviour of the tunnel.

Other potential risks

Seasonal fluctuations of the groundwater level can change effective stresses in the soil and affect soil properties. However, it is generally assumed that there is no great fluctuation during construction. In other words, the effect of the groundwater fluctuation is only considered for long-term analysis (see Figure 20).

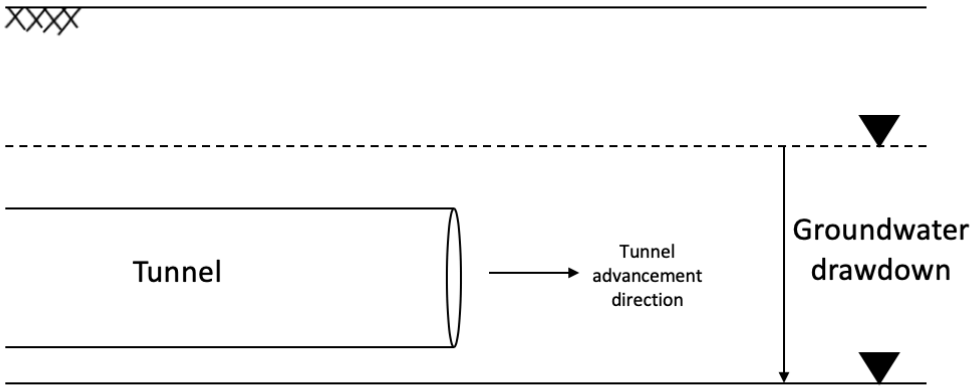

Figure 20. Groundwater drawdown

3.2.2 Risk analysis

In risk analysis, we identify all the hazards and their causes. Failing to capture any specific hazard will lead to complete negligence of it in future steps.

3.2.2.1 Fault tree analysis: short-term

Identification of risk sources

With the aid of fault tree analysis, the causes of the ground surface settlement during construction can be graphically shown. In addition to provide an overall picture about the influential active risk agents during construction, fault tree analysis also provides the mathematical tool to calculate the probability of ground subsidence.

Figure 21 shows the fault tree analysis for the short-term settlement of a straight tunnel section. As mentioned in the previous parts, ground subsidence is mainly because of the volume loss that occurs at the face along the shield and at the tail. The settlement induced by lining deformation is mainly a long-term problem, which will be addressed in the designated analysis.

Face loss is primarily due to failing in the provision of adequate face support. Settlement occurs if the cutter wheel does not provide sufficient support to the face. On the other hand, excessive thrust from the cutter wheel may result in negative face loss, which can lead to heave on the ground surface. This is more critical in the case of pile foundations which will be discussed later in the risk evaluation part. Variation of the geological

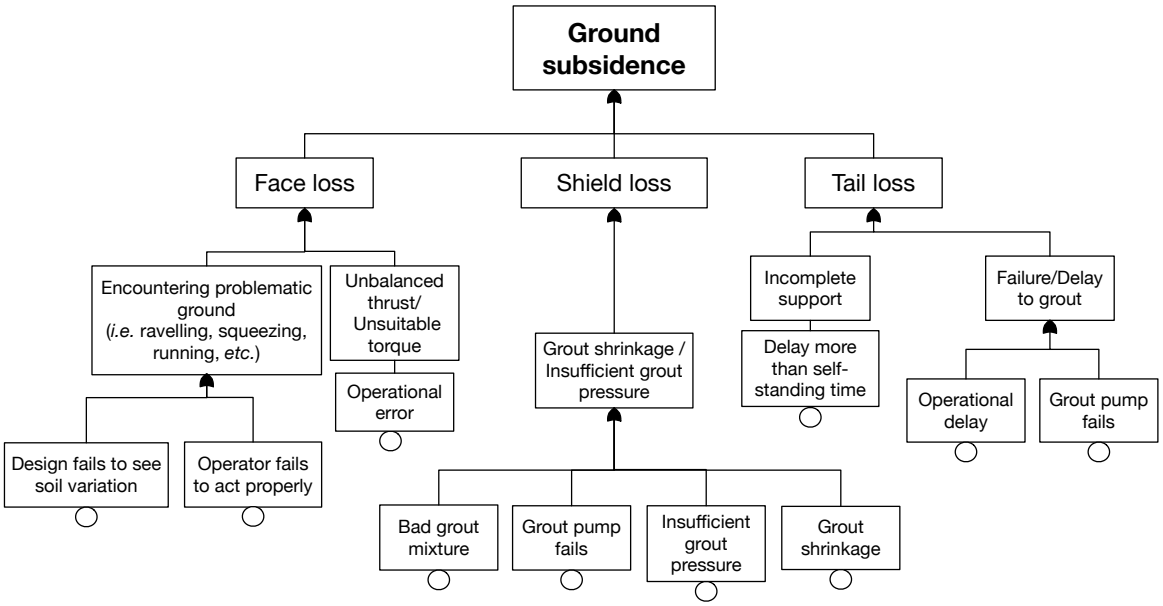

Figure 21. Fault tree analysis: short-term – straight section

condition and problematic ground soil that are overlooked may induce more face loss, particularly when the operator cannot properly counteract the situation. The experience and skills of the operating team are important for a successful TBM driving.

Figure 22 shows the fault tree representation of a curved section, where the main concern is how to consider the effect of the over-excavation at curves. The major difference between the short-term settlement along the shield along straight and curved sections is the settlement induced by extra over-excavation at curves. In this case, the shield loss occurs because of extra-over excavation and grouting problems (shown by an "AND" gate in Figure 22). Grout-related problems, namely insufficient grouting pressure, shrinkage, bad mixture, *etc.* are other causes of the shield loss. Tail loss is mostly caused by grout problems as well as lack of on-time support for the tunnel.

Fault tree analysis is performed by a series of bottom-up calculations. Knowing the probability of the base faults (*i.e.* faults that are indicated by a circle below them in the fault tree), the faults are calculated level-by-level, by considering which type of gate the faults are connected to.

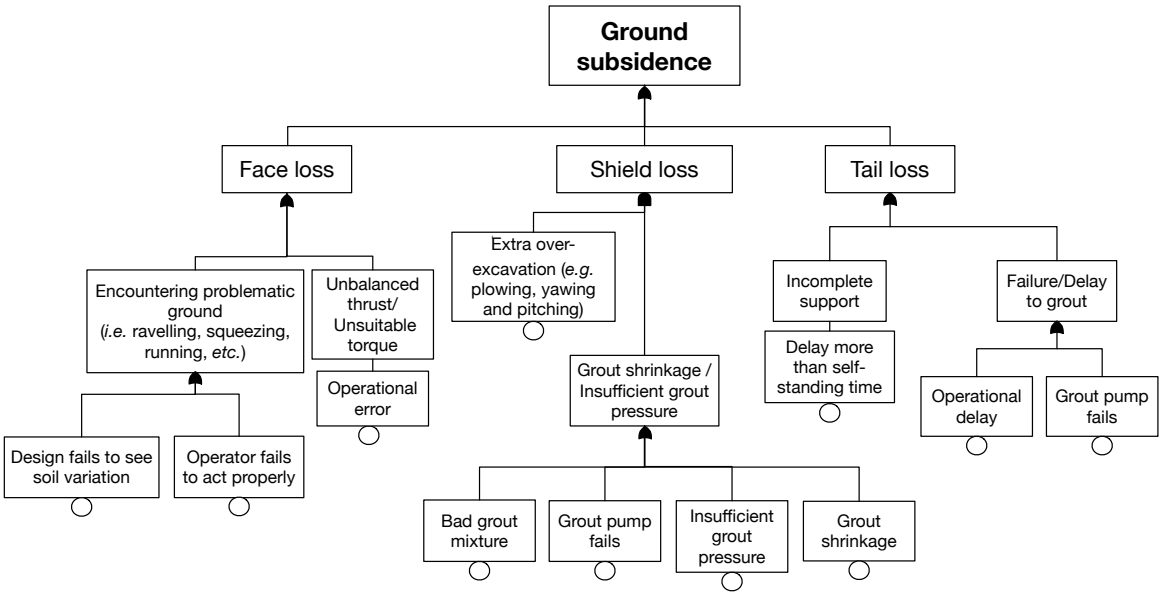

Figure 22. Fault tree analysis: short-term – curved section

Risk analysis based on fault tree

After all the risk sources are identified and investigated, the risk analysis can be performed to calculate the associated risk. Here, the scale of the uncertainty is crucial. Therefore, it is essential to examine the problem from different façades, which enables the risk analyst to better identify the boundaries of the problem for a better engineering judgment.

Recalling that the ultimate goal of RM plan is to address the associated risk of building settlement and damage induced by tunnelling, we should first determine the major components namely buildings that are directly exposed to risk. This can be called "pre-event vulnerability assessment", which provides more information than just reporting a building's weak spots per se. It also includes recognizing the categories and properties of different buildings and provides information about how buildings are "prone" to settlement.

To achieve this goal, we must identify the buildings, which are directly affected by tunnelling activity and their locations. To acquire such information, it is beneficial to project the tunnel's map on the city map, for instance, by using a GIS software. This provides an overview of the boundaries of the problem and also a quick view on its configuration in total. Figure 23 represents this projection in a schematic way.

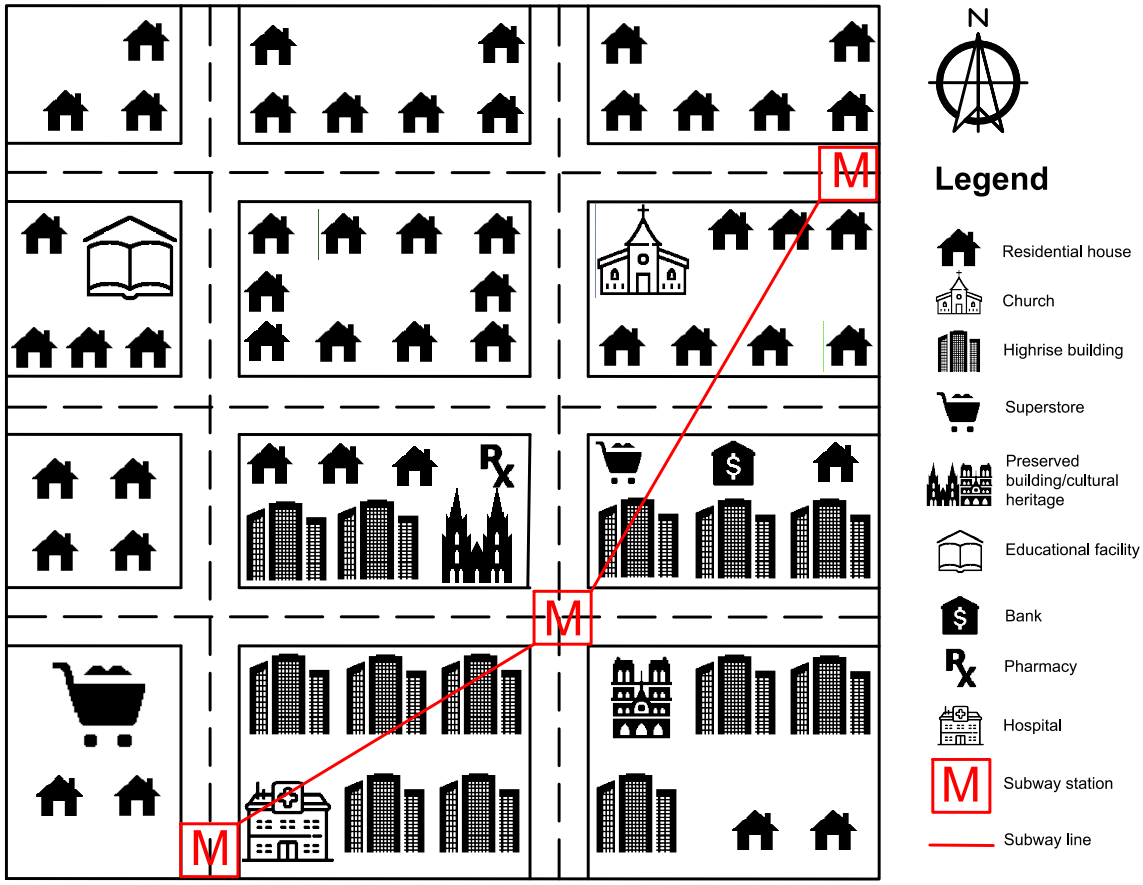

Figure 23. Schematic projection of the tunnel on the urban city map

During the process of excavation, three different zones emerge along the advancement direction. Zone 1, depicted by cyan colour in Figure 24, is always ahead of the tunnel up to 2D (two times the diameter of the tunnel) (Loganathan, 2011). Zone 2 is alongside the tunnel and distances 2D from the centreline (Bowles, 1996), and Zone 3 is also alongside the tunnel advancement direction. According to Peck (1969), Zone 3 is located at 3i from the centreline with i being the transverse settlement trough width parameter:

$$\mathrm{i} = \frac{1.15\mathrm{R}}{(\tan\beta)^{0.4}}\left(\frac{\mathrm{H}}{2\mathrm{R}}\right)^{\frac{0.9}{(\tan\beta)^{0.2}}} \qquad \textit{(Eq. 3-1)}$$

$$\beta = 45° + \frac{\varphi}{2} \qquad \textit{(Eq. 3-2)}$$

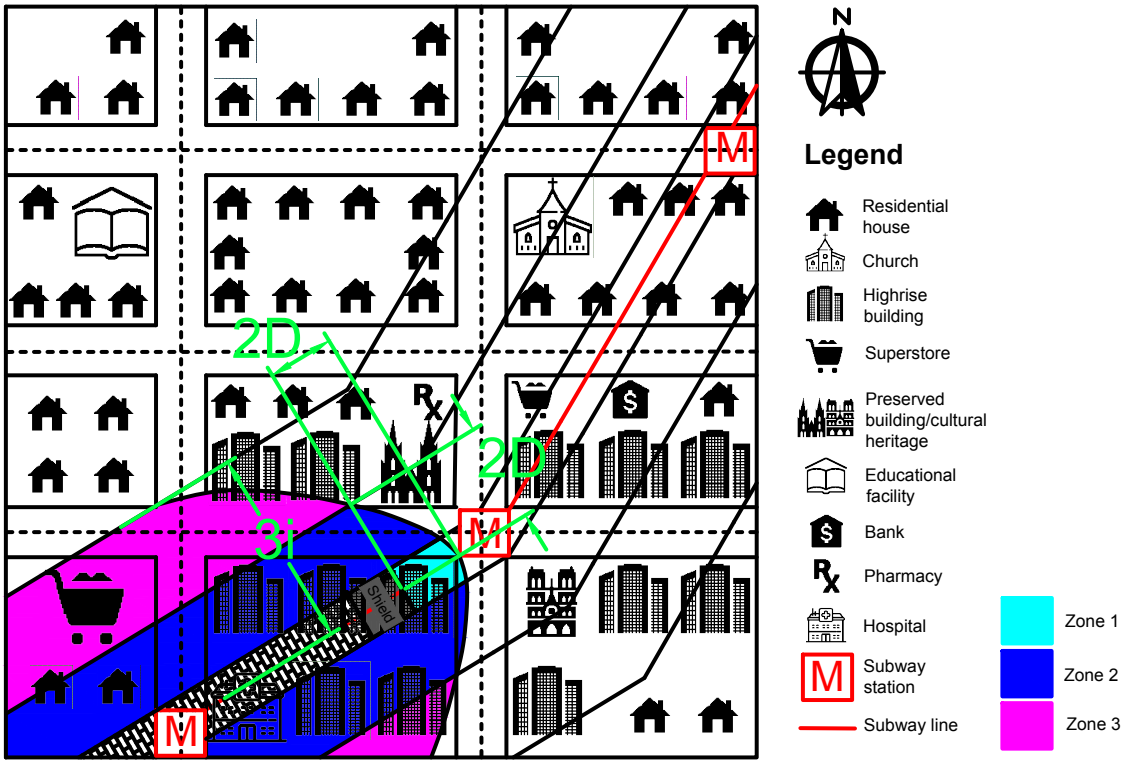

Figure 24. Tunnel's influential zones and their dimensions: Zone 1 (Loganathan 2011), Zone 2 (after Bowles, 1996) and Zone 3 (after Peck, 1969)

where φ is the angle of internal friction of soil, H is the depth of tunnel centreline and R is tunnel's radius. Eq. (3-1) is based on the relation obtained by Loganathan (2011) in his analytical solution for surface settlement that is between normalized $\frac{i}{R}$ and $\frac{H}{2R}$ parameters.

After the excavation of this section of the tunnel is completed, the final maintenance of the tunnel is provided by tunnel lining. The completed section is depicted in Figure 25.

It should be noted that the method described here was first introduced to evaluate the effect of tunnelling on pile foundations (Loganathan, 2011). However, since the extension of these zones are solely based on ground movement, these zones exist, regardless if the surface buildings have pile foundations or not.

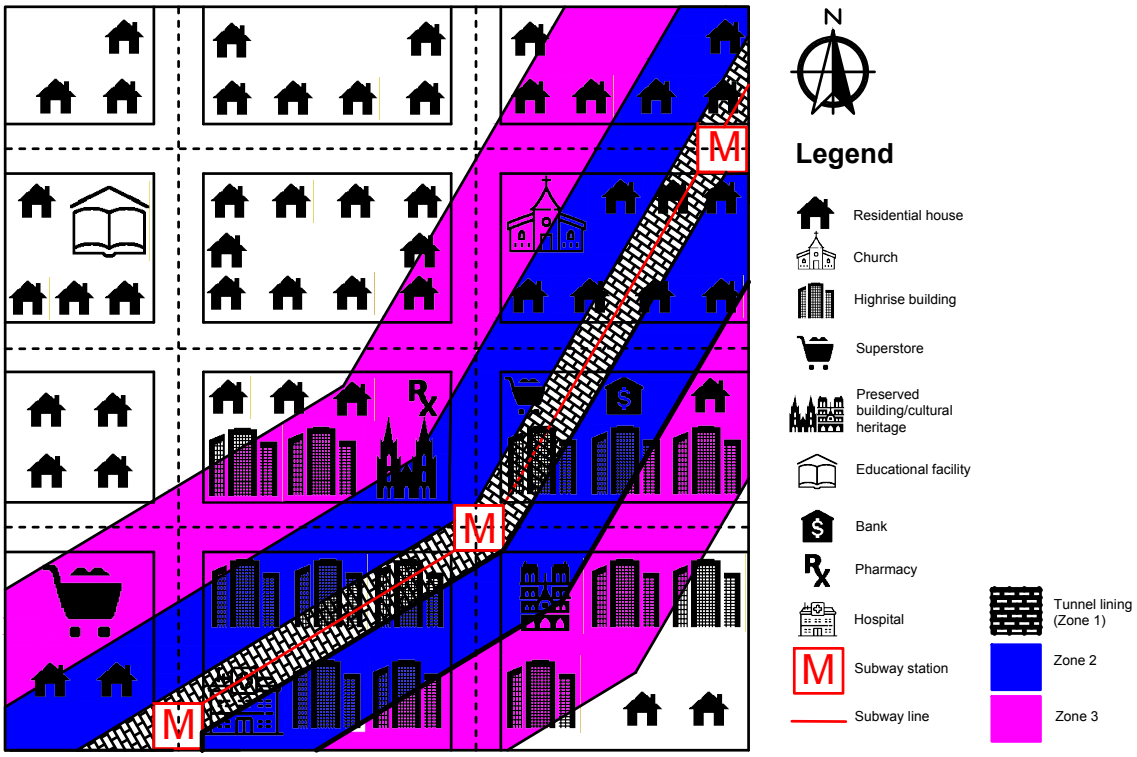

Figure 25. Tunnel influential zones: completed - Zone 2 (after Bowles, 1996) and Zone 3 (after Peck, 1969)

3.2.2.2 Building database

Recalling Eq. (2-21), in order to evaluate the risk of tunnel-induced settlement, we need to know the intensity of the consequences. The intensity of the detrimental effects of tunnel-induced settlement on the buildings is related to the physical vulnerability of the building and the distance of the vulnerable asset (in our case surface buildings) to the tunnel. Therefore, it is useful to categorize the affected buildings in terms of their age, and their location with respect to tunnel, in the form of a building database. For each class of buildings, a specific class of risk evaluation with a specific methodology is used to calculate the risk.

To establish the building database, a unique ID is assigned to each building. Having a unique ID provides the opportunity for further development of the database by adding more entities. In addition to the ID, we should also identify the purpose of the building, its functionality and the level of service it provides. Such information is important for defining the limit-state functions for buildings when performing the reliability analysis.

In the building database, a score is assigned to each building. This score is calculated based on the characteristics and the location of the building as follows:

1. Score for building age: the buildings are put into these subcategories in terms of their age: up to 20 years, from 20 years to 100 years and more than 100 years. The scores corresponding to these age categories are 2, 1 and zero, respectively.
2. Score for building location: the risk associated to buildings of different age or type in different tunnelling zones (*i.e.* 1 to 3) is different. The scores assigned to the outer zone, Zone 3, is 2 while Zone 1, which is located above the tunnel, has zero score.

After the scores are determined, a building is assigned to a class based on the total score: if the score is 4 or 5, the building is in Class 3. If the score is 3 or 2, the class will be 2 and otherwise the class is 1. The purpose of providing buildings with a score is to identify buildings having lower scores since these buildings requires more attention and in-depth evaluation. Table 4 represents the features of the building database in a tabular form.

ID	Purpose	Foundation type			Age			Tunnelling affected zone			Preserved building		Building category		
		Shallow	Deep	Other	0-20	20-100	>100	TZ1	TZ2	TZ3	Yes	No	Class 3	Class 2	Class 1
		S	D	O	2	1	0	0	1	2	0	1	(4,5)	(2,3)	(0,1)

Table 4. Building database

The outcome of this classification is six building indices, namely BS1, BS2, BS3, BD1, BD2 and BD3 for buildings on shallow and deep foundations. The letter "S" stands for "shallow" and "D" stands for "deep". Therefore, BS1 represents a Class 1 building with a shallow foundation.

After the buildings are grouped in different classes, they are next projected on the urban map with different colour codes (Figure 26). This provides the big picture of the problem and enables the analyst to have a better insight about the risk exposure. One may also regroup the buildings to build city zones with the same class of buildings. For excavations in different regions of a city, such information can be used to adjust the

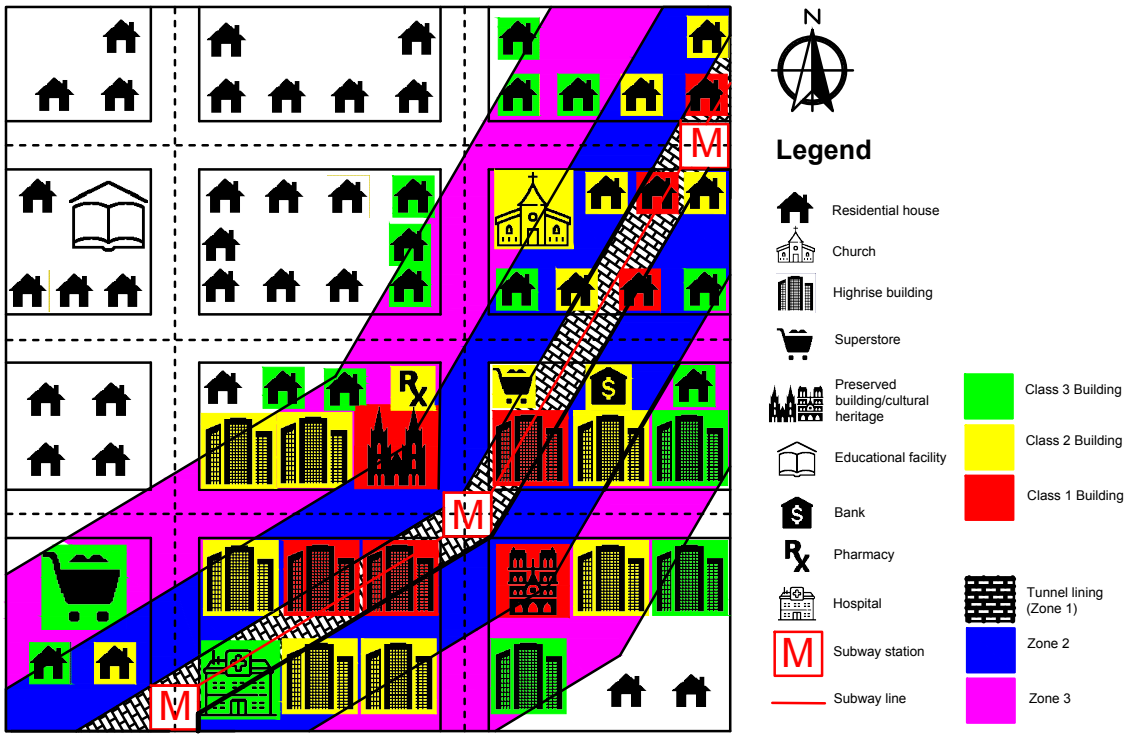

Figure 26. Map of building classes

advancement rate and related properties with new conditions to provide appropriate measures if needed.

The reliability analysis can be performed after the building database is completed. Two different classes of analysis are to be performed based on the foundation type of the building.

Before explaining each class of risk analysis, it has to be clearly stated that the primary purpose of this study is the provision of an RM framework instead of the development of a new method or an analytical solution for ground settlement. Therefore, in some classes of analyses, methods to evaluate ground settlement proposed in the literature are used, with the focus being placed on the applicability of these methods and how to evaluate the associated uncertainty.

Regarding the selection of the analytical or numerical formulations, for each class of analysis, a methodology is suggested to calculate the settlement. Different methodologies for risk settlement calculations are proposed in order to consider

different levels of accuracy required for different building types. For instance, a BS3 building is less critical than a BS1 building due to the fact that it is either less physically vulnerable or located at a further distance from the tunnel. The consequence of tunnel-induced settlement is more critical for Class 1 buildings which requires a more accurate methodology to calculate the settlement risk. However, other proposed relations can also be used in each class, if the analyst finds them to be more appropriate. In other words, this study attempts to provide an overall framework in which different models or limit-state functions can be used to evaluate the risk.

3.2.2.3 Buildings with shallow foundations

SSRABS3: Short-term settlement risk analysis of Class 3 buildings

The settlement risk of Class 3 buildings is determined through short-term settlement risk analysis of Class 3 buildings, SSRABS3, in which "SSRA" stands for short-term settlement risk analysis and "BS3", is the building index for Class 3 buildings on shallow foundation. This class of buildings is relatively less critical since they either have lower physical vulnerability or less exposure, which results in a lower risk. Here, the exposure is described as the distance from the tunnel centreline where the ground undergoes the highest settlement during tunnelling. This class of analysis uses closed-form formulation by Loganathan (2011), which is a modified version of Loganathan and Poulos (1998) formulation. In the method, the ground deformations are determined as follows (Loganathan, 2011):

– Surface settlement:

$$U_{z=0} = \varepsilon_0 R^2 \frac{4H(1-\nu)}{H^2 + x^2} \exp\left(\frac{-1.38x^2}{(H\cot\beta + R)^2}\right) \qquad \textit{(Eq. 3-3)}$$

– Subsurface deformation:

$$U_z = \varepsilon_0 R^2 \left(\frac{z-H}{x^2 + (z-H)^2} + (3-4\upsilon)\frac{z+H}{x^2 + (z+H)^2} - \frac{2z(x^2 - (z+H)^2)}{(x^2 + (z+H)^2)^2}\right) \exp\left(-\left(\frac{1.38x^2}{(H\cot\beta + R)^2} + \frac{0.69z^2}{H^2}\right)\right) \qquad \textit{(Eq. 3-4)}$$

– Lateral movement:

$$U_x = -\varepsilon_0 R^2 x \left(\frac{1}{x^2 + (H - z)^2} + \frac{3 - 4\upsilon}{x^2 + (z + H)^2} - \frac{4z(z + H)}{(x^2 + (z + H)^2)^2} \right) \exp\left(-\left(\frac{1.38x^2}{(H\cot\beta + R)^2} + \frac{0.69z^2}{H^2} \right) \right) \quad \textit{(Eq. 3-5)}$$

where R = tunnel radius,

z = the depth below the ground surface,

H = the depth of the tunnel centreline,

υ = Poisson's ratio of ground soil,

ε_0 = average ground loss,

x = lateral distance from tunnel centreline,

$\beta = 45 + \frac{\phi}{2}$ with ϕ being the angle of internal friction of soil.

The above expressions have been verified by various case studies, centrifuge modelling and numerical analysis using FLAC3D (Loganathan, 2011). It is worth to mention that the Peck's empirical equation for transverse settlement trough (Eq. 2-2) can be used alternatively, for a very quick estimate of the surface settlement.

Eqs. (3-3) to (3-5) can be used to determine ground settlement deterministically based on average or representative values of various parameters. To establish a multi-level risk framework for ground settlement, the parameters in Eqs. (3-3) to (3-5) must be considered as random variables to consider the uncertainty associated with the input data.

This reliability analysis will supply us the probability of failure, which is used to determine the risk of the settlement. Another point which is included in this framework is that if the exceedance probability in one class of analysis is higher than a given threshold (*e.g.* P_{s_1}), the building will be transferred into a lower-number class to be evaluated more accurately. This assures the analyst to pay enough attention to critical buildings of each class. The formulation and how to perform the reliability calculations will be discussed thoroughly in "risk evaluation" part. In this section, we only suppose

that we have an exceedance probability and a settlement threshold for each class of buildings.

CIRIA PR30 (1996) proposed a damage classification based on the building slope and maximum settlement values, as summarized in Table 5. This classification can be used to establish the thresholds of settlement for buildings in Class 3. In this way, the proposed framework in this study can be calibrated with the CIRIA PR30 damage classification. For instance, one may use $10\ \mathrm{mm}$ (the boundary between "negligible" and "slight" risks in CIRIA PR30, 1996) as the threshold to define the limit-state function. If the calculated exceedance probability using this threshold exceeds 20%, it will be required to perform settlement risk assessment of Class 2 buildings (SSRABS2).

Risk category	Maximum slope of building	Maximum settlement (mm)	Description of the risk
1	<1/500	<10	**Negligible**: superficial damage unlikely
2	1/500 to 1/200	10 to 50	**Slight**: possible superficial damage, unlikely to have structural significance
3	1/200 to 1/50	50 to 75	**Moderate**: expected superficial damage and possible structural damage to building, possible damage to relatively rigid pipelines
4	>1/50	>75	**High**: expected structural damage to buildings and rigid pipelines or possible damage to other pipelines

Table 5. CIRIA damage classification (CIRIA PR30, 1996)

SSRABS2: Short-term settlement risk analysis of Class 2 buildings

The settlements of Class 2 buildings (*i.e.* BS2) and the buildings transferred from SSRABS3 are estimated using the method proposed by Burland and Wroth (1974). In this method, depending on the location and mode of settlement, the ground is classified as "hogging" or "sagging" zones; as illustrated in Figure 27.

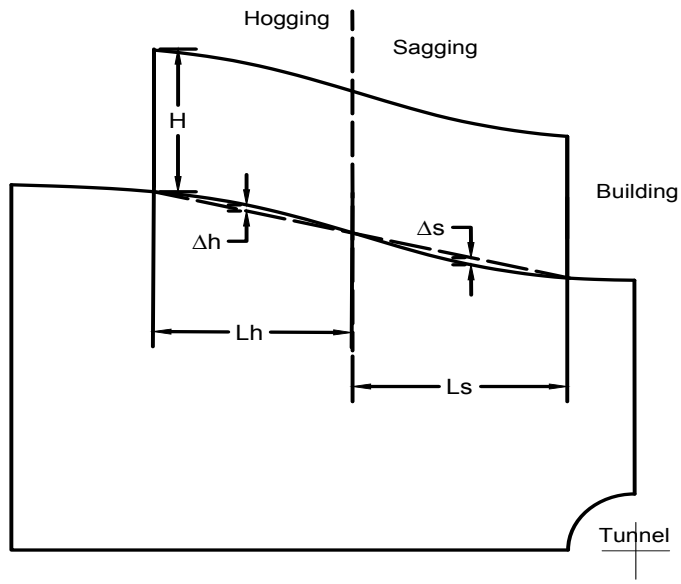

Figure 27. Hogging-sagging zones

Burland and Wroth (1974) simplified the buildings as simple beams. Closed-form solution are developed to determine the strains of buildings in "hogging" and "sagging" zones, respectively. Even though, this approach has its own drawbacks due to the simplifying assumption of considering building as a simple beam, it provides us an improved method for building settlement, by taking into account the nature of ground deformation.

To perform Class 2 settlement analysis, we should first determine the bending strain ε_b, the diagonal strain ε_d and the horizontal strain ε_h of the equivalent beam:

$$\varepsilon_b = \frac{\frac{\Delta}{B}}{\left(\frac{L}{12t} + \frac{3IE}{2tLHG}\right)} \qquad \textit{(Eq. 3-6)}$$

$$\varepsilon_d = \frac{\frac{\Delta}{B}}{\left(\frac{HL^2G}{18IE} + 1\right)} \qquad \textit{(Eq. 3-7)}$$

$$\varepsilon_h = \frac{\Delta}{B} \qquad \textit{(Eq. 3-8)}$$

where Δ = maximum relative settlement at the considered area,

L = the length of the building,

t = the furthest distance of neutral axis to the edge of the equivalent beam (for sagging zone $\mathrm{t} = \frac{\mathrm{H}}{2}$ and for hogging zone $\mathrm{t} = \mathrm{H}$)(Loganathan, 2011),

H = the height of the building,

E = Young's modulus of the building (equivalent beam),

G = shear modulus of the building (equivalent beam),

I = the moment of inertia of the equivalent beam, (for sagging zone $\mathrm{I} = \frac{\mathrm{H}^3}{12}$ and hogging zone $\mathrm{I} = \frac{\mathrm{H}^3}{3}$), and

B = the length of the building interacting with the horizontal movement.

The total diagonal strain $\varepsilon_{\mathrm{ds}}$, is determined from the horizontal strain ε_{h} and diagonal strain ε_{d}:

$$\varepsilon_{\mathrm{ds}} = \varepsilon_{\mathrm{h}}\left(\frac{1-\nu}{2}\right) + \sqrt{\varepsilon_{\mathrm{h}}^2\left(\frac{1-\nu}{2}\right)^2 + \varepsilon_{\mathrm{d}}^2} \qquad \textit{(Eq. 3-9)}$$

where υ is Poisson's ratio of the equivalent beam.

The total bending strain is calculated as:

$$\varepsilon_{\mathrm{bs}} = \varepsilon_{\mathrm{b.max}} + \varepsilon_{\mathrm{h}} \qquad \textit{(Eq. 3-10)}$$

in which $\varepsilon_{\mathrm{b.max}}$ is the maximum bending moment, which is calculated at the furthest distance from the neutral axis of the equivalent beam and ε_{h} is the horizontal strain.

Finally, the critical strain $\varepsilon_{\mathrm{crit}}$ is determined as:

$$\varepsilon_{\mathrm{crit}} = \max\left(\varepsilon_{\mathrm{bs}}, \varepsilon_{\mathrm{ds}}\right) \qquad \textit{(Eq. 3-11)}$$

According to Burland and Wroth (1974), buildings may have two possible extreme modes of deformation, namely "bending only" and "shearing only". In the case of pure

bending, the crack starts from the outermost fibre of a building as a result of the tensile strain ε_b, whereas for shear, the crack is the result of the diagonal tensile strain ε_d.

Depending on the critical strains, Boscardin and Cording (1989) proposed a classification for different types of damage, as summarized in Table 6.

Damage type	**0**	**1**	**2**	**3**	**4&5**
$\varepsilon_{crit}(\%)$	≤ 0.05	> 0.05 ≤ 0.075	> 0.075 ≤ 0.150	> 0.150 ≤ 0.3	> 0.3

Table 6. Damage classification by ε_{crit}, (after Boscardin & Cording, 1989)

SSRABS1: Short-term settlement risk analysis of Class 1 buildings

Class 1 reliability analysis is performed for the most sensitive and vulnerable buildings in the tunnelling zones. For this class of analysis, due to the possibility of more severe consequences, it is suggested to perform a more rigorous elastoplastic analysis via numerical modelling (*e.g.* FEM) to estimate the settlement induced by tunnelling. Finite Element modelling provides a more accurate stress/strain model as well as an improved accuracy, regarding the magnitude of the settlement.

Performing sensitivity analysis is proven to be helpful to provide the analyst with the perspective of the sensitivity of the results to one or more parameters (variables). This also makes it possible to form an importance ranking list based on the results of sensitivity analysis to identify the priorities. Details of the assessment and the models will be discussed next in the following section on “risk evaluation”.

3.2.2.4 Buildings with deep foundations

The workflow of risk assessment for pile foundations is similar to that for shallow foundations, except that the settlement calculations are based on methods proposed for pile foundations. The buildings go through two classes of reliability assessment based on their building indices (*e.g.* BD2, BD1). The outcome of each class of analysis is an exceedance probability, which is calculated based on the limit-state function defined for each class. Similar to the buildings with shallow foundations, if the exceedance

probability exceeds a threshold value, the building is then transferred from Class 2 to Class 1. It is noteworthy to mention that for a building with pile foundations, it is inappropriate to use green field settlements, since buildings do not settle along the settlement trough; they settle according to the pile's settlement (Loganathan, 2011).

SSRABD2: Short-term settlement risk analysis of Class 2 and Class 3 buildings

According to Table 4, buildings that are indexed as BD2 or BD3 are evaluated throughout this class. The evaluation of settlement in this class uses the "design charts" proposed by Loganathan (2011). Design charts are able to provide reasonable accuracy with negligible computational cost. The limit-state functions are developed based damage classifications (*e.g.* CIRIA PR30, 1996). The base values of settlement, bending stress and lateral deformation are extracted from design charts and then calibrated using the correction factors. The bending stress, pile settlement and lateral deflection are then calculated according to the location of the pile with respect to the tunnel *i.e.* TZ1, TZ2 and TZ3.

The combined stresses in a pile as well as settlement and lateral deflection are calculated according to:

$$\sigma_{max} = \frac{\left(M_{design} + M_{induced}\right)}{Z} + \frac{\left(P_{design} + P_{induced}\right)}{A} \qquad \textit{(Eq. 3-12)}$$

$$\sigma_{min} = \frac{\left(M_{design} + M_{induced}\right)}{Z} - \frac{\left(P_{design} + P_{induced}\right)}{A} \qquad \textit{(Eq. 3-13)}$$

$$\nu_{max} = \nu_{design} + \nu_{induced} \qquad \textit{(Eq. 3-14)}$$

$$\rho_{max} = \rho_{design} + \rho_{induced} \qquad \textit{(Eq. 3-15)}$$

where Z = section modulus,

M_{design} = the design bending moment (also called "as-built" bending moment),

$M_{induced}$ = the tunnel-induced bending moment,

P_{design} = the design axial force,

$P_{induced}$ = the tunnel-induced axial force,

ν_{design} = the design settlement of the pile,

ν_{induced} = the tunnel-induced settlement of the pile,

ρ_{design} = the design lateral deflection of the pile,

ρ_{induced} = the tunnel-induced lateral deflection of the pile.

These induced stresses in pile and the corresponding pile deformations may be different based on the location of a building with respect to the tunnel zones *i.e.* TZ1, TZ2 and TZ3.

SSRABD1: Short-term settlement risk analysis of Class 1 buildings

Similar to SSRABS1, this class of settlement analysis for buildings with deep foundations utilizes numerical modelling due to the importance of this class of buildings. Here, FEM is used to perform reliability analysis on a single pile or a group of piles. If required, sensitivity analysis is performed to check how different parameters affect the results and to what extent. The details will be discussed in the "risk evaluation" section.

Risk evaluation flowchart (short-term)

Figure 28 presents the flowchart of RM for short-term settlement risk analysis. This flowchart provides the workflow necessary to perform RM. In addition, it is vital for development of a software based on the proposed framework.

The framework of RM consists of three parts, which are enclosed by dashed-line rectangles in the flowchart. The first part is pre-tunnelling building indexing. In this part, the tunnel is projected onto the city map and various affected zones are identified. Buildings at different location and of different characteristics are indexed and added to a database. Next, the buildings are classified as either shallow foundations or deep foundations. Then, based on their score, the risks associated with each building are evaluated in different classes. The level of accuracy and details as well as the computational cost and time required will increase, as more rigorous analyses are required as in Class 1.

Each class of analysis provides a building with an exceedance probability (or reliability index) based on the limit-state function defined for this class. At the end, the building's database is updated with probabilities of failure of buildings. It is extremely important to be aware that only the probability of failure of buildings in the same class are

comparable. That is why future risk remedies and decisions should not be made based on the probability of failures without considering the evaluation classes.

The outcomes of the short-term risk analysis are summarized in one building report and one map. The map is called short-term risk map or “SRM”. This map simply depicts the affected tunnelling zone and settlement depth in that area. This map is beneficial for long-term settlement evaluations, which eventually provides the total settlement map.

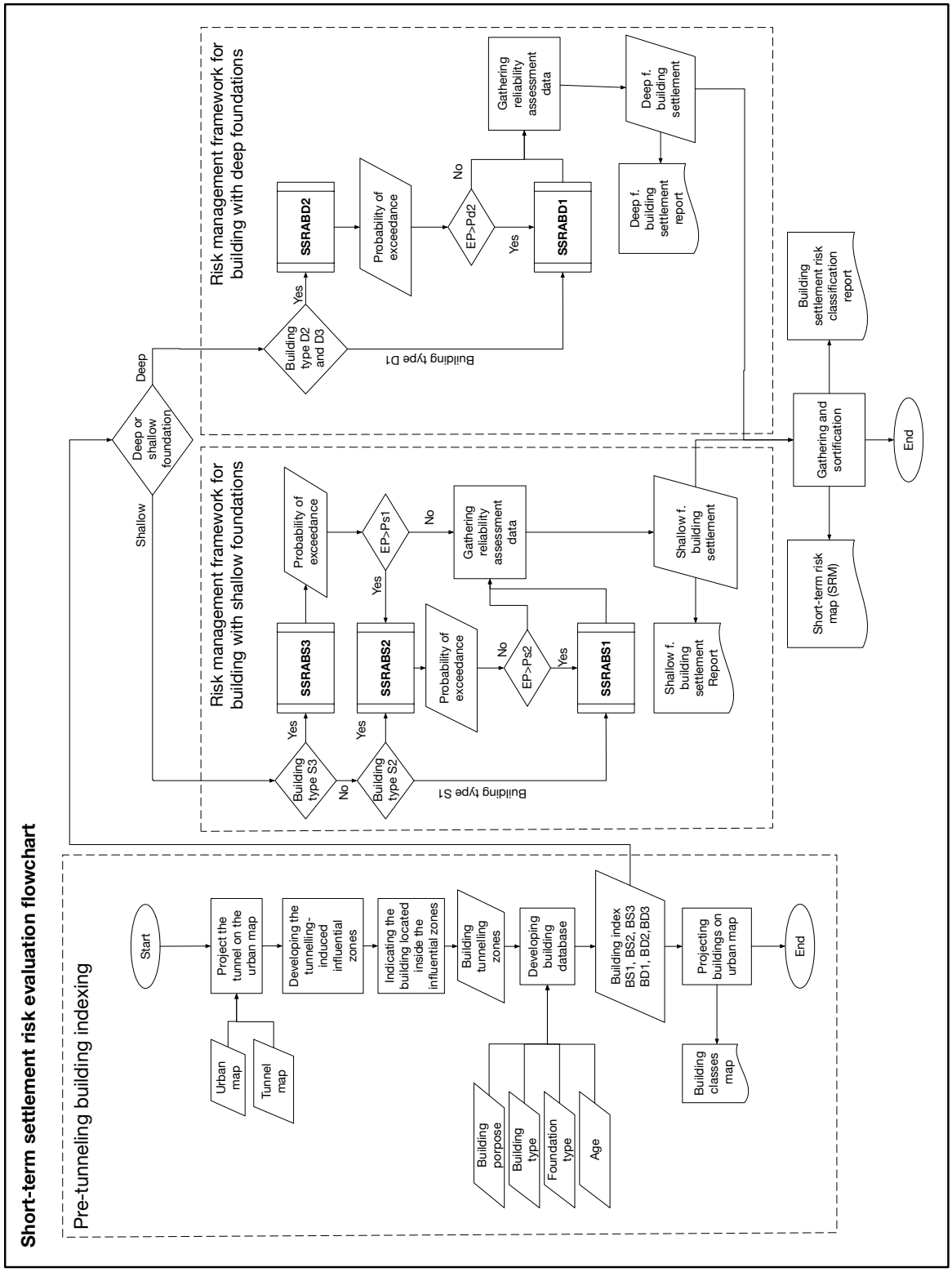

Figure 28. Risk management framework for short-term settlement risk

3.2.3 Risk evaluation

This section discusses the risk formulations for each class of short-term settlement risk analysis (SSRA) and the corresponding models. The risk calculations will be performed with the help of reliability analysis. Probabilistic methods are utilized to evaluate the uncertainties of various parameters involved in the models. Random variables are used to introduce these uncertainties in the analysis. The reliability analysis also requires limit-state functions, which should be defined for each class, based on the criteria introduced previously.

3.2.3.1 Buildings with shallow foundations

SSRABS3: Short-term settlement risk evaluation for Class 3 buildings

For shallow foundations, Class 3 analysis uses settlement calculation proposed by Loganathan (2011) for different types of ground movements as given in Eqs. (3-3) to (3-5). Figure 29 shows the models as well as the parameters associated in this class of analysis and the link between them. This flowchart also depicts the pathways of error propagation. Table 7 lists the parameters involved in the SSRABS3.

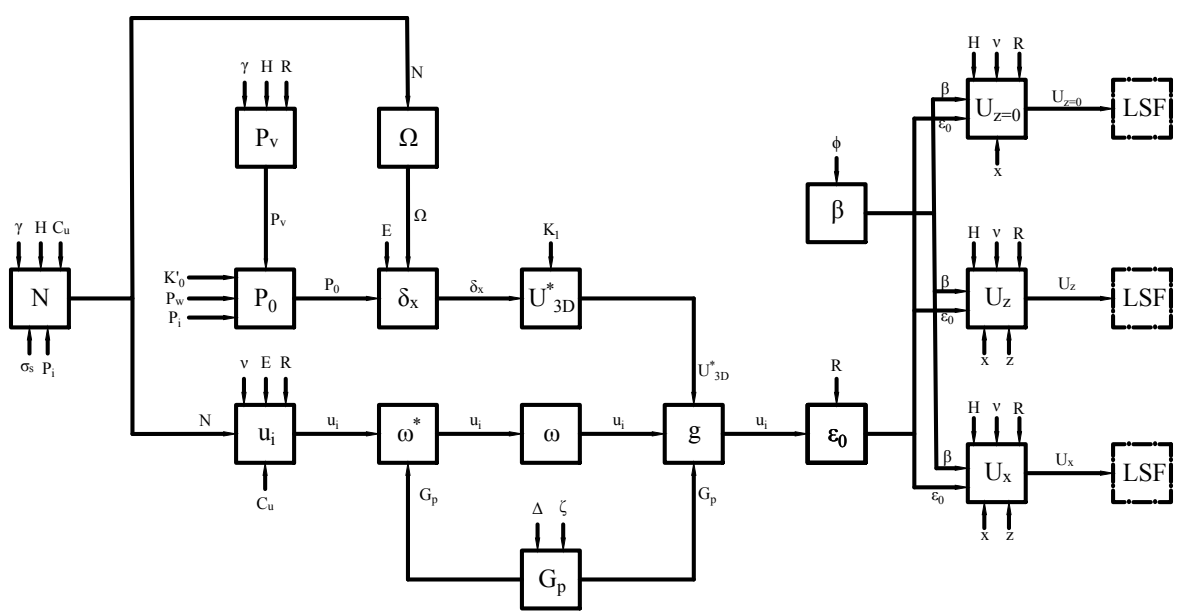

Figure 29. Model for Class 3 reliability analysis of shallow foundations

Symbol	Description	Type
H	Depth of the tunnel axis level	Random variable
ν	Soil's undrained Poisson's ratio	Random variable
R	Tunnel radius	Random variable
X	Lateral distance from tunnel centreline	Constant
Z	Depth below the ground surface	Constant
ϕ	Internal friction angle of soil	Random variable
γ	Unit weight of overburden soil	Random variable
C_u	Undrained shear strength of soil	Random variable
P_i	Tunnel supporting pressure	Random variable
P_w	Pore water pressure	Random variable
K_0	Earth pressure at rest	Random variable
E	Undrained soil's modulus	Random variable
K_1	Volume ratio	Constant
Δ	Thickness of the tail piece	Random variable
Z	Required clearance for erection of tail piece	Random variable
σ_s	Surcharge	Random variable

Table 7. List of parameters in Class 3 reliability analysis for shallow foundations

To consider the uncertainty in the parameters as well as the model itself, the parameters are defined stochastically as random variables. The type of the random variable is not specified in Table 7 and left to the discretion of the analyst. For instance, the dimension-related parameters as well as resistance parameters may be defined using lognormal distribution since they have to be restrictedly positive. On the other hand, lateral distance from tunnel centreline and the depth may be determined as constant values.

Referring to Table 5, CIRIA PR30 (1996) considers four classes for building damage; the threshold of maximum settlement for having a "negligible" damage is $10\ \mathrm{mm}$. As a result, we may define the limit-state function of this class of analysis as:

$$\mathrm{LSF}_{\mathrm{Class\ 3}} = 10\ [\mathrm{mm}] - \mathrm{U}_{z=0} \qquad \textit{(Eq. 3-16)}$$

In this way, the results of the proposed frameworks are consistent with the practical code and will provide the analyst with a virtue of comparison.

The exceedance probability is estimated by reliability analysis, for instance, by using FORM. If the probability is higher than a selected level (say 20%), the building will be transferred to Class 2 for a more in-detail investigations.

SSRABS2: Short-term settlement risk evaluation for Class 2 buildings

In Class 2 reliability analysis, Burlnad and Wroth (1974) method is used to determine the building damage. This class of analysis has a less complex structure comparing to the Class 3 analysis, but it provides improved accuracy for the risk evaluation as well as the movements and damage of buildings. The reliability analysis models and parameters are shown in Figure 30:

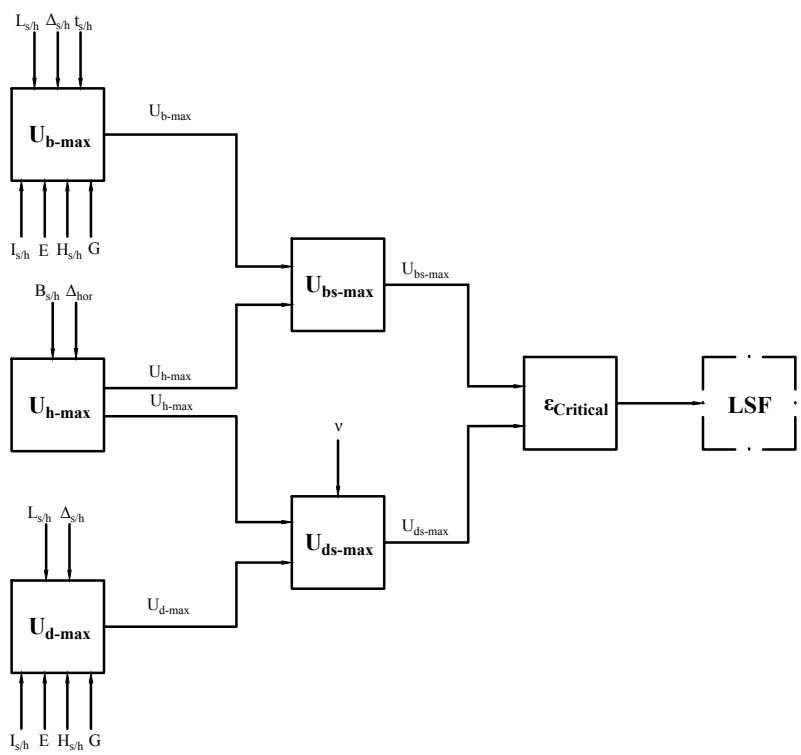

Figure 30. Model for Class 2 reliability analysis of shallow foundations

Table 8 provides the list of parameters considered in SSRABS2. The S/h sub-index stands for buildings in sagging or hogging zones. Eqs. (3-6) to (3-11) are used to calculate strains

of building for sagging and hogging zones. The maximum value of strains is selected as the critical value.

To define the limit-state function used for this class of analysis, the criteria developed by Boscardin and Cording (1989) is used. They proposed five classes of damage based on the critical strain with the threshold being 0.3%, which corresponding to the limit between Class 3 and Class 4&5. Therefore, the limit-state function is chosen as:

$$\mathrm{LSF}_{\mathrm{Class\ 2}} = 0.3\ [\%] - \varepsilon_{\mathrm{Critical}} \qquad \textit{(Eq. 3-17)}$$

in which $\varepsilon_{\mathrm{Critical}}$ is determined from Eq. (3-11).

Symbol	Description	Type
$L_{s/h}$	Length of sagging / hogging zone	Random variable
$\Delta_{s/h}$	Maximum relative settlement	Random variable
$I_{s/h}$	Moment of inertia of the equivalent beam	Random variable
E	Building's Younge's modulus	Random variable
H	Building height	Random variable
$B_{s/h}$	Length of the building interacting with horizontal movement	Random variable
Δ_{hor}	Horizontal movement	Random variable
G	Building's shear modulus	Random variable
ν	Building's Poisson's ratio	Random variable

Table 8. List of parameters in Class 2 reliability analysis for shallow foundations

Alternatively, it is possible to define the limit-state function based on other limit values proposed by Boscardin and Cording (1989) for other classes of damage. It is also possible to define a limit-state function for each damage class and then perform the evaluation.

SSRABS1: Short-term settlement risk evaluation for Class 1 buildings

For Class 1 reliability assessment for shallow foundations, numerical modelling such as FEM is required to estimate ground deformation induced by tunnelling. To achieve this goal, an FEM model needs to be established for the building-ground-tunnel system with proper selection of constitutive models for various materials. The FEM analysis should be performed by considering the random variation of material properties to provide probabilistic results.

For each specific case, a specific threshold is defined for limit-state function. This threshold is precisely chosen for the target building. It is also possible and sometimes mandatory to preform sensitivity analysis on the threshold value to find out how the geosystem is responsive to the uncertainties. This series of analysis will provide us not only with the building's behaviour due to tunnelling activities, but also the behaviours of the foundation, soil and the tunnel structure itself. Class 1 analysis is generally comprehensive and time-consuming. Hence, it is required only for a special comprehensive analysis, to be performed only for a special section containing important building(s) with high risk.

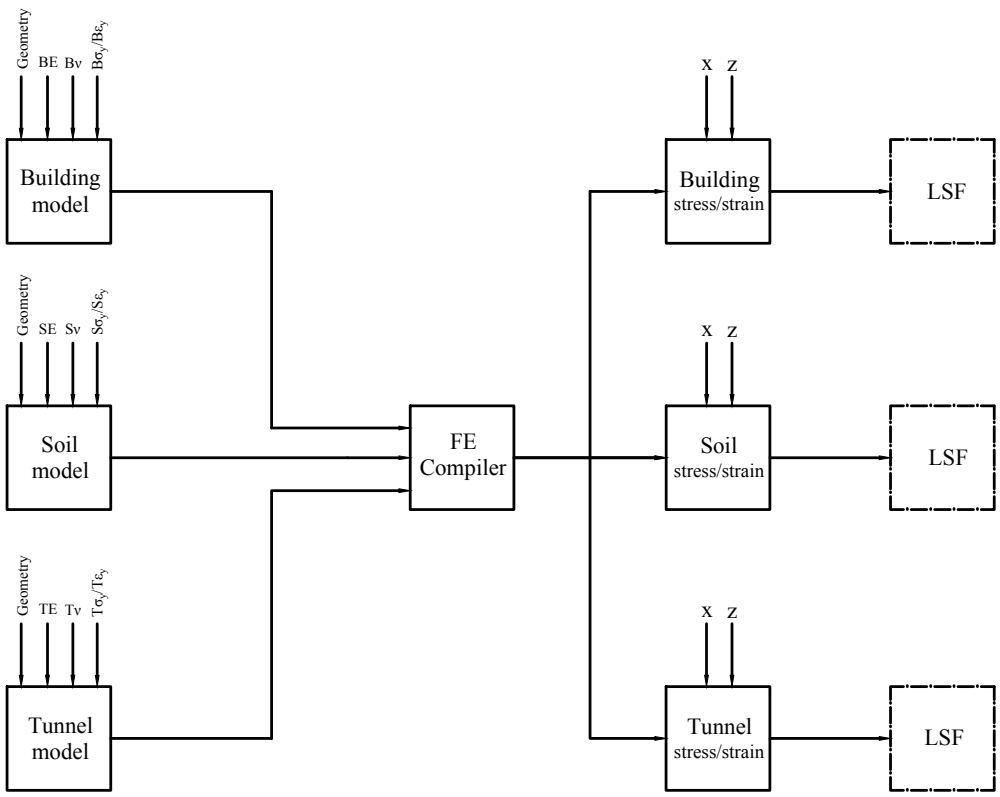

Figure 31. Model for Class 1 reliability analysis of shallow foundations

Figure 31 presents the model for Class 1 reliability analysis and the considered parameters are summarized in Table 9. It should be mentioned that, in Class 1 risk analysis, possible uncertainties with respect to the dimensions for instance beam dimension, lining thickness, *etc.* are generally ignored in the reliability analysis.

Symbol	Description	Type
Geometry	Geometry	Constant
BE	Building's Younge's modulus	Random variable
Bν	Building's Poisson's ratio	Random variable
$B\sigma_y/B\varepsilon_y$	Building's yield stress/strain	Random variable
SE	Soil's Younge's modulus	Random variable
Sν	Soil's Poisson's ratio	Random variable
$S\sigma_y/S\varepsilon_y$	Soil's yield stress/strain	Random variable
TE	Tunnel's Younge's modulus	Random variable
Tν	Tunnel's Poisson's ratio	Random variable
$T\sigma_y/T\varepsilon_y$	Tunnel's yield stress/strain	Random variable
x	Lateral distance from tunnel centreline	Random variable
z	Depth below the ground surface	Random variable

Table 9. List of parameters in Class 1 reliability analysis for buildings with shallow foundations

3.2.3.2 Buildings with deep foundations

There are two classes of reliability assessment for buildings with deep foundations.

SSRABD2: Short-term settlement risk evaluation for Class 2 buildings

Class 2 analysis is performed to evaluate the settlement risk of pile foundations with indices BD3 and BD2, while BD1 buildings are directly evaluated via Class 1 analysis due to the primary higher expected risk. To counterbalance the level of details and accuracy with time and computational cost, it is better to employ a more practical method to evaluate the response of the piles to the induced forces and bending moments using the design charts as described in Section 2.3.2.1.

The model for Class 2 settlement risk evaluation and parameters are depicted in Figure 32, while the parameters involved in this class of analysis are listed in Table 10. The volume loss model in SSRABD2 is identical to SSRABS3 therefore, volume loss parameters are not repeated in Table 10. The concept of design charts has been discussed in Chapter 2 and the charts are provided in Appendix I. It should be noted that the "basic" parameters and the correction factors are extracted from the design charts

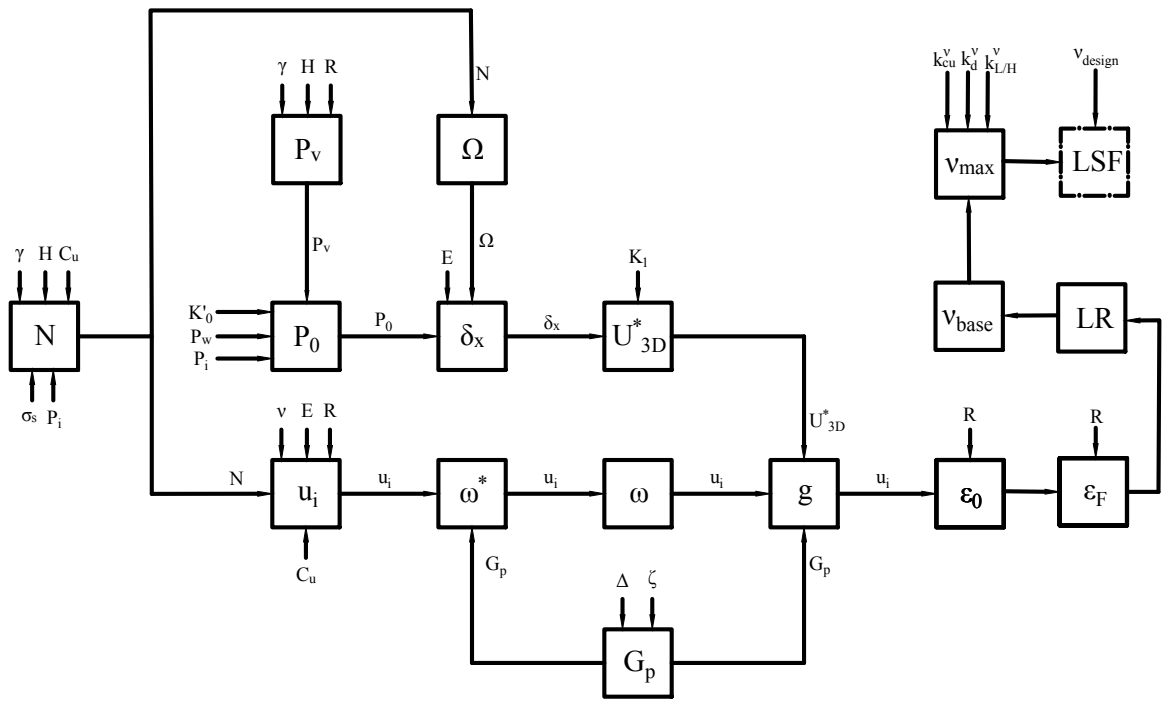

Figure 32. Model for Class 2 reliability analysis of deep foundations

Symbol	Description	Type
k_{cu}^{ν}	Settlement correction factor for undrained shear strength	Random variable
k_{d}^{ν}	Settlement correction factor for pile diameter	Random variable
$k_{L/H}^{\nu}$	Settlement correction factor for length to tunnel axis ratio	Random variable
ν_{design}	Design pile settlement	Random variable
R	Tunnel radius	Random variable

Table 10. List of parameters in Class 2 reliability analysis for deep foundations

visually therefore, there is a human error involved in addition to the uncertainty exist in modelling and developing of these charts, which requires them to be defined in the form of random variables.

The limit-state function for pile settlement is defined by comparing the sum of the design settlement ν_{design} and the tunnel-induced settlement $\nu_{induced}$ with the threshold

value of $10\ \mathrm{mm}$ from a damage classification (*e.g.* CIRIA PR30, 1996). The limit-state function for "negligible" damage based on CIRIA PR30 is:

$$\mathrm{LSF}_{\mathrm{Class\ 2}} = 10[\mathrm{mm}] - (\nu_{\mathrm{design}} + \nu_{\mathrm{induced}}) \qquad \textit{(Eq. 3-18)}$$

By performing reliability analysis, we obtain the exceedance probability. If this probability of failure is more than a selected level (say 20%), then the building is transferred to Class 1 where it is evaluated through a more rigorous way using numerical analysis.

SSRABD1: Short-term settlement risk evaluation for Class 1 buildings

Similar to what has been proposed for buildings on shallow foundations, a numerical model addressing the tunnel-foundation-structure interaction is employed due to the complexity of the geosystem and possibility of a high-level consequence. The sensitivity analysis is again significantly beneficial to provide a better insight about the most influential characters. The schematic view of the model is similar to what have proposed for buildings with shallow foundations nevertheless the parameter's details are different.

3.2.4 Updated building database and risk register

The risk evaluation analysis yields the exceedance probability (or reliability index) of the threshold value for each particular limit-state function. The risk associated to the settlement of buildings does not only depend on the exceedance probability, but also the limit-state function, used to evaluate the risk. As a result, it is necessary to include the building class given that the class of risk analysis and its index are included in the risk register. Risk register is a concise report exhibiting at-risk items as well as their associated risk and the status of the required countermeasures. Proper development, inscribing and updating this report is absolutely important for future reference and risk communication between different management levels. Table 11 shows the proposed risk register for the framework of RM.

Recalling previous discussion on the establishment of the building database, an ID is defined as "primary" entity. Defining the primary entity is obligatory in database

ID	Building index	Class of analysis	Exceedance probability	Mitigation measures				Last update
				Not needed (N)	Approved(A)	Initiated(I)	Completed(C)	
B10000001	BS1	Class 1	0.02	N				15/10/2019

Table 11. Risk register

development to link different characteristics defined using various reports in different chronological orders and even with different data types.

In addition to ID, the building index as well as the class of analysis are included. These two entities are requisite to properly interpret the exceedance probability of the building. The mitigation measures and their completion status are also a part of the database: the “approved” status means that the assigned counteract is approved by not yet “initiated”. The ongoing action is labelled as “initiated” and after completion is “completed”.

Table 11 includes example entries for a building. The format of the building ID is designed in a special way to address also other types of structures, *e.g.* tunnel, which may be appended to the database later. The first letter indicates the type of structure, for instance, “B” stands for buildings. The second two numbers show the foundation type, if applicable: 10 is for shallow foundations and 20 for deep ones. Therefore, the ID given as an example in Table 11 represents a building with shallow foundation. As such, the risk register provides us with an instant knowledge about the building type (from the ID) and the classes. The time of last update is to be used for future references to the database.

The three pillars of a RM framework should be used during design and construction of the tunnel. The associated risk of tunnelling is not only during the construction; in fact, a considerable risk threatens the system during the operation of the system especially in

soft grounds in urban areas. Therefore, another framework is required to identify the risk and deal with it even after completion of the tunnel.

3.3 Risk management framework during operation (long-term)

3.3.1 Risk identification

The risk of long-term tunnel-induced settlement, in contrast to the short-term risk, is not only associated with the building and the overlying structures but also to the tunnel itself. The main focus of long-term RM will be on the mechanism of consolidation settlement, its causes and how to quantify it. The associated uncertainties will be addressed in risk evaluation section similar to what has been proposed for short-term RM.

As discussed in Chapter 2, many factors affect the long-term performance of a tunnel. However, the fundamental mechanism of the delayed ground movement is primarily the dissipation of excess pore pressure (either positive or negative) in soil around the tunnel induced by excavation and grouting. This problem needs to be addressed before we can assess the associated risk.

In comparison with other shield tunnelling methods (*e.g.* open shield), EPB reduces the ground movement significantly. When constructing a tunnel using EPB, the shield, the cutting wheel and the lining provide the support in different parts of the tunnel to maintain the equilibrium of the system. Higher or lower forces or displacements will induce excess pore pressure in the ground and cause ground movements eventually. The face pressure is usually slightly higher than the exerted overburden pressure to minimize the ground loss and the associated settlement. The higher face pressure, however, will cause additional shear deformation of soil and excess pore pressure in front of the cutter wheel, which will be dissipated later and cause consolidation settlement. Therefore, over-pressurizing the tunnel face may diminish the ground movement during construction but may induce severe post-construction settlement. Tail voids are inevitable during tunnelling; a gap is formed due to the tunnelling process which is immediately filled with grout. However, not only the compaction grouting exerts stress on the surrounding soils generating excess pore pressure, the grout itself may shrink and dewatered. The higher the amount of grout and the higher the grouting pressure during

injection, the more the induced consolidation settlement subsequently. Excessive backfilling is another contributor to the consolidation settlement of the tunnel.

In addition to the effect of excess pore pressure dissipation, long-term ground settlement may be induced by other mechanisms. Leaking of the tunnel liner and groundwater level variation have been identified as factors causing long-term settlement (Shen *et al.*, 2014).

The tunnel lining is designed to sustain the surrounding ground soil by undergoing designated strains. These designated strains do not imperil the tunnel. However, under some circumstances, unexpected additional stresses on the tunnel lining may lead to uneven deformation and damage the water tightness of the lining. A longitudinal differential settlement is one of the reasons. Moreover, groundwater drawdown due to urbanization leads to subsurface settlement. Development in cities forms a great amount of surcharge on tunnels. All these factors contribute to differential settlement.

The differential settlement may also be induced by soil layer alteration. The tunnel may pass different soil layers intersecting the tunnel line. When the material properties (*e.g.* permeability and compressibility) of these soil layers are significantly different, the rest of the settlement of different tunnel sections may vary, which amplifies the differential settlement.

Recently, studies have been conducted to investigate the effect of train-induced stress and the generation of excess pore water pressure in soil and the long-term settlement (*e.g.* Haung *et al.*, 2018). The loading caused by train passage and the low permeability of the soft clay leads to continuous accumulation of the excess pore water pressure. Even though the quantity of the excess pore water pressure and soil deformation due to each single passage is low, the accumulation of deformation over time makes notable accumulative settlement induced by cyclic train loading.

3.3.2 Risk analysis for long-term settlement

3.3.2.1 Influence diagram analysis

The risk identification for long-term settlement shows that various events affect the development of long-term settlement. In addition, the influences of those factors are

coupled. The influence diagrams can be used to address the relations between various factors, including interconnections and possible consequences.

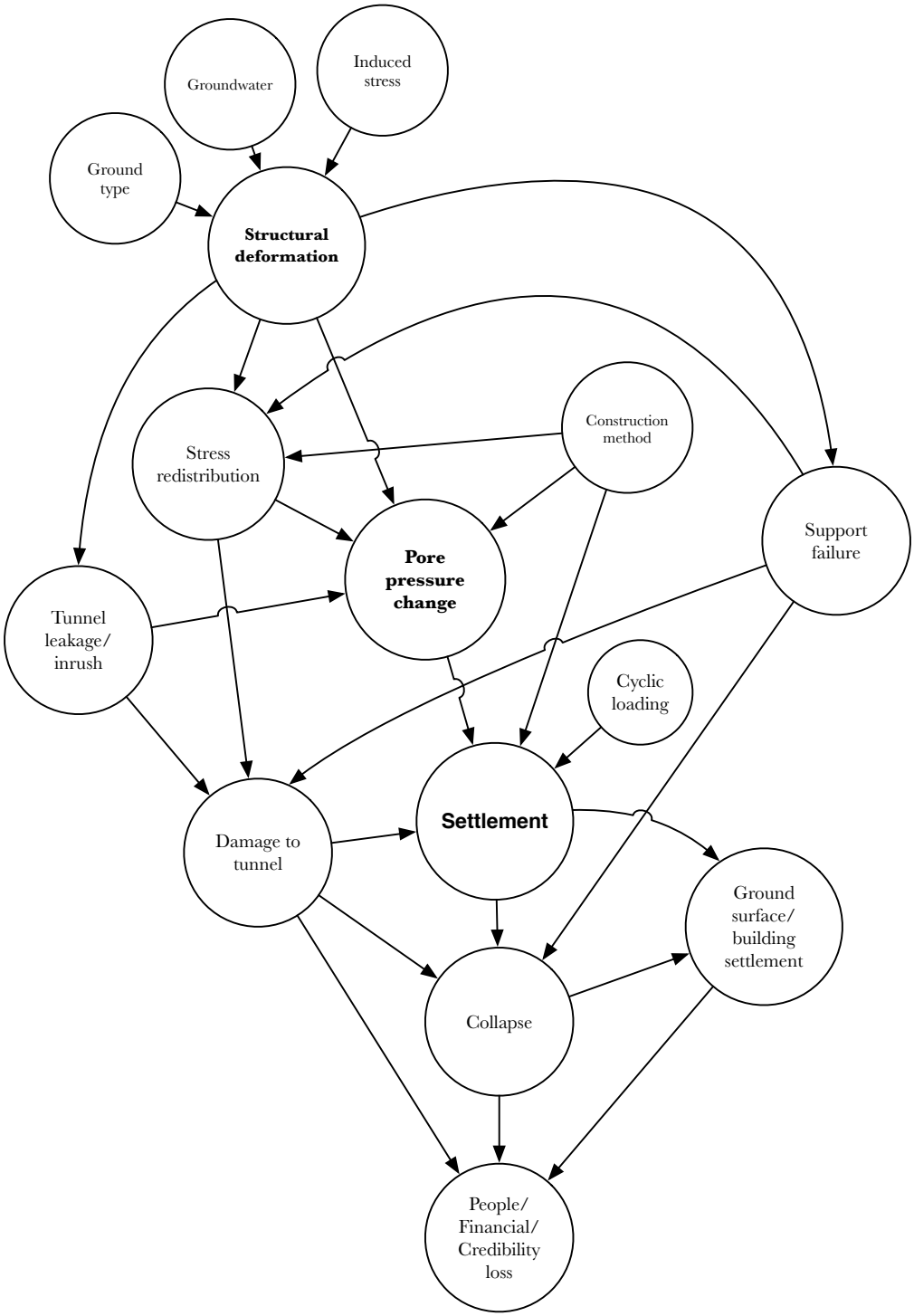

Figure 33. Influence diagram of long-term tunnel settlement

Figure 33 depicts the influence diagram of the long-term settlement in soft clay. The influence diagram shows how different base factors influence and stimulate the next ones to forms a cascading situation leading to different catastrophic consequences *e.g.* loss of lives. The advantage of influence diagrams is that they are able to represent causes and effects as well as the relationships all in one place. Therefore, an influence chart can be used for a consequence analysis.

Two main influential factors of the influence diagram in Figure 33 are structural deformation and pore water pressure. The type of soil, the amount of surcharge, the depth of the cover (*i.e.* the depth of the overburden) and the groundwater level are all influential factors for the stresses developed in soil. As mentioned before, the structural deformation causes variation of stresses and pore water pressure in the tunnelling zone. It also increases leakage of the tunnel lining and facilitates consolidation settlement. Extremely severe structural deformation may even lead to failure of tunnel segments or even partial collapse.

The method of excavation (*e.g.* open-shield, slurry or EPB) imposes different stress conditions on the tunnel face and the surrounding soil. Cyclic loading induced by trains contributes to accumulative consolidation settlement, as discussed previously.

3.3.2.2 Fault tree analysis

Although influence diagram is able to provide us valuable information about the structure of the problem, it is inadequate to deliver in-depth details. Therefore, for a multi-level risk analysis, it is necessary to consider the causes in a more systematic way, for instance, by developing a fault tree diagram. Figure 34 shows a fault tree diagram demonstrating the main contributors of the ground subsidence as well as the possible causes.

In Figure 34, seven major causes are considered for ground subsidence as the common and most problematic sources. Significant differential settlement is often observed at the connections between tunnels and station. There are different stress and pore pressure regimes adjacent to the tunnel-station connection due to the different structural types and different construction method. In addition, the waterproofing methods are not the same for different construction techniques. As such, the connection between the tunnel structures is prone to differential settlement and

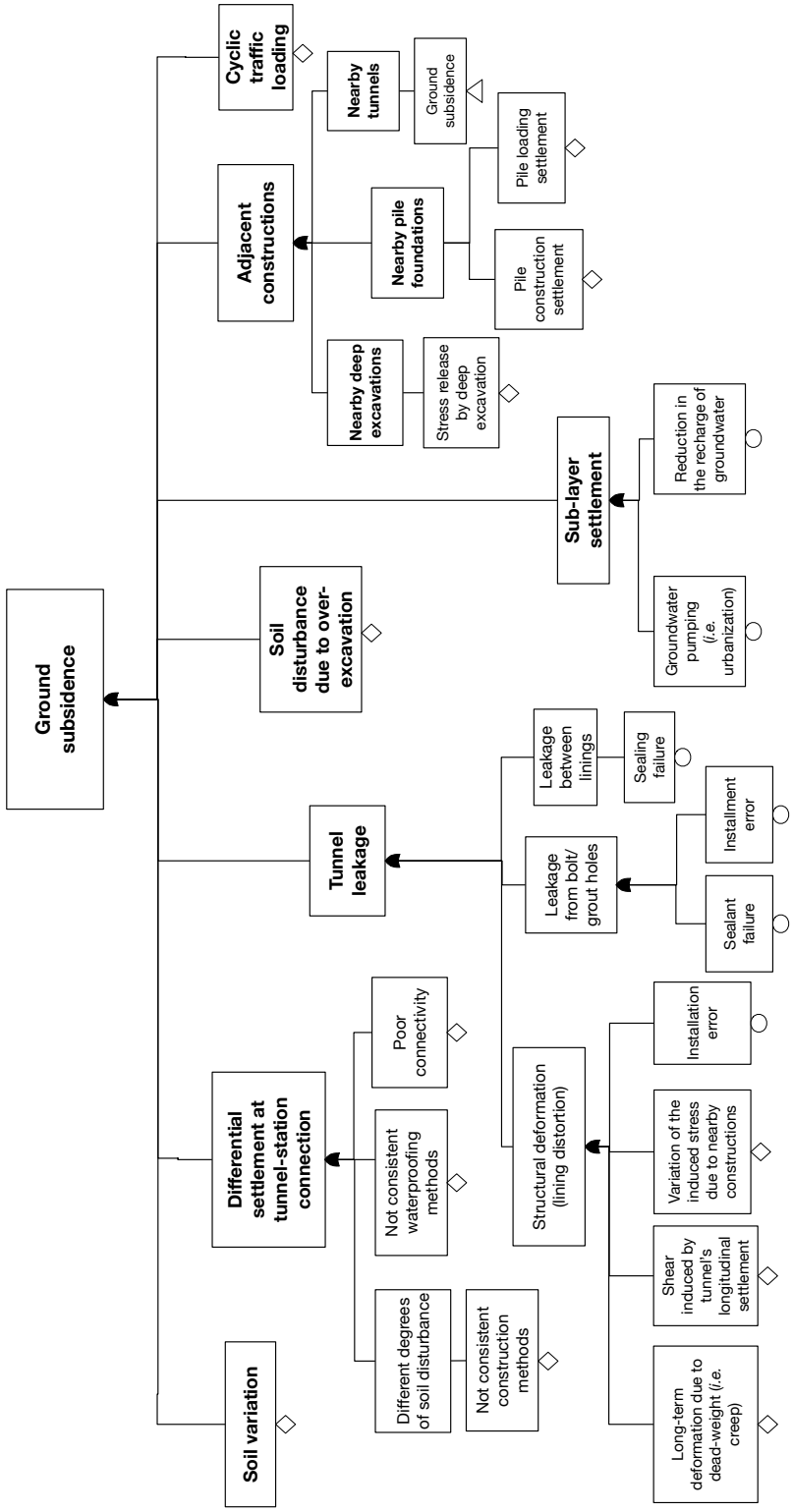

Figure 34. Fault tree analysis for long-term settlement

structural damage. As it is previously stated, tunnel leakage changes the pore-pressure regime by dissipating the excess pore water pressure, leading to an increase in the effective stress and subsequently a settlement. This leakage may be due to either excessive lining deformation or failure of the watertight at joints of concrete lining.

This fault tree analysis provides a descriptive, mathematical tool to know the main contributor to ground subsidence and their causes. By knowing the likelihood of the base faults, a bottom-up calculation will provide us the total probability of subsidence. An example of the fault tree analysis will be provided in Chapter 5.

3.3.2.3 Event tree analysis

Fault tree analysis is the most efficient approach to assess the probability of failure of a system, by knowing the probability of failure of each "component". However, it suffers from lack of flexibility in defining what-if scenarios. Therefore, event tree analysis may be used as a complementary tool to fault tree analysis to define possible scenarios after the occurrence of a particular event. In other words, fault tree analysis is the best tool to address the post-event risk, while event tree analysis is the most efficient tool for pre-event risk analysis and scenario development.

Considering the initial event as just the existence of a tunnel in soft ground may trigger a few sub-events. For instance, a tunnel may be constructed by driving EPB in a single layer or through multiple soil layers. Two tunnels with the same configuration may have different settlement mechanisms. The tunnel constructed in single layer generally has less differential settlement than the one passing through multi-layers of soils (see Figure 35).

An event that requires special attention is the differential deformation of a tunnel below a river. Seasonal variation of water level in the river tends to affect the effective stresses in the ground and hence tunnel deformation, depending on the ground soil properties, particularly the permeability. When a section of tunnel, connecting to a train station, is built in multiple soil layers under the downtown area, most severe differential settlement tends to occur.

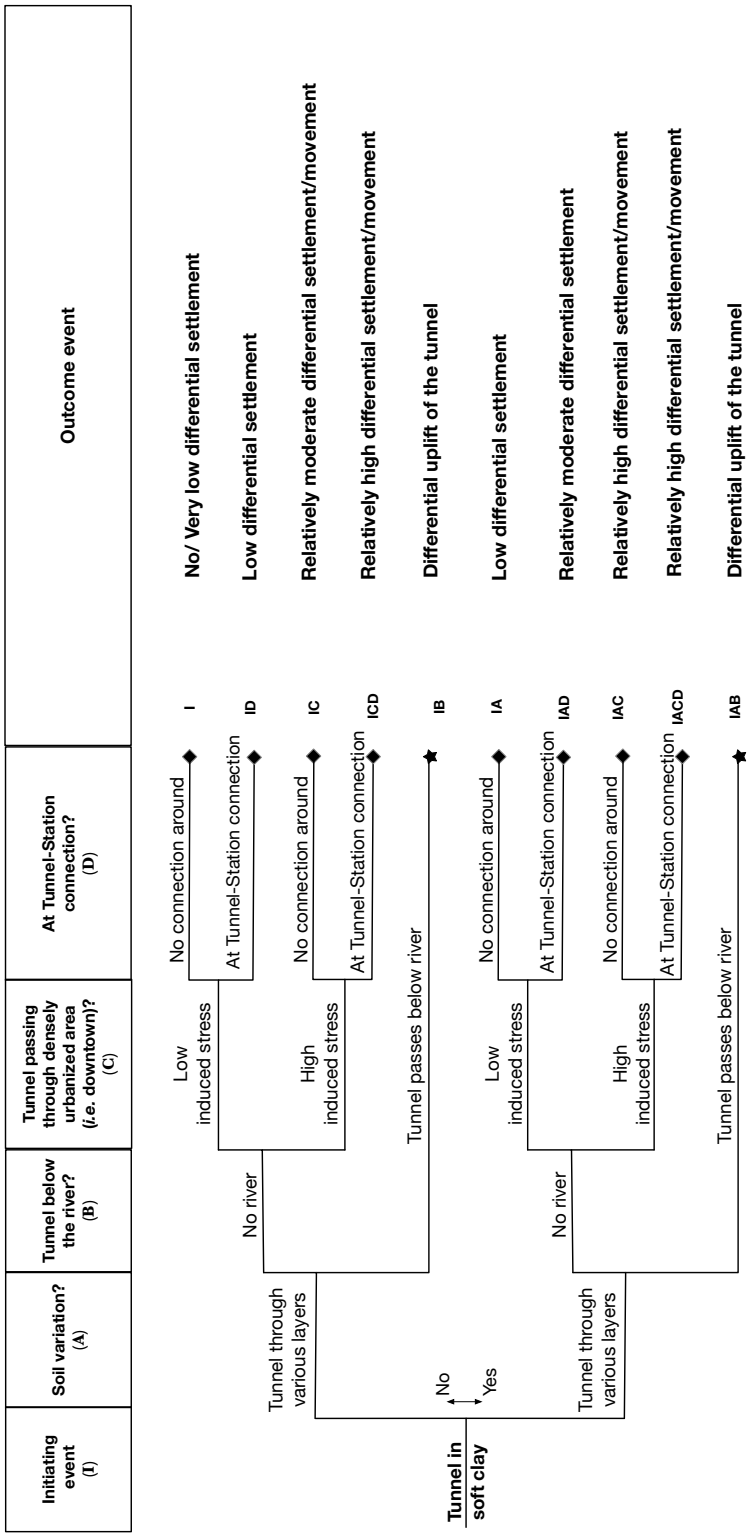

Figure 35. Event tree analysis for long-term settlement

According to the event tree (Figure 35), event I corresponds to the lowest differential settlement. For the other events, a quantitative comparison is required to check which event contributes more to long-term settlement and which scenario has the highest occurrence probability, as a part of the event tree analysis. As mentioned before, event tree analysis is a common analytical tool in many fields for pre-event analysis providing the event probabilities. An example of how to use the event tree is provided in next chapter.

3.3.2.4 Consequence tree analysis

A consequence tree is analytically identical to an event tree. However, the goal of consequence analysis is to describe the post-event situations, similar to a fault tree. In other words, if "differential settlement" is located at the core event of a bow-tie diagram with two wings, the event tree is on the cause wing and the consequence tree is on the consequence wing.

Herein, the consequence of having a differential settlement is taken into account to see how far this initial event can provoke following events and what are the repercussions (Figure 36). The immediate consequence of differential settlement is considered as the first subsequent event, leading to tunnel leakage, eventually ground surface settlement and surface building damage. The ground subsidence and ground surface settlement are introduced as two events. In this way, it is possible to capture the effect of the depth and movement propagation that actually induces the surface settlement. For a deeply buried tunnel, the effect of the differential settlement of the tunnel may not reach the ground surface and cause no damage to surface buildings.

The probability of each scenario is determined from the probability of the preceding complementary events. If the events are considered as independent (no correlation), then the probability of an outcome event is the multiplication of the probability of the MECE (mutually exclusive and collectively exhaustive) events.

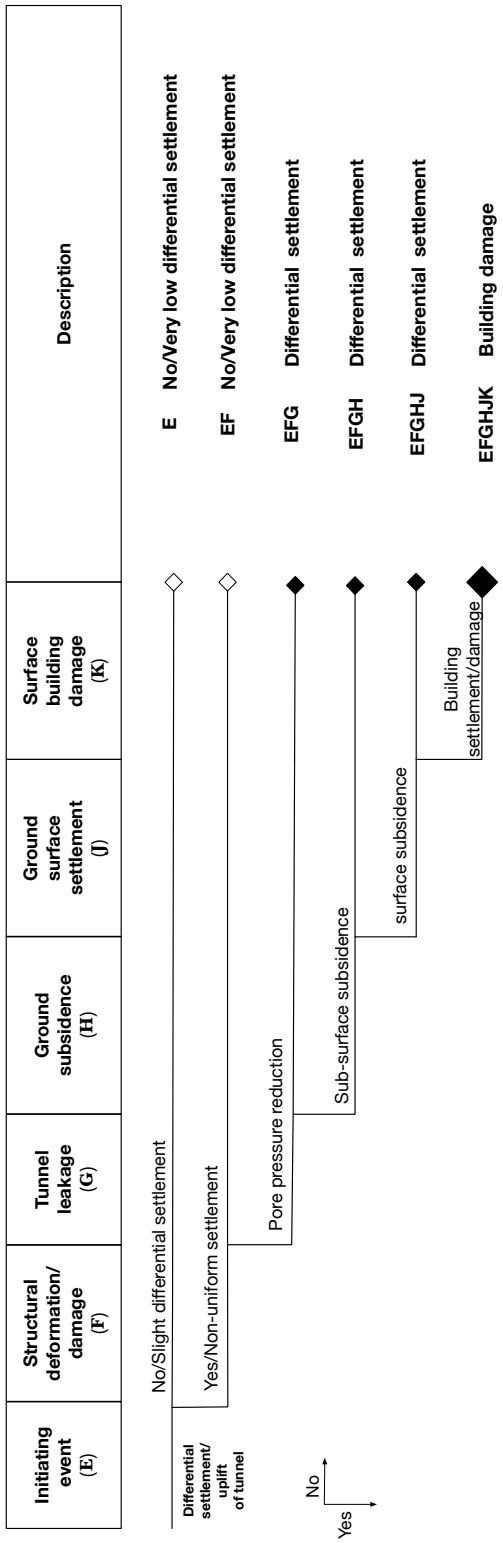

Figure 36. Consequence tree analysis for long-term settlement

3.3.3 Risk evaluation

The outputs of the event tree and consequence tree analyses inform us about the severity of the differential settlement in different tunnel sections. This information can be used to classify the overlying buildings in different sections of a tunnel, into two classes. Critical buildings *i.e.* the buildings that, according to event tree analysis, are located above the sections with relatively high differential settlements (*e.g.* events ICD and IACD) are evaluated in Class 1 long-term settlement risk analysis (LSRAC1) and buildings with less critical situations are evaluated in Class 2 long-term settlement risk analysis (LSRAC2).

Similar to the risk evaluation for the short-term settlement, the risk evaluation for long-term settlement involves quantifying the risk using probabilistic methods. The multi-level risk due to parameters, models and results are determined and the effect of these uncertainties are evaluated, in the form of an exceedance probability. Again, the workflow will be presented in the form of a flowchart. By completing this section, it is possible to integrate the results of the short-term and long-term analyses and to evaluate the risk of total settlement which will be addressed in an example in Chapter 4.

LSRAC2: Long-term settlement risk analysis for Class 2 buildings

LSRAC2 utilizes the method proposed by Laver *et al.* (2016) to estimate ground movement at different locations, as cited in Chapter 2. Laver *et al.* (2016) proposed a procedure to calculate the long-term movement of the surface, considering the effect of the tunnel underneath. This section will focus on the model and the parameters needed for reliability analysis.

The procedure starts by defining the dimensionless surface settlement (DS). According to the Laver *et al.* (2016), DS is equal to zero for a fully impermeable lining. In order to address the problem of tunnel leakage, an equivalent tunnel permeability can be estimated, by assuming that the permeability of a broken watertight follows Cubic Law (Witherspoon *et al.,* 1980).
The tunnel equivalent permeability is then defined as:

$$k_{t\_equ} = \frac{n * k_{joint} * s_j + k_{concrete} * (t_p - n * s_j)}{t_p} \qquad \textit{(Eq. 3-19)}$$

with

$$k_{joint} = \frac{g s_j^2}{12 \upsilon_w} \qquad \textit{(Eq. 3-20)}$$

in which n is the number of joints/segments, g is gravitational acceleration of earth, s_j is the aperture of the watertight between two adjacent segments, υ_w is the kinematic viscosity of water, $k_{concrete}$ is the permeability of the tunnel segment (which is assumed to be zero in our analysis), and t_p is the tunnel outer perimeter. The tunnel equivalent permeability k_{t_equ} is then substituted with tunnel's permeability in the method proposed by Laver *et al.* (2016). Then, the maximum settlements, horizontal displacement and tensile and compression strains are calculated and eventually the settlement or, in general, movement at any distance. Table 12 summarizes the parameters and their descriptions. The model for LSRAC2 is shown in Figure 37.

Symbol	Description	Type
s_j	Watertight's joint	Random variable
g	Gravitational acceleration of earth	Constant
ν_w	Kinematic viscosity of water	Random variable
n	number of segments/joints	Constant
ε_0	Volume loss	Random variable
D	Tunnel diameter	Random variable
γ_w	Unit weight of water	Constant
k_h	Horizontal permeability of soil	Random variable
k_v	Vertical permeability of soil	Random variable
t_L	Thickness of the lining	Random variable
C_{clay}	Clay cover depth	Random variable
H	Depth of tunnel axis	Random variable
t	time	Constant
E'_d	Equivalent drained stiffness of soil	Random variable
L_c	Depth of tunnel axis below water table	Random variable
x	Horizontal distance from tunnel centreline	Constant

Table 12. List of parameters in Class 2 reliability analysis for long-term settlement risk assessment

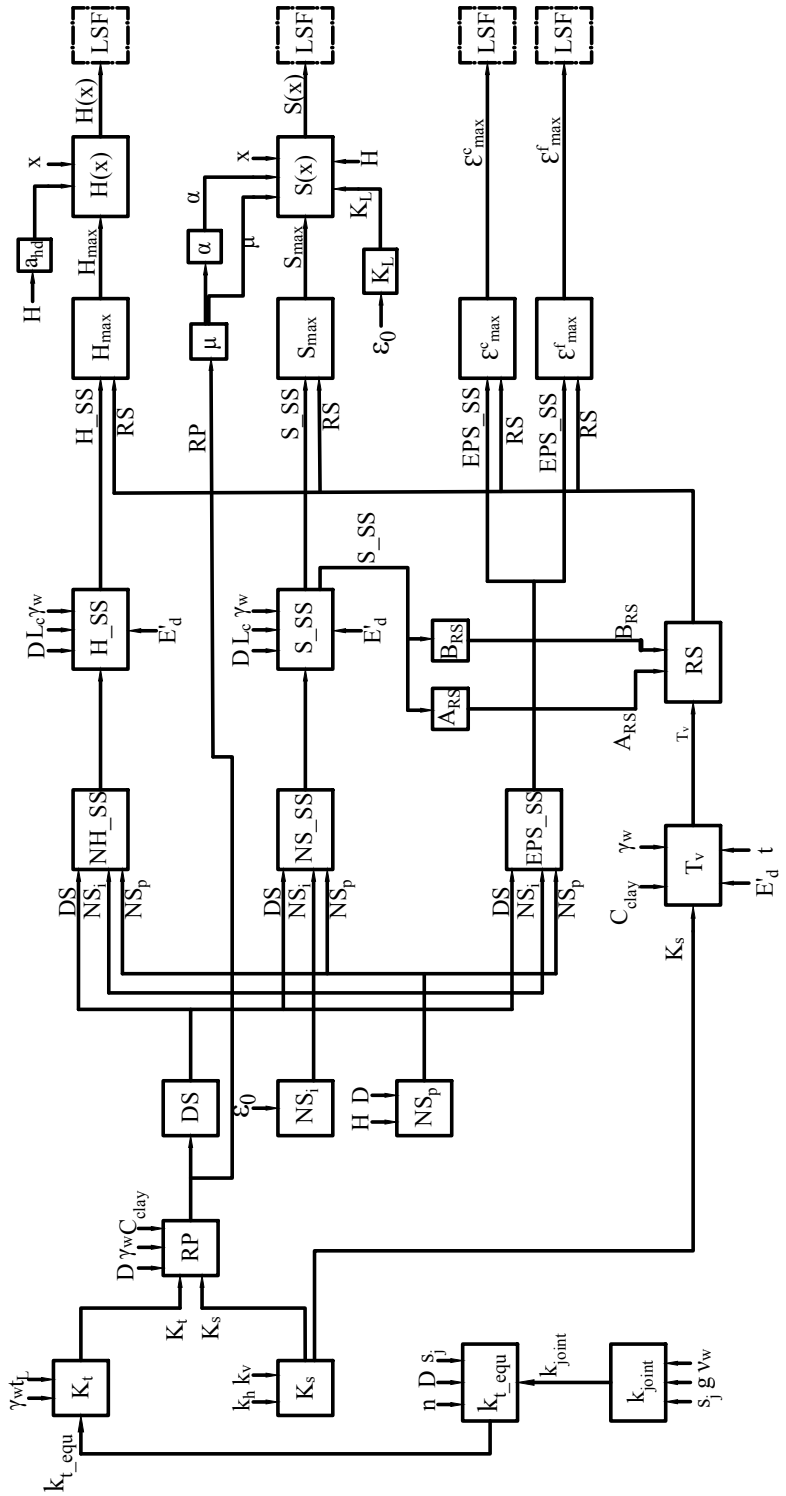

Figure 37. Model for Class 2 reliability analysis for long-term settlement

Laver *et al.* (2016) introduced a nondimensional settlement parameter $\mathrm{NS_i} = -4.4\varepsilon_0$, for the case of having fully impermeable lining. For a fully impermeable lining in stiff clay, shearing induces dilation and negative excess pore water pressure, which in long term results in heaving. This is shown by a negative sign in their proposed formula. This behaviour is opposite in soft clays and shearing induces compaction which leads to settlement in long term. This is modified in our model by changing the sign and the magnitude of the $\mathrm{NS_i}$ formula, based on assuming that the behaviour is opposite but with different correlation to volume loss ε_0. This assumption needs further analyses and field data to be verified which is out of the scope of this research. For our risk analysis, we assume that the nondimensional settlement parameter is $\mathrm{NS_i} = 2\varepsilon_0$. Further details are provided in Chapter 4.

LSRAC1: Long-term settlement risk analysis for Class 1 buildings

Similar to SSRABS1 and SSRABD1, this class of settlement risk analysis required numerical modelling (*e.g.* FEM) of the soil-tunnel interaction to obtain detailed information of the system, including stresses, excess pore water pressure, ground and tunnel deformation (one may refer to the descriptions in previous sections).

Figure 38 depicts the workflow of performing risk assessment for long-term settlement risk. This framework starts with classifying buildings based on the results of the event tree analysis and calculate the corresponding settlement risk via the designated class.

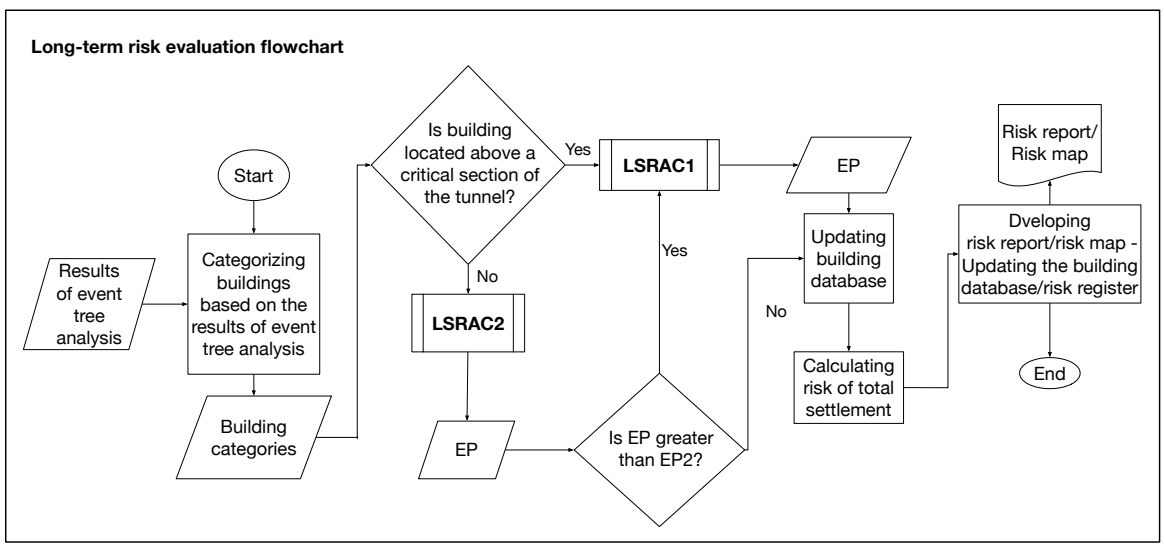

Figure 38. Risk management framework for long-term settlement risk

3.4 Limitations of the proposed risk evaluation methodologies

Different classes of risk evaluations (*e.g.* SSRABS3, SSRABS2, *etc.*) have been proposed to evaluate the risk of settlement of the surface buildings. The proposed limit-state functions are introduced, based on the foundation type, in order to evaluate the risk of damage to the surface buildings. It is possible to define other limit-state functions to address the risk of damage to surface structures based on other modes of deformation (*e.g.* tilt, rotation, *etc.*). The accuracy and the level of the details, encapsulated in each class of risk evaluation, depends on the class of evaluation. The class of evaluation is selected according to the building score. For instance, for BS3 buildings, a closed-form solution is used to calculate the ground settlement. In this method, the soil behaviour is simplified and the effect of the stress state, stress history and constitutive parameters are not considered. Consequently, this closed-form solution (*i.e.* SSRABS3) only provides an approximation to the actual surface settlement which can only be used for buildings with low vulnerability. SSRABS3 methodology tends to oversimplify the risk of settlement, which may lead to disastrous consequences for sensitive buildings. Another important point to mention is about the validity of parameters, defined in each risk evaluation class. For instance, the stability number N, may not be used for the face of the tunnel for very deep tunnels.

For BS2 buildings (which are more critical than BS3 buildings), it is proposed to evaluate the developed critical strain $\varepsilon_{\mathrm{critical}}$ (Burland and Wroth, 1974). Critical strain is a more accurate indicator of the tunnel-induced damage to the surface buildings comparing to the green-field surface settlement. However, SSRABS2 is not proposed for very critical buildings (*i.e.* BS1). Assuming building as a simple, isotropic, linear-elastic beam and neglecting the soil-structure interaction introduce errors in prediction of the foundation behavior, which may cause catastrophic consequences for sensitive buildings. Numerical modelling can address the effect of the stress state, stress history, soil-structure interaction as well as the progressive induced deformation due to tunnelling. However, the numerical modelling is computationally expensive and time-consuming. This is the reason that numerical modelling is only proposed for the critical buildings (*i.e.* Class 1 buildings).

The limitations on using the proposed framework for settlement risk calculation is restricted to the applicability of the method used for settlement calculation. For instance, the gap parameter proposed by Lee *et al.* (1992), used in our SSRABS3 and

SSRABD2 models, is valid for fully saturated soft clay. The assumptions behind the proposed relation for gap parameter may not be valid for the cases of partially saturated soft soils. Geometry of the tunnel (*i.e.* depth to radius ratio $\mathrm{H/R}$) is another important indicator for applicability of the settlement calculation methods. SSRABS3 and SSRABD2 may not provide reliable results in cases of having very small or very large $\mathrm{H/R}$ ratio.

3.5 Outcomes of the RM analyses

The outcomes of RM analyses can be presented using risk registers and risk maps. Risk register can be a report, generated from the building (structure) database, after the database has been updated with the results of risk analyses.

3.5.1 Updating building (structure) database

A risk register has already been proposed in short-term risk analysis. If the short-term risk register is available at the time of performing long-term risk assessment, it would be beneficial to update this risk register with the calculated risk associated with the long-term settlement (Table 13).

ID	**Building index**	**Building score**	**SSRA**		**LSRA**		**Mitigation measures**					**Last update**
			Class of analysis	Exceedance probability	Class of analysis	Exceedance probability	**Action required**	**status**				
								Not needed (N)	Approved(A)	Initiated(I)	Completed(C)	

Table 13. Updated building database

The risks associated with short-term and long-term settlements can eventually be integrated to assess the risk of total settlement. The limit-state function of the total settlement can be established using any damage classification *e.g.* CIRIA PR30 (1996). In this way, the uncertainties involved in parameters, models, and even human factors are taken into account. Three types of uncertainties cited previously in this work are all evaluated in different levels, for spatial variation, parameter uncertainty, model uncertainty and even human behaviour.

3.5.2 Developing the risk map

Risk maps are another type of risk communication tool, which provides valuable information regarding the settlement risk. Herein, the risk map can be produced by combining the short-term and long-term settlement risk data. Figure 39 shows an example of a risk map in which different buildings with different classes and different exceedance probabilities are depicted with different colours. This map provides a quick and informative mean of risk communication. It is also possible to project the tunnel line on the risk map to realize which sections of the tunnel are located in high risk zone and which section is in low risk zone. In this way, it is possible to extend the concept of zoning into the tunnel lines and show them with different colour codes, based on their associated risk of settlement. It is also informative to sign the critical points (*e.g.* the connection between tunnel and station) with a specific symbol on the map to show their locations (see Figure 40).

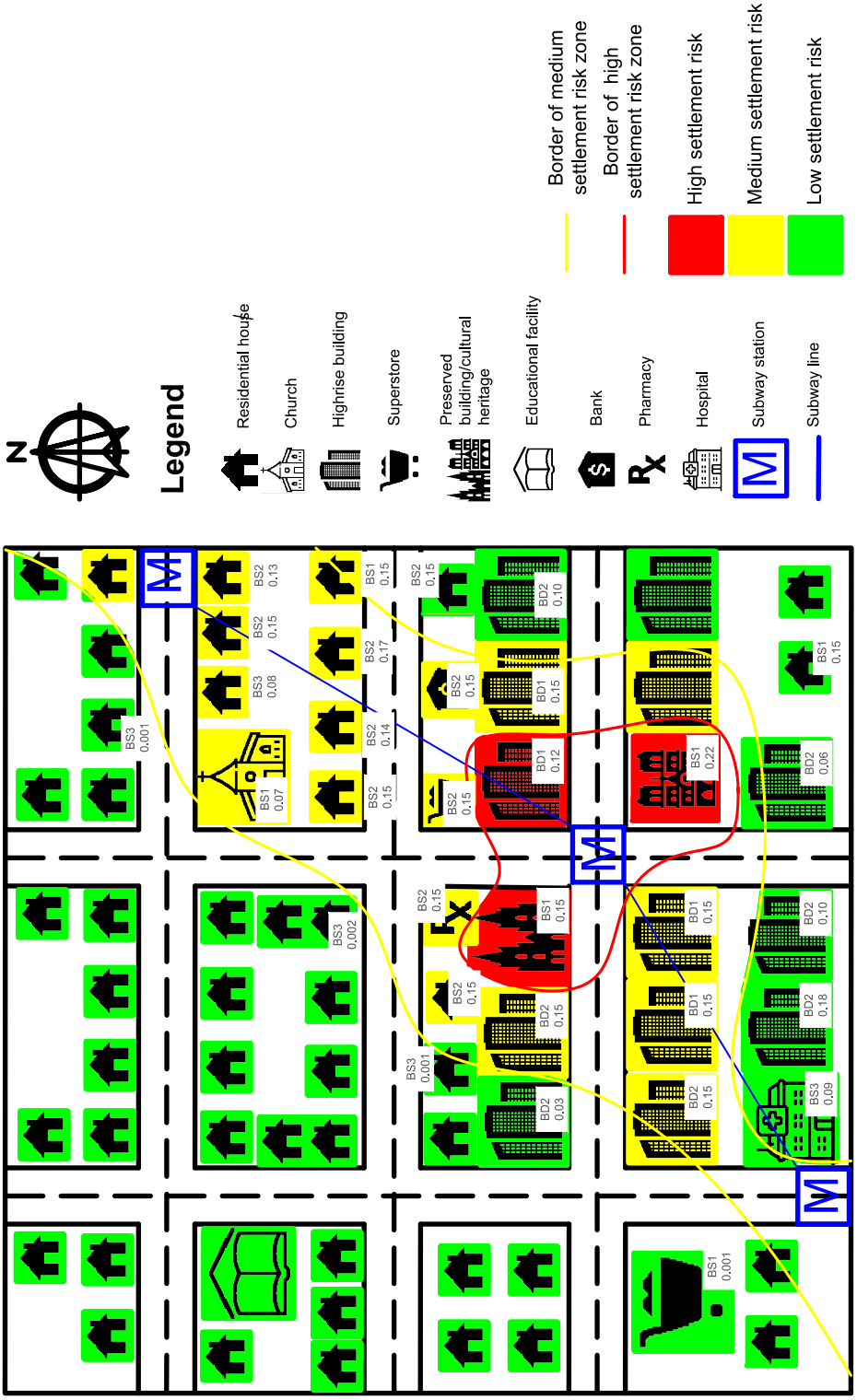

Figure 39. Risk map – an example

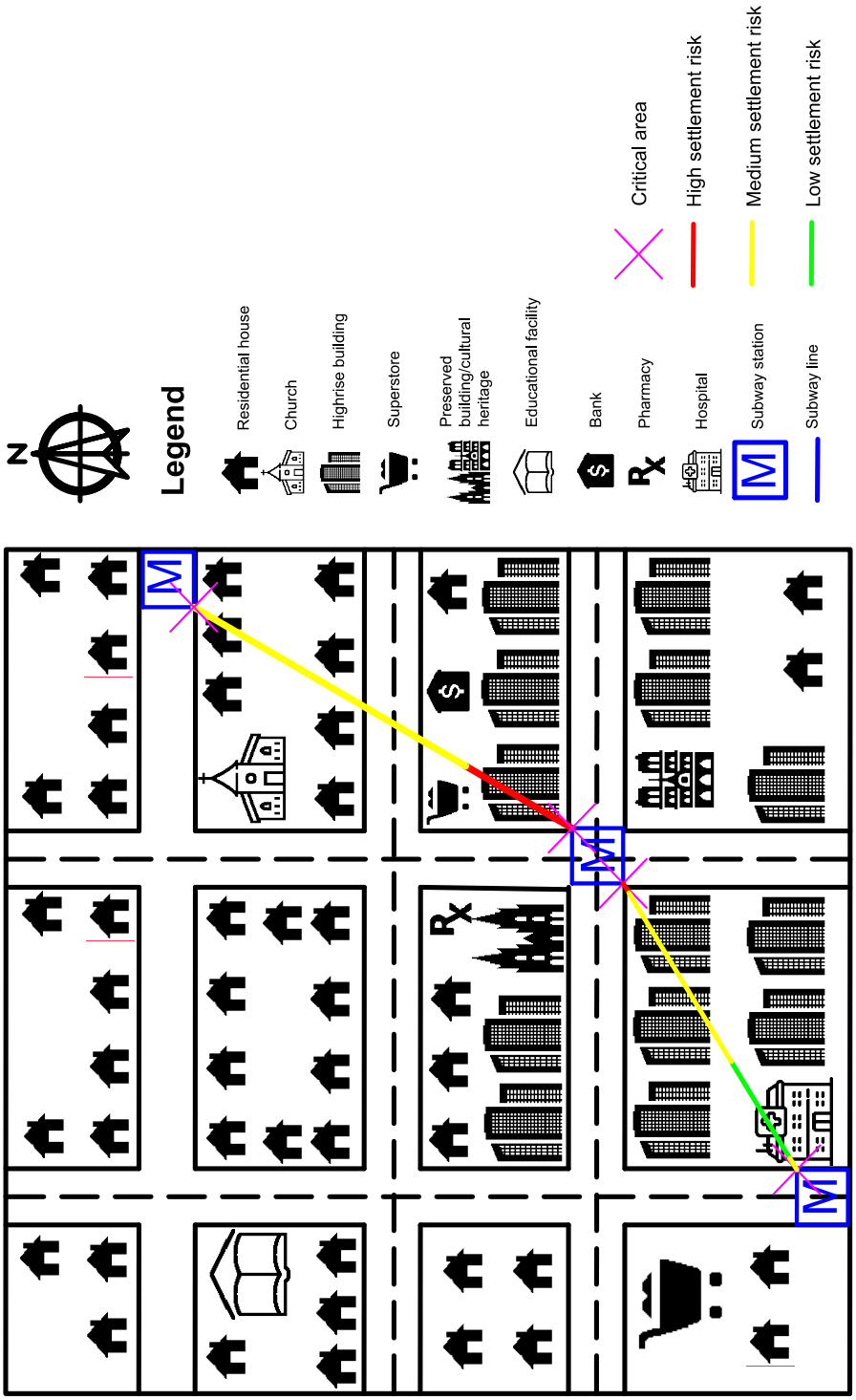

Figure 40. The settlement condition of tunnel and the critical areas – an example

Chapter 4. Implementation of the multi-class risk analysis

In this chapter, the framework for multi-class risk analysis developed in Chapter 3 is implemented in an example problem. Each step of the framework is demonstrated and the final probability of failure (or reliability index) is reported. No specific effort is made for the selection of the values of the parameters and the threshold values of the limit-state functions, which are technically left to the discretion of the analyst or to be determined by various agencies for different types of projects. The examples only demonstrate the procedures of risk analysis and are not real case studies. Moreover, the preparation parts, *e.g.* pre-tunnelling indexing, are not presented here since they have been discussed in detail in Chapter 3.

Rt risk tool is utilized in this chapter to perform the reliability calculations. It is a non-commercial reliability and optimization facilitator developed in C++ (Mahsuli and Haukaas, 2013). Rt is capable of performing FOSM, FORM, SORM and sampling analysis. It also provides ranking for model's parameters based on the alpha and gamma importance vectors. The software also provides the bridge between the external software suites performing the numerical analysis (*e.g.* ABAQUS, ANSYS, *etc.*) and the reliability calculations. It recalls the FE solver many times to perform the numerical modelling for statistical analyses. A number of built-in probabilistic models (*e.g.* Poisson's pulse model, moment magnitude, simple damage curve, *etc.*) are included in the software's library. Nevertheless, the software permits the analysts to define their own models. The software is also suitable for designing purposes. For instance, the value of a decision variable (*e.g.* amount of grout) can be determined by optimization. The availability, flexibility, reliability and agility of the software makes it one of the options available for performing reliability analysis.

The parameters are defined as either constant or random variables. Then, the parameters are gathered together to form the models. The output of one model becomes the input of the next one up to the final model which is used in the limit-state function. Therefore, the inputs of our reliability analysis are random variables, functional forms of the models, and the limit-state functions. The outputs are exceedance probability and reliability index.

4.1 Example of short-term risk management

4.1.1 Risk analysis

In this example, we assume that the tunnel projection and pre-tunnelling building indexing have been completed as described in Chapter 3. Consequently, we start by fault tree analysis for short-term risk evaluation.

4.1.1.1 Fault tree analysis

(a) Straight section of a tunnel

Figure 21 represented the fault tree of the straight section of a tunnel. For this fault tree analysis, a probability of happening (failure) is assigned to each of the base events in the analysis (Table 14).

Base fault	Likelihood
Design fails to see soil variation	2×10^{-3}
Operator fails to act properly	5×10^{-3}
Operational error	1×10^{-3}
Bad grout mixture	1×10^{-3}
Grout pump fails	1×10^{-4}
Insufficient grout pressure	5×10^{-3}
Grout shrinkage	1×10^{-4}
Delay more than self-standing time	5×10^{-5}
Operational delay	1×10^{-3}
Grout pump failure	1×10^{-4}

Table 14. Short-term analysis: base faults of a straight section

Selection for some of the likelihoods in Table 14 requires socio-behavioural modelling and people-machine interactions. Some other likelihoods, *e.g.* pump failure, is usually

available by the manufacturer. However, some of these values may be disputable and require supplementary data for reliable estimates. For example, the probability of delay more than self-standing time may be much lower in tunnels excavated via EPB machines. However, one of the main goals of risk analysis is to consider the effect of the rare events.

After obtaining the probabilities of the base faults, the fault tree analysis can be performed in a bottom-up manner. The calculations are straight forward since we are only dealing with "OR" gates and the head event of each branch of the fault tree, consists of faults that are MECE. The probability of the head fault is then determined as the summation of the sub faults. In particular, the ground subsidence probability is calculated as:

$$\begin{aligned} \mathrm{P(ground\ subsidence)} &= \mathrm{P(face\ loss)} + \mathrm{P(shield\ loss)} + \mathrm{P(tail\ loss)} \\ &= (8 \times 10^{-3}) + (6.2 \times 10^{-3}) + (1.15 \times 10^{-3}) \\ &= 1.535 \times 10^{-2} \end{aligned}$$

Figure 41 shows the solved fault tree with the ground subsidence probability of 1.535×10^{-2}.

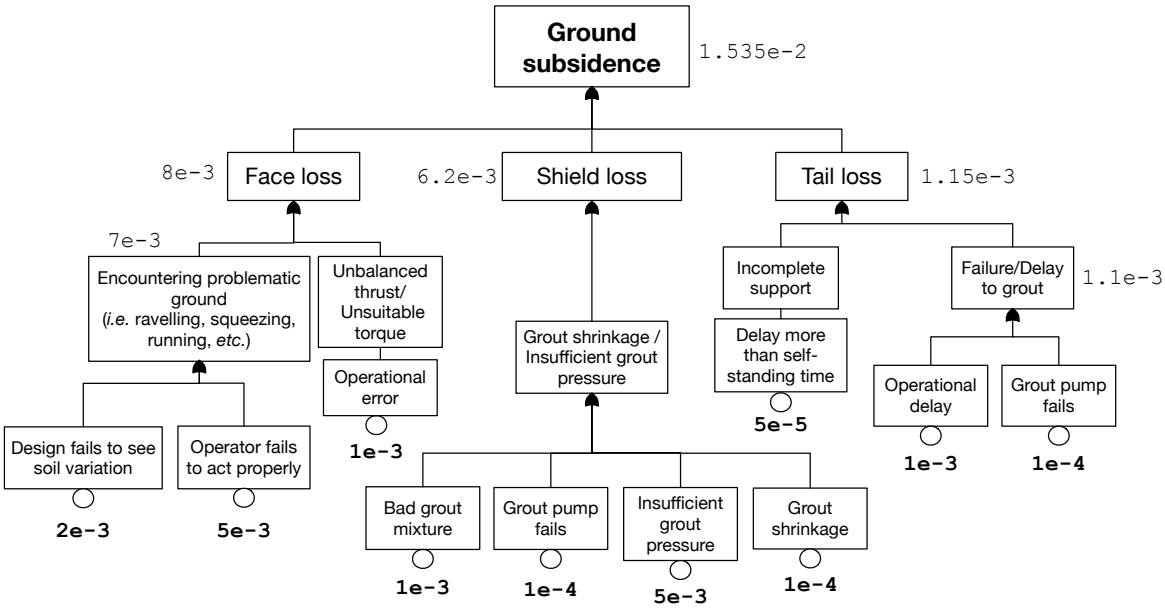

Figure 41. Short-term fault tree for straight section - solved example

(b) Curved section of a tunnel

The risk analysis for short-term settlement of curved sections of the tunnel can be performed following the fault-tree in Figure 22. In this analysis, the probability of the extra over-excavation is added under the shield loss. For fault tree analysis consisting AND gates, the cutsets have to be defined, with the probability $\mathrm{P(shield\ loss)}$ being calculated as

$$\begin{aligned}\mathrm{P(shield\ loss)} &= \mathrm{P(extra\ overexcavation\ \&\ bad\ grout\ mixture)}\\ &\quad +\mathrm{P(extra\ overexcavation\ \&\ grout\ pump\ fails)}\\ &\quad +\mathrm{P(extra\ overexcavation\ \&\ insufficient\ grout\ pressure)}\\ &\quad +\mathrm{P(extra\ overexcavation\ \&\ grout\ shrinkage)}\\ &= (6\times10^{-1}\times1\times10^{-3})+(6\times10^{-1}\times1\times10^{-4})+\\ &\quad (6\times10^{-1}\times10^{-2})+(6\times10^{-1}\times1\times10^{-4})\\ &= 6.72\times10^{-3}\end{aligned}$$

For a curved tunnel section, the likelihood of settlement induced by shield loss is relatively higher than that of straight sections, due to presence of more voids to be filled up with grout. Another way to determine $\mathrm{P(shield\ loss)}$ is to first solve the "OR" gate and then solve the upper "AND" gate:

$$\begin{aligned}\mathrm{P(shield\ loss)} &= (1\times10^{-3}+1\times10^{-4}+1\times10^{-2}+1\times10^{-4})*6\times10^{-1}\\ &= 1.12\times10^{-2}*6\times10^{-1}\\ &= 6.72\times10^{-3}\end{aligned}$$

As a result, the ground subsidence probability for curved section is:

$$\mathrm{P(ground\ subsidence)} = 1.587\times10^{-2}$$

as shown in Figure 42.

Over-excavation is somehow inevitable during excavations at curves. However, there might be cases where extra over-excavation happened due to operational errors, variable ground conditions, *etc.* Nevertheless, this fault has not developed further in the fault tree. Instead, a relatively high likelihood is assigned in this example.

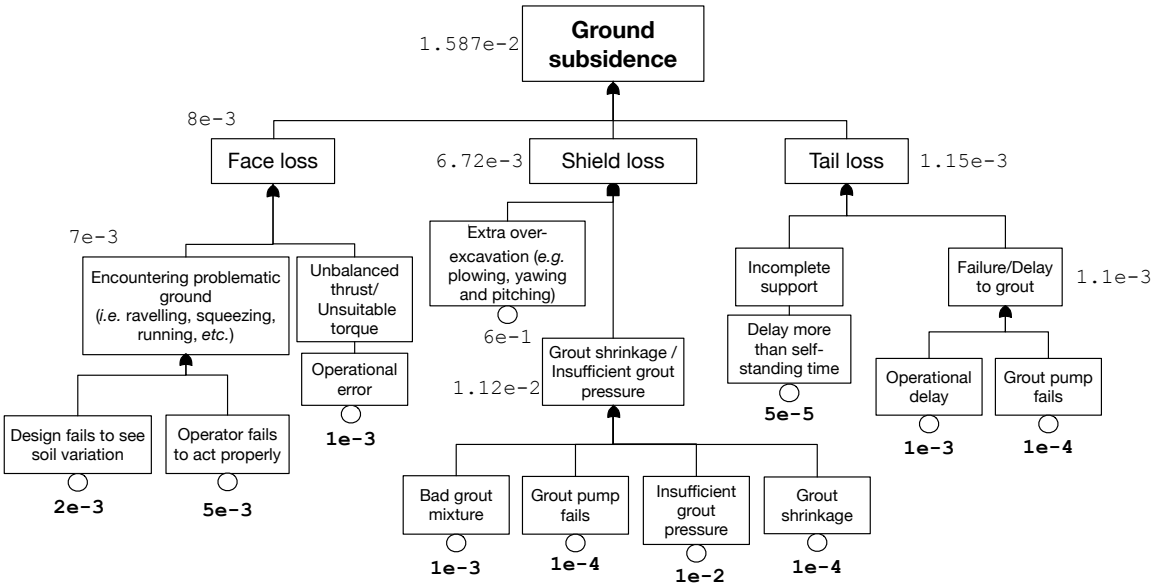

Figure 42. Short-term fault tree for curve section - solved example

4.1.2 Risk evaluation

Chapter 3 introduced different classes of assessment for short-term evaluation: three classes for shallow foundations and two classes for deep foundations. Different mathematical procedures have been developed for each class of risk assessment. In particular, Class 1 assessments for both shallow and deep foundations, are to be performed with the help of numerical modelling (*e.g.* FE simulations). The extent of analysis and the level of details required to perform this type of analysis is out of the scope of this research. However, as it is already stated, Rt risk tool is capable of recalling external FE software packages to perform FE analysis.

4.1.2.1 SSRABS3: Settlement risk evaluation for Class 3 buildings

As stated in section 3.2.2.3, the index of this class of buildings is BS3. Figure 29 presents the model used to perform the calculation, while the method by Loganathan (2011) is used to evaluate ground movement.

To perform the reliability analysis, the SSRABS3 model, as shown in Figure 29, has to be imported to the Rt risk tool environment. Rt risk tool is composed of two complementary parts. In the first part, all the random variables, constants, models and limit-state functions have to be defined. In the second part, the methodology and the mathematical tools required for evaluation are selected and then the analysis will be

performed. Table 15 shows the list of the parameters, their values and the labels used in SSRASB3 code.

The Rt risk tool is able to visualize the model's interconnections. In this way, not only the trace of the error propagation is detectible, but also a representation of a multi-level risk analysis is readily available. It shows how the parameters affect the models and how the models affect the upper-level models up to the limit-state function. In this class, three limit-state functions are defined to address the surface, the subsurface and the lateral movements. The graphical models are depicted in Figure 43.

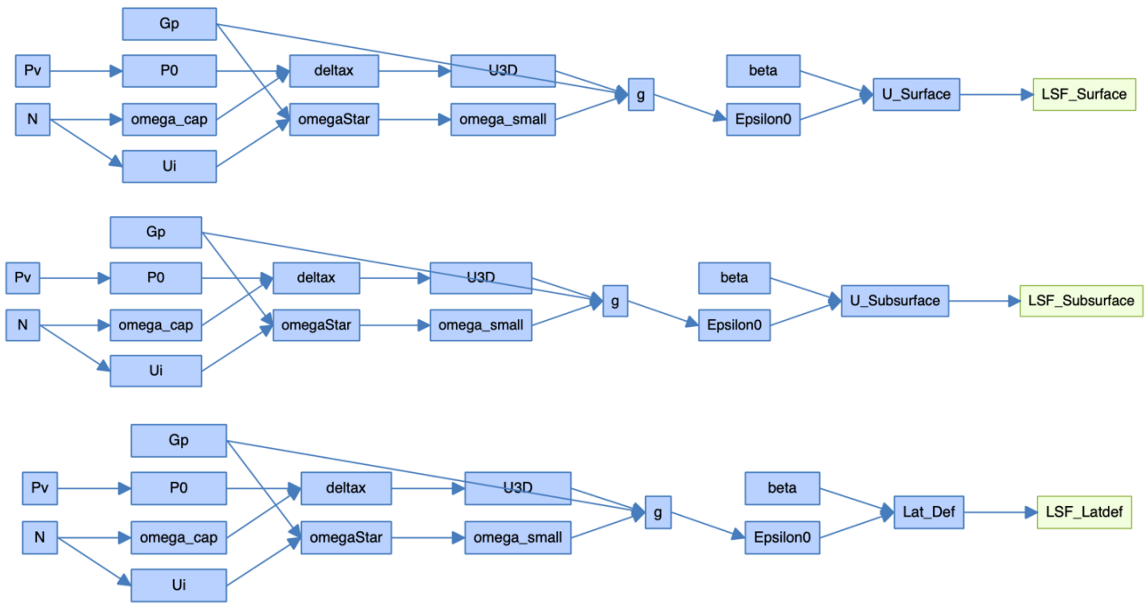

Figure 43. SSRABS3 - Rt risk tool model

The three models involved in Figure 43 are identical except for the last blue box on the right (*i.e.* U_surface, U_Subsurface and U_Def models). Different mathematical expressions are used to calculate the surface settlement, the subsurface settlement and the lateral deformation. Limit-state functions may be different based on the threshold that we define for settlements or deformation.

After defining the parameters, models and limit-state functions, the reliability analysis is performed. This is done under the tab "methods" in Rt risk tool. The available options are FOSM, FORM, SORM and sampling which are defined in Chapter 2. The results of the FORM analysis will be discussed in this section while the comparison of different

Symbol	Label	Distribution type	Descriptive parameters
H	H	lognormal	$\text{Mean} = 20\ \text{m}, \text{Std. Dev.} = 0.01\ \text{m}$
ν	Nuu	lognormal	$\text{Mean} = 0.48, \text{Std. Dev.} = 0.005$
R	R	lognormal	$\text{Mean} = 5\ \text{m}, \text{Std. Dev.} = 0.01\ \text{m}$
X	x	constant	$\text{Value} = 0$, above the tunnel centreline
Z	z_sub	constant	$\text{Value} = 0$, for surface movement
ϕ	phi	lognormal	$\text{Mean} = 35°, \text{Std. Dev.} = 1°$
γ	gamma	lognormal	$\text{Mean} = 17\ \frac{\text{kN}}{\text{m}^3}, \text{Std. Dev.} = 0.5\ \frac{\text{kN}}{\text{m}^3}$
C_u	Cu	lognormal	$\text{Mean} = 60\ \text{kPa}, \text{Std. Dev.} = 1\ \text{kPa}$
P_i	Pi	lognormal	$\text{Mean} = 340\ \text{kPa}, \text{Std. Dev.} = 0.5\ \text{kPa}$
P_w	Pw	lognormal	$\text{Mean} = 147\ \text{kPa}, \text{Std. Dev.} = 0.5\ \text{kPa}$
K_0	K0	lognormal	$\text{Mean} = 1, \text{Std. Dev.} = 0.04$
E_u	E	lognormal	$\text{Mean} = 10500\ \text{kPa}, \text{Std. Dev.} = 100\ \text{kPa}$
K_1	K1	lognormal	$\text{Mean} = 0.8, \text{Std. Dev.} = 0.03$
Δ	Delta	lognormal	$\text{Mean} = 0.035\ \text{m}, \text{Std. Dev.} = 0.001\ \text{m}$
σ_s	sigmaS	lognormal	$\text{Mean} = 100\ \text{kPa}, \text{Std. Dev.} = 1\ \text{kPa}$
ζ	Zeta	lognormal	$\text{Mean} = 0.003\ \text{m}, \text{Std. Dev.} = 5 \times 10^{-4}\ \text{m}$

Table 15. List of parameters and their values in SSRABS3

methods and how to use them in a complementary format to check the results are left to the end of this section.

Recalling from Chapter 2, the task of FORM analysis is to linearize the limit-state function at a "design" point, satisfying the FORM convergence criteria. In order to

perform the FORM analysis, a nonlinear constraint solver which is called "stepper" must be established. After the starting point and the step size are selected, an algorithm called "iHLRF" is used to find the design point (Zhang and Der Kiureghian, 1997).

The limit-state threshold is selected as $0.01\ \mathrm{m}$. According to CIRIA PR30 (1996), $0.01\ \mathrm{m}$ is the maximum allowable settlement to have a "negligible" damage to buildings (Table 5). By performing a FORM using the above data, the probability that the damage is more than "negligible" (settlement larger than $10\ \mathrm{mm}$) is 0.0004 and the reliability index β equals 3.33. The calculation was completed in 0.284 seconds with 9 iterations.

Rt risk tool also provides us with the parameter's ranking, based on the alpha importance measure. In this case, the most influential parameters are: soil's unit weight γ, coefficient of effective earth pressure at-rest K_0 and volume ratio $K1$. The full ranking is sorted in Table 16, based on the absolute value of α. Recalling from Chapter 2, the sign of alpha importance measure for load and resistance random variables is positive and negative respectively.

Symbol	Description	Alpha importance measure
γ	Soil's unit weight	0.7660
K_0	Coefficient of earth pressure at-rest	0.6236
K1	Volume Ratio	0.1110
Δ	Thickness of the tailpiece	0.0780
ν	Soil's Poisson's ratio	-0.0556
P_i	Tunnel supporting pressure	-0.0327
E_u	Soil's undrained modulus	-0.0282
ζ	clearance required for the erection of the lining	0.0191
R	Tunnel's radius	0.0175
H	Tunnel centreline depth	0.0101
P_w	Pore water pressure	-0.0028

Table 16. SSRABS3 – alpha importance measure

As discussed in Chapter 3, a Class 3 building with 20% probability of exceedance of the settlement of $10\ \mathrm{mm}$ (upper limit of "negligible" damage class) should be transferred to SSRABS2. If in the previous example, the tunnel supporting pressure decreases to

$300\ \mathrm{kPa}$, by performing a FORM analysis, the probability of exceedance would be 0.30, which indicates that the building has to be transferred to SSRABS2.

4.1.2.2 SSRABS2: Settlement risk evaluation for Class 2 buildings

SSRABS2 utilizes the method proposed by Burland and Wroth (1974) to estimate the short-term settlement. This method partitions the building into sagging and hogging zones, then calculates the corresponding critical strains. Their maximum strain will be the developed critical strain, which is used in the proposed damage criteria. Our calculations are based on the parameters in Table 17.

Symbol	Label	Distribution type	Descriptive parameters
L_s	BL_sag	lognormal	$\mathrm{Mean} = 14\ \mathrm{m}, \mathrm{Std.\ Dev.} = 0.01\ \mathrm{m}$
L_h	BL_hog	lognormal	$\mathrm{Mean} = 4\ \mathrm{m}, \mathrm{Std.\ Dev.} = 0.01\ \mathrm{m}$
Δ_s	BDelta_sag	lognormal	$\mathrm{Mean} = 0.002\ \mathrm{m}, \mathrm{Std.\ Dev.} = 0.0001\ \mathrm{m}$
Δ_h	BDelta_hog	lognormal	$\mathrm{Mean} = 8 \times 10^{-4}\ \mathrm{m}, \mathrm{Std.\ Dev.} = 0.0001\ \mathrm{m}$
E/G	EGratio	lognormal	$\mathrm{Mean} = 2.6, \mathrm{Std.\ Dev.} = 0.05$
H	BH	lognormal	$\mathrm{Mean} = 4.5\ \mathrm{m}, \mathrm{Std.\ Dev.} = 0.01\ \mathrm{m}$
Δ_{hor}	Deltah	lognormal	$\mathrm{Mean} = 0.01\ \mathrm{m}, \mathrm{Std.\ Dev.} = 0.001\ \mathrm{m}$
ν	BNuu	lognormal	$\mathrm{Mean} = 0.3\ , \mathrm{Std.\ Dev.} = 0.02$
B_s	BB_sag	lognormal	$\mathrm{Mean} = 14\ \mathrm{m}, \mathrm{Std.\ Dev.} = 0.01\ \mathrm{m}$
B_h	BB_hog	lognormal	$\mathrm{Mean} = 4\ \mathrm{m}, \mathrm{Std.\ Dev.} = 0.01\ \mathrm{m}$

Table 17. List of parameters and their values in SSRABS2

The methodology used for SSRABS2 is based on the deflections and strains of the building, which are generally small. This is the reason for selecting very small values for standard deviations in Table 17, otherwise, the quality of the data would be in question. Based on the parameters listed in Table 17, the FORM yields that the probability of

exceedance of 0.3% critical strain is 0.075, while the reliability index β being 1.43. The model developed in Rt risk tool is shown in Figure 44.

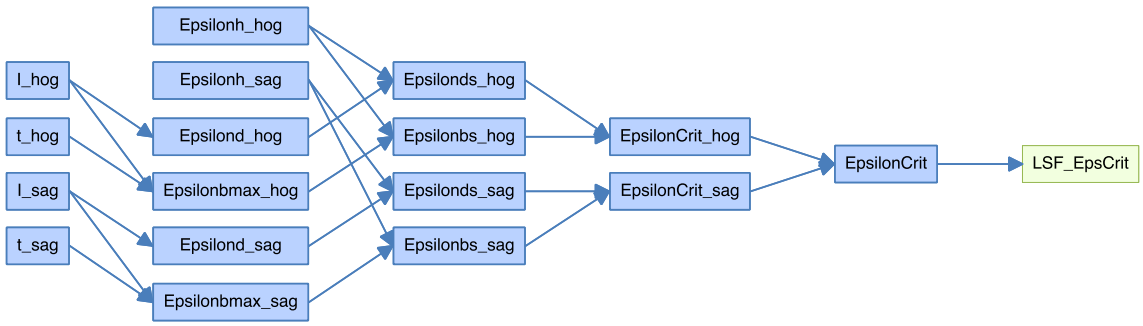

Figure 44. SSRABS2 - Rt risk tool model

The importance ranking of the parameters exhibits that exceedance probability is highly sensitive to the change in horizontal displacement. In fact, 20% increase in the amount of the horizontal displacement, from $10\,\mathrm{mm}$ to $12\,\mathrm{mm}$, will rise the exceedance probability by 61%. Moreover, the ratio $\mathrm{E/G}$ has direct influence on the stiffness of the building and its resilience toward settlement. An increase of 38% in the ratio results in decrease of the exceedance probability from 0.075 to 0.06. The parameters are sorted in Table 18 based on their ranking.

Symbol	**Description**	**Alpha importance measure**
Δ_{hor}	Horizontal movement	0.9980
Δ_{h}	Maximum relative settlement of hogging zone	0.0566
$\mathrm{B_h}$	Length of the building interacting with Δ_{hor} - hogging zone	-0.0261
$\mathrm{E/G}$	Ratio of building's Young's modulus to building's Poisson's ratio	-0.0083
$\mathrm{L_h}$	Length of hogging zone	0.0010
H	Building height	-0.0009

Table 18. SSRABS2 - alpha importance measure

According to the damage classification proposed by Boscardin & Cording (1989) (Table 6), 0.3% critical strain is the threshold between Class 3 and Class 4&5. Based on our evaluations, the probability of exceeding 0.3% critical strain is 7.5%. Since this probability is below 20%, there is no need for a more in-detail evaluation (*e.g.* via SSRABS1).

4.1.2.3 SSRABD2: Settlement risk evaluation of Class 2 buildings

Buildings with deep foundations, indexed as BD3 and BD2, are evaluated in this class of risk assessment. The procedure to calculate the induced values of stress and settlement are summarized in Chapter 2.

The values of the design stress in the pile is available from the calculations of the superstructure on the top. The immediate settlement of the pile can be determined from the method proposed by Bowles (1996) or a more rigorous formulation proposed by Randolph and Wroth (1979). Figure 45 represents this workflow of the models up to the limit-state function. In our example, it is assumed that the pile is $16\ \mathrm{m}$ long with the diameter of $0.6\ \mathrm{m}$ and it is located $10\ \mathrm{m}$ from the tunnel centreline.

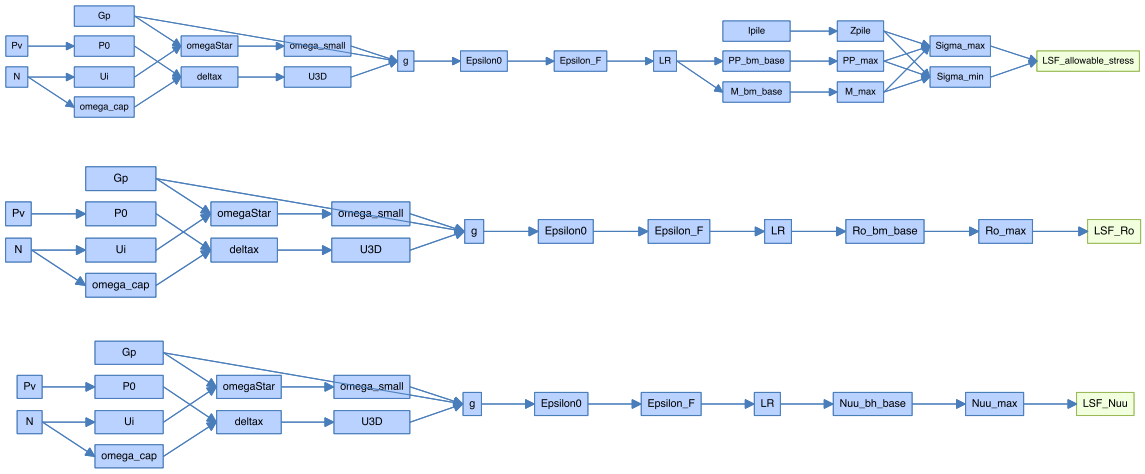

Figure 45. Bending stress, lateral deflection and pile settlement models - Rt risk tool

List of the parameters used in this class of analysis is summarized in Table 19. The average ground loss required for SSRABD2 is imported from the ground loss model, that is defined in SSRABS3. Only the pile settlement is discussed in the example, since it is

assumed that the magnitudes of the deformations and their associated stresses are considerably below the stresses causing the pile to reach its failure (yield) stress.

Symbol	Label	Distribution type	Descriptive parameters
k_{cu}^{ν}	Knuu_cu	constant	$\text{Value} = 1$
k_{d}^{ν}	Knuu_d	lognormal	$\text{Mean} = 0.99, \text{Std. Dev.} = 0.01$
$k_{L_p/H}^{\nu}$	Knuu_lph	lognormal	$\text{Mean} = 0.99, \text{Std. Dev.} = 0.01$
k_{cu}^{ρ}	Kro_cu	constant	$\text{Value} = 1$
k_{d}^{ρ}	Kro_d	lognormal	$\text{Mean} = 0.98, \text{Std. Dev.} = 0.01$
$k_{L_p/H}^{\rho}$	Kro_lph	lognormal	$\text{Mean} = 1.1, \text{Std. Dev.} = 0.01$
ν_{b-raw}	Nuu_bh_raw	lognormal	$\text{Mean} = 0.0055\ \text{m}, \text{Std. Dev.} = 0.0001\ \text{m}$
$\rho_{max-raw}$	Ro_bm_raw	lognormal	$\text{Mean} = 0.0035\ \text{m}, \text{Std. Dev.} = 0.0001\ \text{m}$
ν_{design}	Nuu_design	lognormal	$\text{Mean} = 0.004\ \text{m}, \text{Std. Dev.} = 0.0001\ \text{m}$
ρ_{design}	Ro_design	lognormal	$\text{Mean} = 0.002\ \text{m}, \text{Std. Dev.} = 0.0001\ \text{m}$

Table 19. List of parameters and their values in SSRABD2

The limit-state function is based on CIRIA PR30 (1996) damage classification (Table 5). If the limit-state function is framed based on "negligible" risk, the building settlement should be less than $10\ \text{mm}$. The limit-state function is then expressed as:

$$\text{LSF}_{\nu} = 0.01 - (\nu_{design} + \nu_{max\ \_induced}) \qquad \textit{(Eq. 4-1)}$$

Performing a FORM analysis based on this limit-state function results in a reliability index of 3.54 and the probability of exceedance of 2.06×10^{-4}, which means that there is 0.02% chance that the settlement of the pile exceeds $10\ \text{mm}$. Sorting the parameters based on alpha importance factor discloses that the soil's unit weight γ, coefficient of earth pressure at-rest K_0, and the volume ratio K_1 are the most influential parameters.

These parameters are on the top of the ranking since their standard deviations are relatively larger. The alpha measure ranking is summarized in Table 20.

Symbol	Description	Alpha Importance Measure
γ	Soil's unit weight	0.7553
K_0	Coefficient of effective earth pressure at-rest	0.6164
K1	Volume Ratio	0.1142
ν_{b-raw}	Settlement of the "base" case (raw value)	0.1060
ν_{design}	Design value of pile settlement	0.0985
Δ	Thickness of the tailpiece	0.0762
$k^{\nu}_{L_p/H}$	Correction factor for pile's length	0.0588
k^{ν}_{d}	Correction factor for pile's diameter	0.0588
P_i	Tunnel supporting pressure	-0.0320
E	Soil's undrained modulus	-0.0290
ζ	Clearance required for the erection of the lining	0.0187
R	Tunnel's radius	0.0177
H	Tunnel centreline depth	0.0128
P_w	Pore water pressure	-0.0028

Table 20. SSRABD2 – alpha importance measure

Based on the results of SSRABS3 and SSRABD2 evaluations, it is concluded that the any further investment to improve the accuracy of the parameters should focus on the importance ranking list. In other words, in case of investment, the resources should first be allocated to better estimate the soil's unit weight γ and the coefficient of earth pressure at rest K_0. For SSRABS2, investments should be first done to mitigate the horizontal displacement of the building Δ_{hor}.

4.1.2.4 Utilizing other reliability methods

Rt risk tool is able to perform FOSM, FORM, SORM and sampling. FORM is considered as the main method of analysis due to its low cost and accuracy. Nevertheless, in the case of confronting convergence issues, a FOSM analysis would be an alternative to determine the value of the reliability indices. Typically, problems that are extremely safe or with extremely low reliability index exhibit the problem of convergency. Performing

FOSM analysis makes it possible to trace if the problem of convergency is due to being out of range or other issues (*e.g.* numerical errors).

In the examples presented in 4.1.2.1 – 4.1.2.3, the risk analyses were conducted using FORM analysis, which has a valuable balance between computational cost and accuracy. Alternatively, we can carry out FOSM analysis, based on the second-moment data. Sampling is another method which necessitates more computational time and cost relative to FORM analysis. It generates a large number of samples and calculate the limit-state value for each single of the samples. Eventually, the probability of exceedance is calculated by counting the number of samples which exceeded the limit-state threshold over the total number of samples. Repeating SSRABD2 using sampling analysis generates the exceedance probability of 1.7×10^{-4}, and the reliability index of 3.58 in which the total number of samples is 100000. The results of sampling are notably close to the result of the FORM analysis. However, the sampling analysis lasts for 261.3 seconds, which is remarkably higher than 0.167 seconds required to complete the FORM analysis. The advantage of sampling method is that it does not approximate the limit-state function using a first-order approximation. Instead, it requires a large number of samples, more time and higher computational cost.

The other alternative is SORM analysis. SORM approximates the limit-state function with a second-order approximation and therefore, provides a more accurate results comparing to FORM. However, it is prone to convergency problem. Recalculating SSRABD2 using SORM analysis results in the probability of failure of 2.02×10^{-4} and reliability index of 3.53, which is almost identical to the results of the FORM analysis. Therefore, it can be concluded that FORM analysis is the most efficient method to perform reliability calculations in our RM framework.

4.2 Example of long-term risk management

4.2.1 Risk analysis

Similar to the previous section, this section presents the fault tree and event tree analyses of the long-term settlement. The risk evaluation and uncertainty analysis will further be addressed in the risk evaluation.

4.2.1.1 Fault tree analysis

Figure 34 depicted the fault tree analysis of the long-term ground subsidence. In this section, the likelihoods of the sub-main faults are brought in Table 21. The probability of the base faults as well as the calculations are provided in Figure 46. The probability of long-term ground subsidence is calculated as 6.91×10^{-1}.

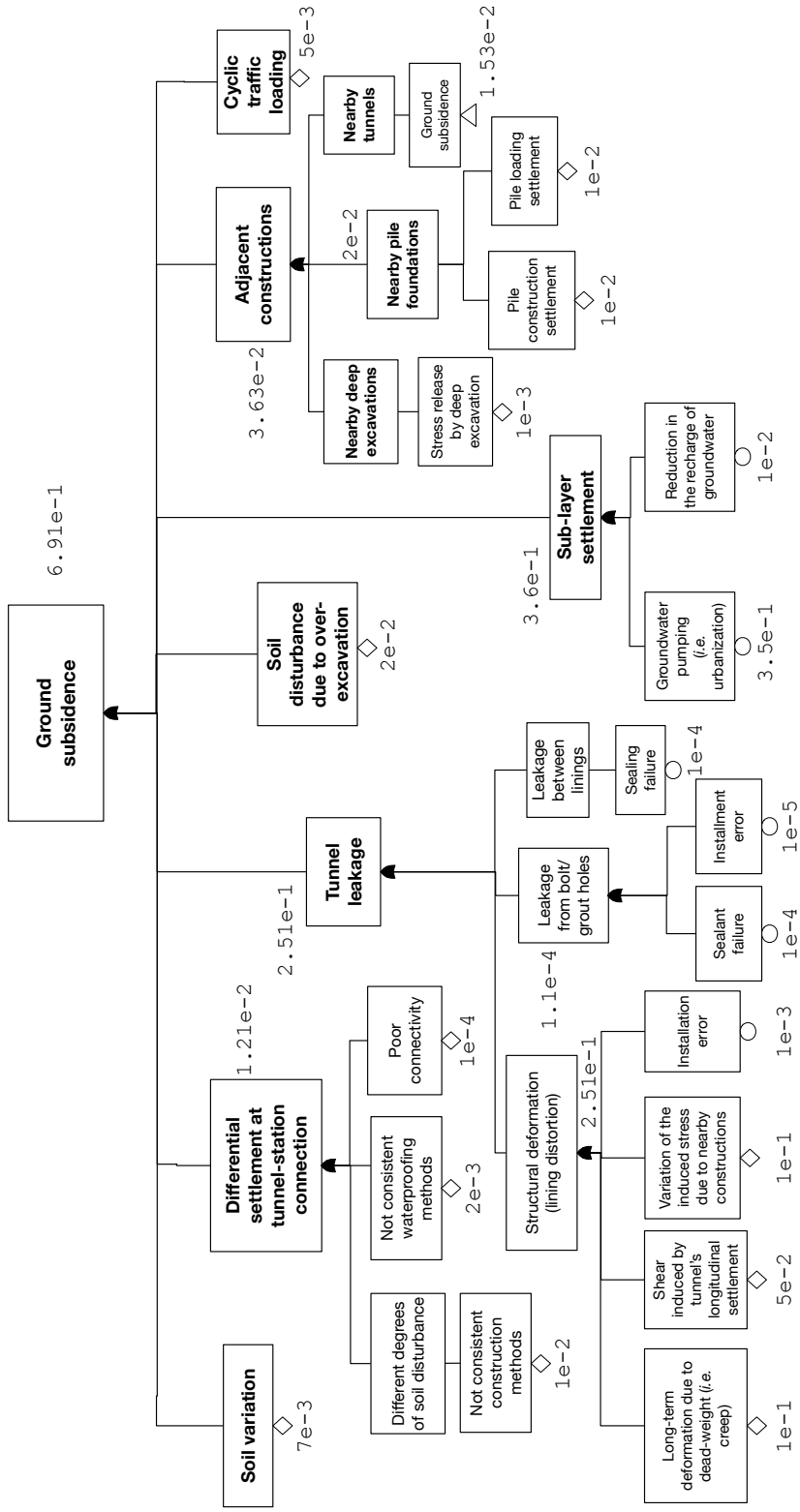

Figure 46. Long-term fault tree analysis - solved example

Sub-main fault	Likelihood
Soil variation throughout the tunnel	7×10^{-3}
Differential settlement at tunnel-station connection	1.21×10^{-2}
Tunnel leakage	2.51×10^{-1}
Soil disturbance due to over-excavation at curves	2×10^{-2}
Sub-layer settlement	3.6×10^{-1}
Adjacent construction	3.63×10^{-2}
Cyclic loading	5×10^{-3}

Table 21. Long-term analysis: sub-main faults

Based on this fault tree analysis, the probability of ground subsidence is:

$$\begin{aligned}&\mathrm{P}(\text{ground subsidence})\\&\qquad = \mathrm{P}(\text{soil variation} \cap \text{differential settlement} \cap \text{tunnel leakage}\\&\qquad \cap \text{soil disturbance} \cap \text{sublayer settlement} \cap \text{adjacent construction}\\&\qquad \cap \text{cyclic loading}) = 0.6914\end{aligned}$$

4.2.1.2 Event tree analysis

Recalling the event tree analysis shown in Figure 35, considering the existence of a tunnel in soft clay with the probability of occurrence of 1, succeeding events can be developed regarding the location of the tunnel section under investigation; *e.g.* events A, B, C, D. By assuming a probability of occurrence for each single event, the probability of a cascading (domino) scenario (*e.g.* event ICD) can be calculated. Our calculations are based on the assumption that these events are independent. Therefore, the probability of the outcome event is the multiplication of the marginal probability of the series of events. This is obvious from the Bayes' theorem that since two following events are assumed independent, the probability of their intersection is the product of probability of occurrence of each of them. As a result, the probability of an event, *e.g.* IACD, is calculated as:

$$\begin{aligned}\mathrm{P(IACD)} &= \mathrm{P(tunnel\ in\ clay} \cap \mathrm{through\ various\ layers} \cap \mathrm{no\ river} \cap \mathrm{high\ surcharge} \\ &\quad \cap \mathrm{at\ tunnel\text{–}\ station\ connection)} \\ &= 1 * 0.7 * 0.8 * 0.9 * 0.7 = 3.528 \times 10^{-1}\end{aligned}$$

The completed event tree is shown in Figure 47.

4.2.1.3 Consequence tree analysis

The consequence tree analysis was depicted in Figure 36. This consequence tree exhibits the aftermath of occurrence of a differential settlement for a tunnel in soft clay. In order to perform the calculation, the probability of the initial event is chosen to be equal to the highest probability of settlement, calculated in the event tree analysis (IACD event with the probability of settlement of 3.528×10^{-1}). The probability of undergoing structural deformation is considered as the sum of the probability of the differential settlement and the structural deformation (since these are two agents directly inducing the structural deformations). The probability of tunnel leakage is also imported from the results of the fault tree analysis. It should be noted that the consequence analysis pictures the repercussions of the differential settlement however, these consequences may also cause more differential settlements. This then leads to a recursive chain of events. For instance, the structural deformation is the cause of the differential settlement, but differential settlement may cause additional structural deformation and subsequent settlement as well. Nevertheless, it is absolutely essential to realize that the probabilities selected here are based on the assumption that these events are independent; which means that the two sub-faults of a main fault are independent and also remain independent during the iterative procedure mentioned above. The results of the consequence analysis are presented in Figure 48. The methodology of a consequence tree calculation is identical to event tree analysis.

4.2.2 Risk evaluation

4.2.2.1 LSRAC2: Long-term settlement risk evaluation for Class 2 buildings

Long-term settlement risk analysis for Class 2 buildings is carried out using the method to determine ground deformation proposed by Laver *et al.* (2016). This analysis only involves the calculation of the vertical displacement. However, the horizontal displacement and horizontal strains can be calculated as well.

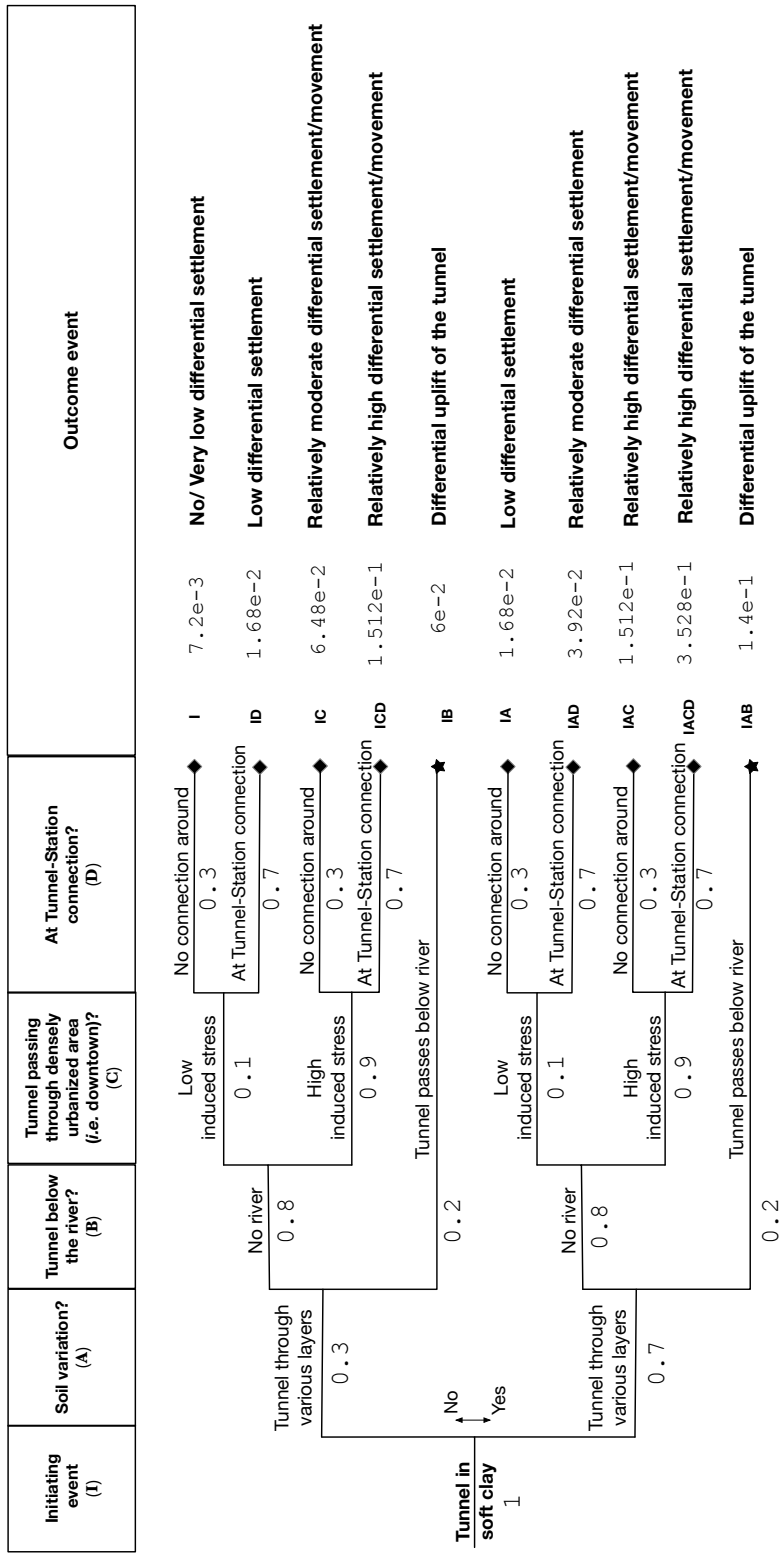

Figure 47. Long-term event tree analysis - solved example

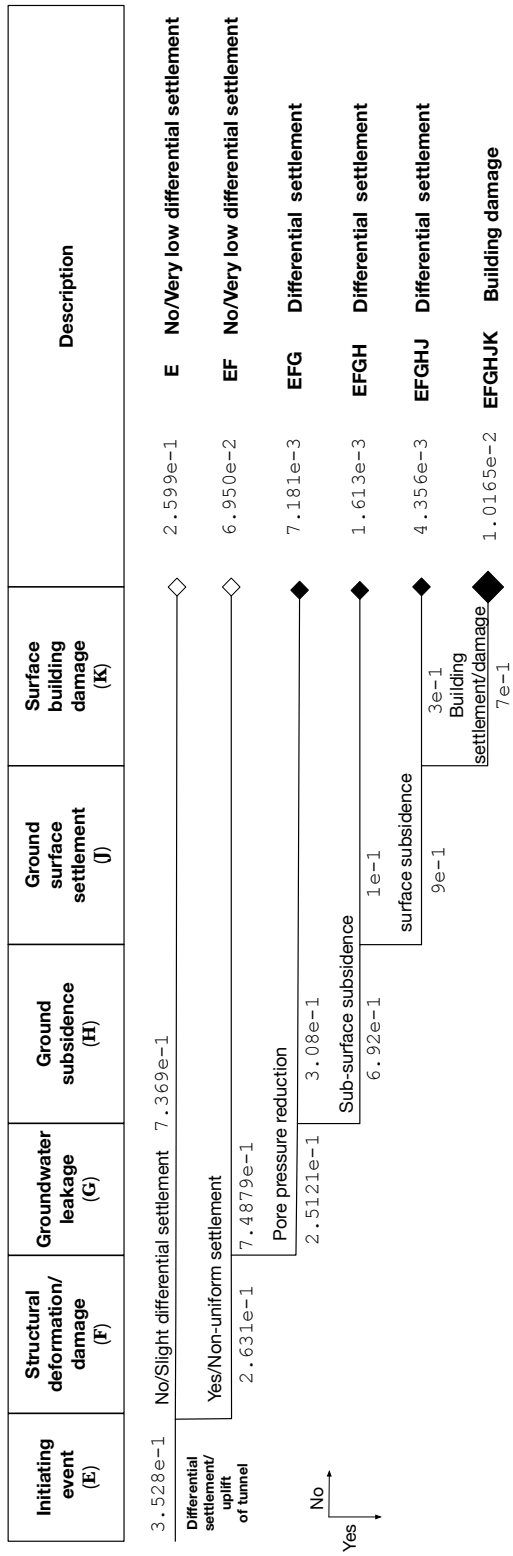

Figure 48. Long-term consequence tree analysis - solved example

The model developed for long-term settlement in Rt risk tool is provided in Figure 49 (left). The parameters used in LSRAC2 are listed in Table 22. The average value of the ground volume loss ε_0 is assumed to be around 0.004 $(\text{Mean} = 0.004, \text{Std. Dev.} = 0.0005)$. Our analyses show that based on the parameters listed in Table 22, the probability that the long-term settlement exceeds $10\,\text{mm}$ ("negligible" damage, according to CIRIA PR30, 1996) is 0.113, and the reliability index of 1.21. The importance alpha measures demonstrate that, the watertight aperture s_j, viscosity of the water ν_w, and volume loss ε_0 are on the top of the ranking list of the influential parameters with importance measures of 0.999, -0.0132 and 0.0105, respectively.

Symbol	Label	Distribution type	Descriptive parameters
γ_w	gammaw	constant	$\text{Value} = 9.8\ \frac{\text{kN}}{\text{m}^3}$
s_j	sj	lognormal	$\text{Mean} = 5 \times 10^{-6}\ \text{m}, \text{Std. Dev.} = 0.0001\ \text{m}$
ν_w	visc	lognormal	$\text{Mean} = 1.004 \times 10^{-6}\ \frac{\text{m}^2}{\text{s}}, \text{Std. Dev.} = 1 \times 10^{-6}\ \frac{\text{m}^2}{\text{s}}$
ε_0	eps0	lognormal	$\text{Mean} = 0.4\%, \text{Std. Dev.} = 0.05\%$
t	t	constant	$\text{Value} = 1.5 \times 10^8\ \text{s}$
k_h	kh	lognormal	$\text{Mean} = 1 \times 10^{-8}\,\frac{\text{m}}{\text{s}}, \text{Std. Dev.} = 1 \times 10^{-9}\,\frac{\text{m}}{\text{s}}$
k_v	kv	lognormal	$\text{Mean} = 1 \times 10^{-8}\,\frac{\text{m}}{\text{s}}, \text{Std. Dev.} = 1 \times 10^{-9}\,\frac{\text{m}}{\text{s}}$
L_c	Lc	lognormal	$\text{Mean} = 15\ \text{m}, \text{Std. Dev.} = 0.1\ \text{m}$
E'	E_prime	lognormal	$\text{Mean} = 15000\ \text{kPa}, \text{Std. Dev.} = 100\ \text{kPa}$
g	grav	constant	$\text{Value} = 9.8\ \frac{\text{m}}{\text{s}^2}$
t_l	tl	lognormal	$\text{Mean} = 0.35\ \text{m}, \text{Std. Dev.} = 0.01\ \text{m}$

Table 22. Class 2 assessment parameters – long-term settlement risk assessment

4.3 Total settlement risk analysis (TSRA)

After conducting the risk evaluations for immediate and consolidation settlements, it is possible to calculate the total settlement risk. Similar to previous calculations, any relevant damage classification can be utilized to define thresholds and determining limit-state functions. Considering CIRIA PR30 (1996) damage classification for "slight" damage (50 mm settlement), the probability that the total settlement exceeds 50 mm is 0.06 and the associated reliability index β is 1.50. The parameter's ranking is listed in Table 23. The TSRA model is shown in Figure 49 (right).

Symbol	Description	Alpha importance measure
s_j	Watertight aperture	0.9998
ν_w	Water's kinematic viscosity	−0.0135
k_h	Horizontal permeability of soil	−0.0066
k_v	Vertical permeability of soil	−0.0066
γ	Soil's unit weight	0.0050
t_l	Thickness of the lining	−0.0038
K_0	Coefficient of effective earth pressure at-rest	0.0038
ε_0	Volume loss	0.0015
L_c	Depth of tunnel axis below the water table	0.0013
E'	Drained soil's modulus	−0.0013
Δ	Thickness of the tailpiece	0.0006
P_i	Tunnel supporting pressure	−0.0002
ν	Soil's Poisson's ratio	−0.0002
H	Tunnel centreline depth	0.0001
ζ	Clearance required for the erection of the lining	0.0001
R	Tunnel's radius	0.0001
K1	Volume Ratio	-3.42×10^{-6}
E	Undrained soil's modulus	-8.70×10^{-7}
P_w	Pore water pressure	1.42×10^{-7}

Table 23. Total settlement – alpha importance measure

The total settlement model may provide more advantageous information. For instance, how an uncertainty or an error in stability number of the tunnel can propagate in the model up to the total settlement value. The influence of each single parameter is highly

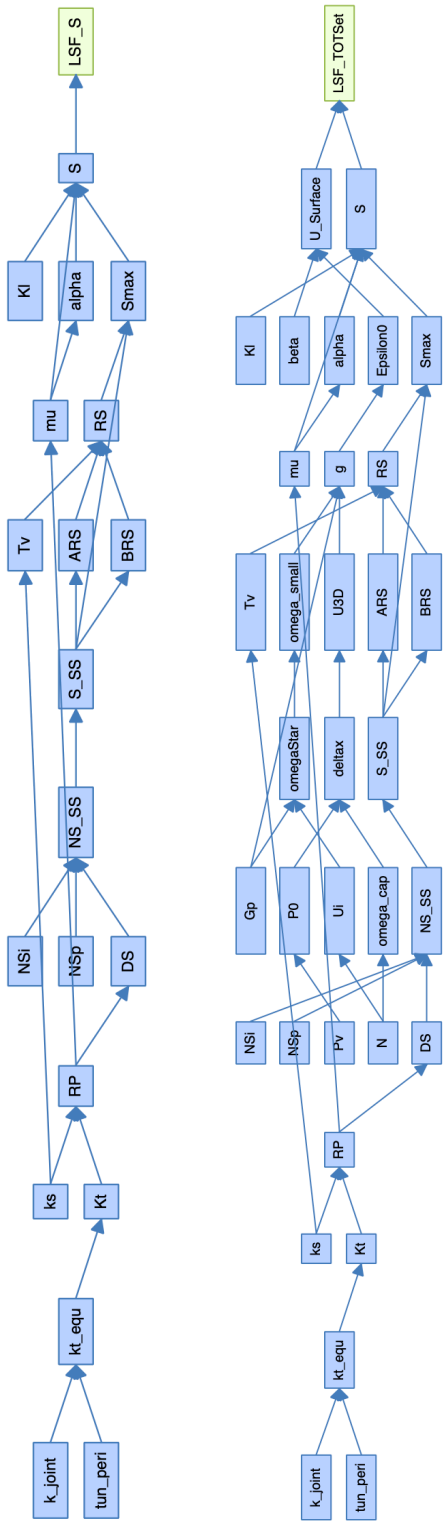

Figure 49. Long-term (left) and total settlement (right) risk evaluation model - Rt risk tool

beneficial to track the most influential parameters in the model. This is important, not only for tunnel designer and construction team to focus more on the most sensitive and critical parameters, but also for project managers and higher-level decision makers to prioritize their needs and allocate their limited resources properly. This is the essence of "risk-based decision making". Only by conducting such multi-level analyses, one may properly address the associated risk of settlement induced by tunnelling. This framework, rather than just being a series of guidelines, is an outlook toward risk and reliability analysis. It contains practical instructions on how to perform reliability analysis while dealing with data of different scales and accuracy. It provides the analyst with meaningful mathematical indicators rather than just providing descriptions on different risk levels. The outcome of settlement risk analysis can be shown on risk maps to provide a better mean of communication between different levels of decision making. In fact, the framework receives the technical data from different engineering aspects, perform the risk analyses, and provides a comprehensible output for managers and decision makers, who may not have an expert knowledge on the tunnelling technical aspects, but they are eager to see the big picture of the problem and its critical parts.

4.4 The effect of introducing parameters' correlation

In all the analyses in this study, the "known" correlations have been introduced between different parameters. However, in reality, there might be some "unknown" correlations, *e.g.* the correlation between soil's drained and undrained moduli (*i.e.* E' and $\mathrm{E_u}$, respectively). In our analysis, it is assumed that drained and undrained soil's moduli are completely independent.

Rt risk tool is capable of considering the correlations between parameters under the Nataf's assumption (1962) discussed in Chapter 2. The results show that based on the influence of the parameter on the limit-state function, introducing correlation alters the results. However, the difference may not be remarkable. For instance, considering an extreme correlation of 0.9 between E' and $\mathrm{E_u}$ in TSRA, the results show an exceedance probability of 0.06 and reliability index of 1.50, which are identical to the results of considering no correlation. Similar situation is observed by introducing correlation between other parameters.

Chapter 5. Conclusion and future work

This study developed a risk management framework to quantify the risk of tunnelling in urbanized area, specifically in soft clay, to meet the need for a more rigorous risk management considering the challenges and multi-scale uncertainties confronted during the tunnelling project and after its completion. The core hazard, which has been targeted in this study, was ground subsidence, both due to the immediate and consolidation settlements. The proposed framework had different risk assessment classes, associated with short-term and long-term settlements, each containing the essential components of a risk management plan; namely, risk identification, risk analysis and risk evaluation. The workflow of each part was then depicted in a flowchart for better visualization and possible extension of the work to develop a software package. The proposed risk management framework provided a better estimation of risk, by considering the vulnerability and exposure of the surface buildings. It also provided multi-level risk evaluation classes, to evaluate the risk according to the sensitivity of the building and the scale of the available data.

In the short-term risk assessment, face, shield and tail losses were identified as the main contributors to the immediate settlement of the ground. Each of them was explained in detail, to address the base faults that cause the main fault. The effect of ground type variation, unbalanced face pressure, grouting deterioration problems and the effect of delayed support were analyzed in a fault tree analysis to calculate the likelihood of the ground settlement. The fault tree analysis was extended to consider the effect of over-excavation at curved sections of a tunnel.

To evaluate the risk of settlement, the buildings were first scored on the scale of 1 to 5 as “building score”, by considering their age, functionality, foundation type and closeness to the tunnel’s centreline. The region of the ground affected by tunnelling was divided into three zones with specific dimensions and with specific scores for the buildings located inside each zone. Six different building types were identified. Each type was evaluated through the designated class of risk assessment, using limit-state functions based on a practical damage classification.

Depending on the required level of accuracy, three classes of settlement risk assessment, namely SSRABS3, SSRABS2 and SSRABS1, were developed for buildings with shallow foundations. For SSRABS3, the settlement calculations were based on the green-

field settlement trough (Loganathan, 2011) and CIRIA damage classification (CIRIA PR30, 1996). FORM analysis was utilized to evaluate the probability of exceeding a designated threshold (*e.g.* $10\,\mathrm{mm}$). For SSRABS2, the settlement was evaluated using a more rigorous method (Burland and Wroth, 1974), which considered the risk of settlement based on the concept of critical strain of buildings. The damage classification proposed by Boscardin and Cording (1989) was utilized to define limit-state functions in SSRABS2. Finally, if the building had a score of 1 or 2 or the building had probability of settlement more than 20% in SSRABS3, the building would be assessed via SSRABS1. For SSRABS1, due to the critical situation of the building as well as possible serious consequences of the collapse (for instance, preserved buildings), it was recommended to use a numerical modelling (*e.g.* FEM) to evaluate the settlement risk. The idea of having different classes of risk assessment with different levels of detail was helpful in order to adjust the required time and resources for a specific type of problem. In this way, for less critical conditions, a less sophisticated model could be used, while more reliable estimate of settlement was required for more sensitive buildings. The same notion was used further for buildings with deep foundations as well as for the long-term risk management plan however, different methods and procedures were recommended for them. For buildings on deep foundations, two classes of assessment were proposed: SSRABD2 utilized design charts, which provided maximum bending stress, pile lateral displacement and vertical settlement, to be compared to the allowable values defined in limit-state function and calculate the probability of exceeding a specific threshold. SSRABD1 was conceptually the same as SSRABS1 where numerical modelling was recommended for settlement calculations.

The second part of the framework dealt with the long-term settlement related to the consolidation of the soft clay. The effect of the groundwater, induced stress, construction method, cyclic train loading and structural deformation were addressed in the form of an influence diagram. A more in-detail analysis was performed using fault tree analysis, where soil variation during tunnelling, differential settlement at tunnel-station connections, tunnel leakage, soil disturbance, the effect of the adjacent construction and the train cyclic loading were discussed as the main causes of long-term ground subsidence. An event tree analysis was performed to develop a series of what/if scenarios and to evaluate the probability of happening of each scenario. These scenarios were identified based on the possibility of having a multi-layered soil along the excavation axis, passage below a river and the possibility of passing under highly populated areas. The outcomes of the event tree analysis provided the most critical

locations of settlement along the tunnel. The outcomes of event tree analysis were used to categorize the buildings for designated settlement risk assessment in different classes. Additionally, a consequence tree analysis was performed to predict the aftermath of differential settlement of the tunnel in soft clay. The differential settlement of the tunnel was considered as the initial event, while the subsequent events include structural deformation, tunnel leakage, ground subsidence, ground surface settlement and subsequently, building settlement. Fault tree, event tree and consequence tree analyses were performed in a complementary format for differential settlement analysis. Fault tree analysis was used for post-settlement risk analysis by knowing the influential factors. Event tree analysis provided a series of possible cascading events to calculate the probability of occurrence of an unexpected event in the future. Consequence tree analysis was an extension to event tree analysis, considering the occurrence of differential settlement.

Two classes of risk evaluation (namely LSRAC2 and LSRAC1) were proposed to evaluate the risk of long-term settlement. Ground surface buildings in different sections affected by a tunnel were classified into two classes, based on the outputs of the event tree and consequence tree analyses. Critical buildings *i.e.* the buildings located above the sections with relatively high differential settlements (*e.g.* events ICD and IACD) were evaluated in Class 1 long-term settlement risk analysis (LSRAC1) and less critical buildings were evaluated in Class 2 long-term settlement risk analysis (LSRAC2).

The methodology used to estimate settlement in LSRAC2 was a modified version of the approach proposed by Laver *et al.* (2016). The effect of the tunnel leakage was considered, by approximating the permeability of a broken watertight. Then, the permeability of the broken watertight and the permeability of the concrete (assumed zero) were used to calculate the equivalent permeability of the tunnel ring. Another assumption made in LSRAC2 analysis about the calculation of nondimensional settlement value for fully impermeable lining $\mathrm{NS_i}$. Shearing-induced dilation behaviour in London clay does not occur in very soft to soft clays (*i.e.* shear induces compaction and therefore, positive excess pore water pressure). Therefore, it was assumed that $\mathrm{NS_i} = 2 * \varepsilon_0$, as a modification to the approach by Laver *et al.* (2016). This assumption needs further elaboration and verification, which is out of the scope of this research. The results of the implementation showed that the consolidation settlement is sensitive

to the aperture of the broken watertight s_j. Therefore, the mitigation measures should first be performed on tunnel's watertight.

Risk maps and risk registers are two means of risk communication used in the proposed framework. The outcomes of the proposed RM plan were visualized using a colour-coded risk map, showing buildings with associated settlement risk. Another risk map was developed to show the associated risk of total settlement for different sections of a tunnel. These risk maps provided risk-based information regarding the magnitude and extension of the settlement risk with respect to the different parts of the tunnel. The risk register was introduced, as a report, generated from the building database, providing information on building (structure) current condition, probability of the settlement (with respect to the structure's class of assessment) and the progress on the required mitigation measures. In fact, our risk management plan received technical data (*e.g.* the average value of the volume loss, the tunnel face pressure, *etc.*), performed the risk analysis and reported the output in the forms of risk maps and risk registers. Such information is comprehensible for managers and decision makers who may not possess a deep knowledge about the technical details. These means of risk communication enable the decision maker to prioritize the problems to be solved and optimize the use of their limited resources.

The risk management framework, proposed in Chapter 3, was implemented in a series of examples in Chapter 4. A post-event risk assessment was performed using fault tree analysis, in which the probability of ground subsidence was evaluated based on the probability of occurrence of its sub-events. A pre-event risk analysis was conducted to estimate the probability of occurrence of a specific scenario including a series of cascading (domino) events. Consequence tree analysis was carried out to evaluate the probability of occurrence of the consequences of tunnel differential settlement. Examples were provided for different classes of settlement risk assessment (*e.g.* SSRABS3, SSRABD2, LSRAC2, *etc.*). The probability of failure was calculated in each case, based on a designated limit-state function. In each class of settlement risk assessment, the parameters were ranked based on their alpha importance measure. For SSRABS3 and SSRABD2, the soil's unit weight γ and the coefficient of earth pressure at rest K_0 were the most influential parameters, respectively. For SSRABS2, the horizontal displacement Δ_{hor} was the most influential factor, with the alpha importance measure of 0.998. The high value of alpha importance measure acknowledges that the

probability of exceedance was highly sensitive to Δ_{hor}. An increase of 20% in amount of the horizontal displacement Δ_{hor}, from $10\,\mathrm{mm}$ to $12\,\mathrm{mm}$, rose the exceedance probability by 61%. In TSRA, the results showed that the analysis was highly sensitive to the aperture of the watertight with alpha measure of 0.999. Based on the results of SSRABS3 and SSRABD2 evaluations, it was concluded that the any further investment to improve the accuracy of the parameters should focus on the importance ranking list. In other words, in case of investment, the resources should first be allocated to better estimate the soil's unit weight γ and the coefficient of earth pressure at rest K_0. For SSRABS2, investments should be done to mitigate the horizontal displacement of the building Δ_{hor}.

For the purpose of reliability analysis, FORM was chosen as the primary probabilistic method in our analysis to conduct the reliability assessments. It provided a proper balance between accuracy and computational costs. Alternatively, SORM and sampling were also mentioned, which necessitate more computational effort comparing to FORM analysis. Performing SORM and sampling instead of FORM in our settlement risk assessments showed that the differences are negligible. Consequently, it was unnecessary to use more mathematically complex methods. Repeating SSRABD2 using sampling analysis generated the exceedance probability of 1.7×10^{-4}, and the reliability index of 3.58 in which the total number of samples was 100000. The results of sampling were notably close to the result of the FORM analysis ($\text{exceedance probability} = 2.06 \times 10^{-4}$ and $\beta = 3.54$). The advantage of sampling method was that it does not approximate the limit-state function using a first-order approximation. It was also a great alternative when confronting convergency problem. However, it required a large number of samples, more time and computational cost. The difference between the results of FORM and SORM were negligible in the example problem. It is concluded that the results of the proposed settlement calculation were not sensitive to the method of the reliability analysis.

The limitations on using the proposed framework were discussed. The proposed framework mainly focused on the risk of settlement for surface buildings. The closed-form formula for settlement calculation, proposed for SSRABS3, tended to oversimplify the soil behavior and did not consider the effect of the stress state, stress history and constitutive parameters. In SSRABS2, it is concluded that assuming building as a simple, isotropic, linear-elastic beam and neglecting the soil-structure interaction introduce errors in prediction of the foundation behavior. Both of these simplifications may cause

catastrophic consequences for sensitive buildings. The applicability of the framework was restricted by the method used for settlement calculation. For instance, in SSRABS3 and SSRABD2, the stability number N may not be used for the stability of the face of the tunnel for very deep tunnels. Also, the assumptions behind the proposed relation for gap parameter may not be valid for the cases of partially saturated soft soils. The geometry of the tunnel (*i.e.* depth to radius ratio $\mathrm{H/R}$) was another important indicator for applicability of the settlement calculation methods. SSRABS3 and SSRABD2 may not provide reliable results in cases of having very small or very large $\mathrm{H/R}$ ratio.

In this study, the "known" correlations were introduced between different parameters. However, in reality, there might be some "unknown" correlations, *e.g.* the correlation between soil's drained and undrained moduli (*i.e.* E' and $\mathrm{E_u}$, respectively). The results show that, based on the influence of the parameters on the limit-state function, introducing correlation may alter the results. However, the difference is negligible.

As the future work, the proposed framework needs to be implemented in a computer code for tunnelling risk assessment. As illustrated in Figure 50, the software should be capable of performing the risk and reliability analysis, to work with software packages (*e.g.*, ArcGIS) and to import CAD files (*e.g.* .dwg, .dxf, *etc.*). The software should also be compatible with database programming languages (*e.g.* written in SQL) in order to provide the risk register, immediately in a form of a report. Rt risk tool is a general probabilistic analysis facilitator which is sufficiently strong in reliability analysis. However, other aspects of the software and its visual features are left undeveloped. In addition, it would be beneficial to have a code, exclusively developed for tunnelling in soft soil, which will help the analyst to perform more reliable risk analysis and develop corresponding risk management strategies.

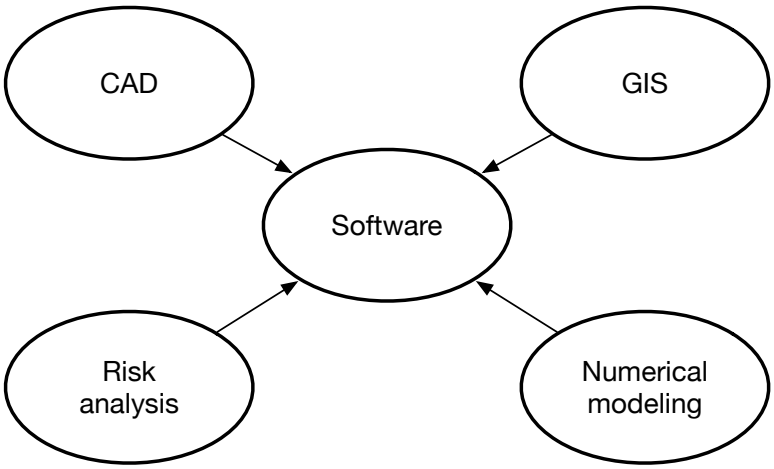

Figure 50. Future work: software's capabilities

References

Addenbrooke TI, Potts DM (2001). *Finite element analysis of St. James Park greenfield reference site*. In: Burland JB, Standing JR, Jardine FM (eds) Building response to tunnelling, vol 1. Thomas Telford, London, pp. 177-194.

Atkinson JH, Potts DM (1977). *Subsidence above shallow tunnels in soft ground*. ASCE Geotechnical Eng Div, pp. 59-64.

Attewell P.B. and Woodman J.P. (1982). *Predicting the dynamics of ground settlement and its derivatives caused by tunnelling in soil*. Ground Engineering, November issue, pp. 13-22.

Attewell, P., & Farmer, I. (1974). *Ground disturbance caused by shield tunnelling in a stiff, overconsolidated clay.* Engineering Geology, 8(4), pp. 361–381. doi: 10.1016/0013-7952(74)90028-3

Becker, D.E. (1996). *Eighteenth Canadian Geotechnical Colloquium: Limit States Design for Foundations. Part II. Development for the National Building Code of Canada.* Canadian Geotechnical Journal, 33(6): pp. 984–1007. doi:10.1139/t96- 125.

Bickel, J. O., Kuesel, T. R., & King, E. H. (1996). *Tunnel engineering handbook*. New York, N.Y: Chapman & Hall.

Bobet A (2002). *Analytical Solutions for Shallow Tunnels in Saturated Ground*. Journal of Engineering Mechanics ASCE 12: pp. 1258–1266.

Boscardin M. D. and Cording E. J. (1989). *Building Response to Excavation-Induced Settlement*, Journal of Geotechnical Engineering, American Society of Civil Engineers, Vol. 115, No. 1, pp. 1-21.

Bowers, K. H., Miller, D. M. & New, B. M. (1996). *Ground movement over three years at the Heathrow Express Trial Tunnel. In Geotechnical aspects of underground construction in soft ground* (eds R. J. Mair and R. N. Taylor), pp. 647–652. Rotterdam: Balkema.

Bowles, J.E. 1988. *Foundation analysis and design. 5th edition*. New York: McGraw-Hill.

Broms, B. B.,and Bennermark, H. (1967). Stability of clay at vertical openings. J. Soi/ Me& Fndn Div. ASCE 93, No. SMl, 71-94.

Burland J. B. and Wroth C. P. (1974). *Settlement of buildings and associated damage. State of the Art Review*, Proceedings, Conference on Settlement of Structures, Cambridge, Pentech Press, London, pp. 611-654.

Burland, J. B. (1995). *Assessment of risk of damage to buildings due to tunnelling and excavation.* Invited special lecture to IS-Tokyo 95. In: 1st International Conference on Earthquake Geotechnical Engineering V3, pp. 1189-1202

Casagrande, A., (1965). *Role of the calculated risk in earthwork and foundation engineering.* Journal of soil mechanics division, ASCE, Vol. 91. No. SM4, p1.

Chi, S.Y., Chern, J.C., Lin, C.C. (2001). *Optimized Back-Analysis for Tunnelling-Induced Ground Movement Using Equivalent Ground Loss Model*. Tunnelling and Underground Space Technology, Volume 16. Issue 3. pp. 159-165.

Chou WI, Bobet A. (2002). *Predictions of ground deformations in shallow tunnels in clay*. Tunnel and Underground Space Technology, pp. 3–19.

CIRIA (1996). *Prediction and effects of ground movements caused by tunnelling in soft ground beneath urban areas.* Construction Industry Research and Information Association, Project Report 30.

Deere, D. V., Peck, R. B., Monsees, J. E., And Schmidt, B. (1969). *Design of tunnel liners and support systems*, Washington, D.C. [Available from National Technical Information Service, Springfield, V A 22161 as NTIS Report PB-183799.]

Di, H., Zhou, S., Guo, P., He, C., Zhang, X., & Huang, S. (2019). *Observed long-term differential settlement of metro structures built on soft deposits in the Yangtze River Delta region of China. Canadian Geotechnical Journal*. doi: 10.1139/cgj-2018-0524

Duddeck, H. (1996). *Challenges to tunnelling engineers.* Tunnelling and Underground Space Technology, 11 (1)(1996), pp. 5-10.

Ercelebi, S.G., Copur, H. & Ocak, I. (2011). *Surface settlement predictions for Istanbul Metro tunnels excavated by EPB-TBM.* Environ Earth Sci (2011) 62: 357. https://doi.org/10.1007/s12665-010-0530-6

Eskesen, S. D., Tengborg, P., Kampmann, J., Veicherts, T. (2004). *Guidelines for tunnelling risk management*. International Tunnelling Association, Working Group No. 2. Tunnelling and Underground Space Technology 19 (2004) pp. 217-237.

Essex, R.J., Ed. (2007). *Geotechnical Baseline Reports for Construction—Suggested Guidelines*. Prepared by the Technical Committee on Geotechnical Reports for the Underground Technology Research Council. Reston, Virginia: ASCE.

Farrell, R., Mair, R., Sciotti, A., and Pigorini, A. (2014). *Building response to tunnelling.* Soils Found., 54(3), pp. 269–279.

Gioda, G. and Swoboda, G. (1999). *Developments and applications of the numerical analysis of tunnels in continuous media.* Int. J. Num. Ana. Meth. Geom., Vol. 23, No. 12, pp. 1393-1405.

Greathead, J. H. (1886). *Patent number 5221, Apparatus to driving tunnels.* The Engineer Volume 61, Morgan-Grampian, pp. 329

Harding, H. (1981). *Tunnelling history and my own involvement.* Toronto: Gloder Associates.

Hasofer, A.M. and Lind, N. C. (1974). *Exact and invariant second-moment code format.* J. Engineering Mechanics Division, ASCE, 100(1), pp. 111–121.

Haukaas, T. (2018). *The First-order Reliability Method – FORM.* Lecture notes of Structural Reliability. University of British Columbia. Retrieved at: http://terje.civil.ubc.ca/reliability/

Heisenberg, W. (1927). *Über den anschaulichen Inhalt der quantentheoretischen Kinematik und Mechanik*, *Zeitschrift für Physik* (in German), **43** (3–4): pp. 172-198.

Herzog M. (1985). *Surface subsidence above shallow tunnels* (in German). Bautechnik 62: pp. 375–377.

Heuer, R.E. (1974). *Important ground parameters in soft ground tunnelling.* Proceedings of Specialty Conference on Subsurface Exploration for Underground Excavation and Heavy Construction, New York: ASCE.

Hosseini, S. A. A., Mohammadnejad, M., Hoseini, S. M., Mikaeil, R., and Tolooiyan, A. (2012). *Numerical and analytical investigation of ground surface settlement due to subway excavation.* Geosciences, Vol. 2, No. 6, pp. 185-191, DOI: 10.5923/j.geo.20120206.06.

Hu, Q., Huang, H. (2014). *The State of the Art of Risk Management Standards on Tunnels and Underground Works in China*. 2nd international conference on vulnerability risk analysis and management (ICVRAM), Liverpool, UK pp. 419-426. 10.1061 /9780784413609.043.

Huang, H.W., Zhang, D. M. (2015). *Quantitative geotechnical risk management for tunnelling projects in China*. 5th international symposium on geotechnical safety and risk, Rotterdam, Netherlands. pp. 61-75.

Huang, Q., Huang, H., Ye, B., Zhang, D., Zhang, F. (2018). *Evaluation of train-induced settlement for metro tunnel in saturated clay based on an elastoplastic constitutive model.* Underground Space, Volume 3, Issue 2, pp. 109-124.

Huang, H.W., Zhang, D.M. (2015). *Quantitative Geotechnical Risk Management for Tunneling Projects in China***.** 5th International Symposium on Geotechnical Safety and Risk, Rotterdam, Netherlands (2015), pp. 61-75, 10.3233/978-1-61499-580-7-61

Ingles O. G., Metacalf, J. B. (1972). *Soil Stabilisation: principle and practice*, Butterworths and Company Publishers Limited, Sydney, Australia.

International Organization for Standardization (2009). *ISO 31000: Risk management-Principles and guidelines*. doi: 10.3403/30202344

International Organization for Standardization (2009). *ISO guide 73: Risk Management Vocabulary*

Kamon, M. & Bergado, D.T. (1991). *Ground improvement techniques. Theme Lecture.* Proc. 9th Asian Regional Conference on Soil Mech. and Foundn. Engg., Bangkok. 2: pp. 521-549.

Komiya, K., Soga, K., Akagi, H., Jafari, M. R. and Bolton M. D. (2001). *Soil consolidation associated with grouting during shield tunnelling in soft clayey ground.* Geotechnique 51. No. 10, pp. 835-846.

Lagerblad B., Fjallberg L. and Vogt C. (2010). *Shrinkage and Durability of Shotcrete*, Proceeding of Shotcrete Elements of a System, ed: Bernard, ES, 2010 Taylor & Francis Group, London, pp. 173-180.

Laver RG, Li Z, Soga K (2016). *Method to evaluate the long-term surface movements by tunneling in London clay*. J Geotech Geoenviron 143(3):06016023

Leca, E., and New, B. (2007). *Settlements induced by tunnelling in soft ground*. Tunnelling and Underground Space Technology, 22: pp.119-149.
Lee, K.M., Rowe, R.K., Lo, K.Y., (1992). *Subsidence owing to tunnelling. I. Estimating the gap parameter.* Canadian Geotechnical Journal 29, pp. 929–940.

Liu, P.L. and Der Kiureghian, A. (1986). *Multivariate distribution models with prescribed marginals and covariances*. Probabilistic Engineering Mechanics, 1(2), pp. 105–112.

Lo, K. Y., Ng, R. M. C., Rowe, R. K. (1984). *Predicting settlement due to tunnelling in clays*. Proc., Tunnelling in Soil and Rock, Geotech III Conf, ASCE, Reston, Va., pp. 48-76.

Loganathan, N. (2011). *An Innovative Method for Assessing Tunnelling-Induced Risks to Adjacent Structures*, PB 2009 William Barclay Parsons Fellowship Monograph 25, Parsons Brinckerhoff Inc., New York, USA

Loganathan, N., and Poulos, H. G. (1998). *Analytical prediction for tunnelling-induced ground movements in clays*. J. Geotech. Geoenviron. Eng., 124(9), pp. 846–856.

Macklin S. R. (1999). *The prediction of volume loss due to tunnelling in overconsolidated clay based on geometry and stability number*. Ground Engng 32, No. 4, pp. 30–33.

Mahsuli, M., & Haukaas, T. (2013). *Computer Program for Multimodel Reliability and Optimization Analysis*. *Journal of Computing in Civil Engineering*, *27*(1), pp. 87–98. doi: 10.1061/(ASCE)cp.1943-5487.0000204

Mair R. J. (1983). *Geotechnical aspects of soft ground tunnelling*. In: Proceedings of international symposium on construction problems in soft soils, Nanyang Technological Institute, Singapore.

Mair, R. J., and Taylor, R. N. (1997). *Theme lecture: Bored tunnelling in the urban environment*. Proc., 14th Int. Conf. on Soil Mechanics and Foundation Engineering, Hamburg, Balkema, Rotterdam, The Netherlands, pp. 2353–2385.

Mair, R. J., Merritt, A. S., Borghi, F. X., Yamazaki, H. & Minami, T. (2003). *Soil conditioning for clay soils.* Tunnels and Tunnel- ling Int., 35, No. 4, pp. 29–32.

Mair, R. J., Taylor, R. N., and Bracegirdle, A. (1993). *Subsurface settlement profiles above tunnels in clays*. Geotechnique, 43, No. 2, pp. 315–320.

Martos F. (1958). *Concerning an approximate equation of the subsidence trough and its time factors.* International Strata Control Congress, Leipzig, pp. 191–205.

Mathew, G. V. and Lehane, B. M. (2013). *Numerical back-analyses of greenfield settlement during tunnel boring.* Can. Geotech. J., Vol. 50, No. 2, pp. 145-152, DOI: 10.1139/cgj-2011-0358.

Melis M., Medina L., Rodriguez J.M. (2002). *Prediction and analysis of subsidence induced by shield tunnelling in the Madrid Metro extension.* Can Geotech J 39:1273–1287.

Mroueh H., Shahrour I. (2002). *Three-dimensional finite element analysis of the interaction between tunnelling and pile foundations*. Int J Numer. Anal Meth Geomech. 26:217–230.

Nataf, A. (1962). *Determination des Distributions de Probabilités dont des Marges sont Donneés*, C.R. Academy of Sciences, 255, pp. 42-43.

Neaupane KM, Adhikari NR (2006). *Prediction of tunnelling-induced ground movement with the multi-layer perception*. Tunnel and Underground Space Technology 21:151–159.

New, B.M., O'Reilly, M.P, (1991). *Tunnelling induced ground movements: predicting their magnitude and effects.* In: 4th International Conference on Ground Movements and Structures, Cardiff, invited review paper, pp. 691–697.

Ocak I. (2009). *Environmental effects of tunnel excavation in soft and shallow ground with EPBM: the case of Istanbul.* Environ Earth Sci 59(2):347–352. doi:10.1007/s12665-009-0032-6.

Ocak I., Seker SE (2013). *Calculation of surface settlements caused by EPBM tunnelling using artificial neural network, SVM, and Gaussian processes*. Environ Earth Sci 69(5):1673–1683. doi:10.1007/s12665-012-2002-7.

O'Reilly, M. P., Mair, R. J., Alderman, G. H. (1991). *Long-term settlements over tunnels: an eleven-year study at Grimsby. Proc Tunnelling '91, London, 14-18 April 1991 pp.55-64. Publ Londen: Elsevier, 1991.*

Park KH (2005). *Analytical solution for tunnelling-induced ground movement in clays.* Tunn Undergr Space Technol, pp. 249–261.

Peck R.B. (1969). *Deep excavations and tunnelling in soft ground*. In: 7th International conference on soil mechanics and foundation engineering, State of the Art Volume, pp. 225–290.

Project Management Institute (2008). *A Guide to the Project Management Body of Knowledge*. ANSI/PMI 99-001-2008, Philadelphia, PA: Project Management Institute. p17.

Qian Q., Lin P. (2016). *Safety risk management of underground engineering in China: progress, challenges and strategies*. J. Rock Mech. Geotech. Eng. 8, pp. 423-442.

Rackwitz, R. and Fiessler, B. (1978). *Structural reliability under combined load sequences*. Computers & Structures, 9, pp. 489–494.

Randolph, M. F., and Wroth C. P. (1979). *A Simple Approach to Pile Design and the Evaluation of Pile Tests*, *ASTM STP* No. 670, pp. 484-499.

Rowe, R.K., and Kack, G.J. (1983). *A theoretical examination of the settlements induced by tunnelling: four case histories*. Canadian Geotechnical Journal, 20: 299-314.

Sagaseta, C. (1987). *Analysis of undrained soil deformation due to ground loss*. Geotechnique 37 (3), pp. 301–320.

Samarasekera, L., and Eisenstein, Z. (1992). *Pore pressures around tunnels in clay*. Canadian Geotechnical Journal, 29:819–831.

Santos Ovıdio J., Celestino Tarćısio B. (2008). *Artificial neural networks analysis of Sao Paulo subway tunnel settlement data*. Tunnel and Underground Space Technol 23(5):481–491.

Schmidt B. (1969). A method of estimating surface settlement above tunnels constructed in soft ground. Can Geotech J 20:11–22.

Schmidt, B. (1974). *Exploration for soft ground tunnels-a new approach, Subsurface exploration and heavy construction*, New England College, Henniker, New Hampshire, American Society of Civil Engineers, New York.

Schmidt, B. (1989). *Consolidation settlements due to soft ground tunnelling*. In: 12th International Conference on Soil Mechanics and Foundation Engineering, Rio, pp. 797–800.

Shen, S. L., Wu, H. N., Cui Y. J., Yin Z. Y. (2014). *Long-term settlement behaviour of metro tunnels in the soft deposit of Shanghai.* Tunnel and Underground Space Technology 40, pp. 309-323.

Shi J., Ortigao JAR, Bai J. (1998). *Modular neural networks for predicting settlement during tunnelling*. J Geotech Geoenv Engrg ASCE 124(5):389–395.

Shirlaw, J.N., Busbridge, J.R., Yi, X. (1994). *Consolidation settlements over tunnels: A review*. Canadian Tunnelling 1994. The Tunnelling Association of Canada. pp. 253-266.

Soga, K., Laver, R. G., Li, Z. (2017). *Long-term tunnel behaviour and ground movements after tunnelling in clayey soils.* Underground Space 2. pp. 149-167.

Stamatelatos, M. (2002). *Fault Tree Handbook with Aerospace Applications*. NASA

Staveren M. V. (2006). *Uncertainty and ground condition: A risk management approach.* Taylor and Francis Group, 711 Third Avenue, New York, NY 10017, USA. p. 125-151.

Suwansawat S. (2002). *Earth pressure balance (EPB) shield tunnelling in Bangkok: ground response and prediction of surface settlements using artificial neural networks*. PhD thesis, Massachusetts Institute of Technology, Department of civil and environmental engineering

Suwansawat S, Einstein HH (2006). *Artificial neural networks for predicting the maximum surface settlement caused by EPB shield tunnelling.* Tunnel and Underground Space Technology 21:133–150

Svenska Geotekniska Föreningen (SGF). *Report 1:2014E, Risk management in geotechnical engineering projects – requirements*, Linköping 2017 (translated to English)

Tamagnini C., Miriano C., Sellari E., Cipollone N. (2005). *Two-dimensional FE analysis of ground movements induced by shield tunnelling: the role of tunnel ovalization*. Riv Ital Geotech 1:11–33.

Vermeer, P. A., Möller, S.C., Ruse, N., (2003). *On the application of numerical analysis in tunnelling*. In: Proceedings of the 12th Asian Regional Conference on Soil Mechanics and Geotechnical Engineering (12 ARC), Singapore, Vol. 2, pp.1539–1544.

Vermeer, P. A. and Bonnier, P. G. (1991). *Pile settlements due to tunnelling.* Proc. 10lh European Conf. on Soil Mechanics and Foundation Engineering, Florence, Balkema,Vol. 2, pp. 869-872.

Verruijt, A., Booker, J.R. (1996). *Surface settlements due to deformation of a tunnel in an elastic half plane.* Technical Note. Geotechnique 46, No. 4, pp. 753–756.

Whitman, R. V. (1984). *Evaluating calculate risk in geotechnical engineering.* J. Geotech. Engrg. 110(2). pp. 143-188.

Witherspoon, P. A., Wang, J. S. Y., Iwai, K., and Gale, J. E., *Validity of cubic law for fluid flow in a deformable rock fracture*, Water Resour. Res., 16, 1016-24, 1980.

Wongsaroj, J., Soga, K., and Mair, R. J. (2013). *Tunnelling-induced consolidation settlements in London clay*. Geotechnique, 63(13), pp. 1103–1115.

Xu K J and Poulos H G (1999). *Principles of Program GEPAN for General Pile Elastic Analysis*, University of Sydney, Dept. of Civil Engineering, Research Report No: R782.

Yao BZ, Yang CY, Yu B., Jia FF, Yu B (2010). *Applying support vector machines to predict tunnel surrounding rock displacement*. Appl Mech Mater 29–32:1717–1721.

Yi, X., Rowe, R.K., and Lee, K.M. (1993). *Observed and calculated pore pressures and deformations induced by an earth balance shield.* Canadian Geotechnical Journal, 30(3): 476–490. doi:10.1139/t93-041.

Zhang, Y., Kiureghian, A. D. (1997). *Finite element reliability methods for in elastic structures*. *ReportUCB/SEMM-97/05, Department of civil and environmental engineering, University of California, Berkeley*.

Zhang Y.-J., Feng X.-T., Jiang, Q. (2015). *Uncertainty Analysis and Risk Management of Underground Cavern Group at Jinping II Hydropower Station.* Stand Alone, 0(Geotechnical Safety and Risk V), pp. 645–651. https://doi.org/10.3233/978-1-61499-580-7-645

Appendix I: Design charts for short and long piles

The design charts (Loganathan, 2011) for short piles (pile length smaller than tunnel centreline depth) and long piles (pile length greater than tunnel centreline depth) are provided in this appendix. First, the charts of induced bending moment M_{bM}, induced settlement ρ_{bM}, induced positive down drag force $+P_{max}$, induced negative down drag force $-P_{max}$ and induced head settlement ν_{max} for the "base" case are provided which are followed by correction factor diagrams for undrained shear strength k_{cu}, pile diameter k_d and ratio of pile length to the tunnel axis level $k_{L_p/H}$.

Design charts for short piles:

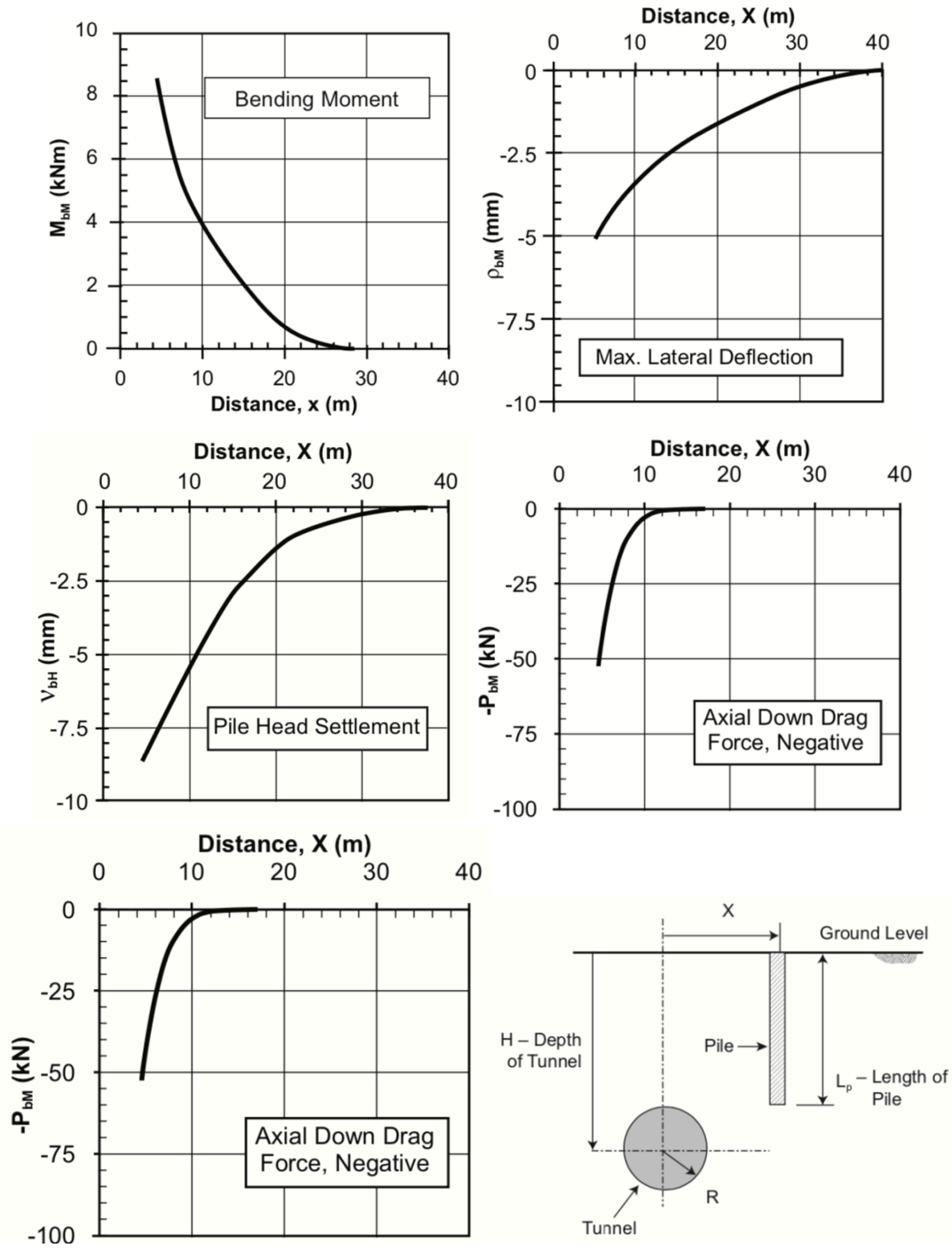

Figure 51. Design charts (short pile) (after Loganathan, 2011)

Undrained shear strength correction factor for short piles:

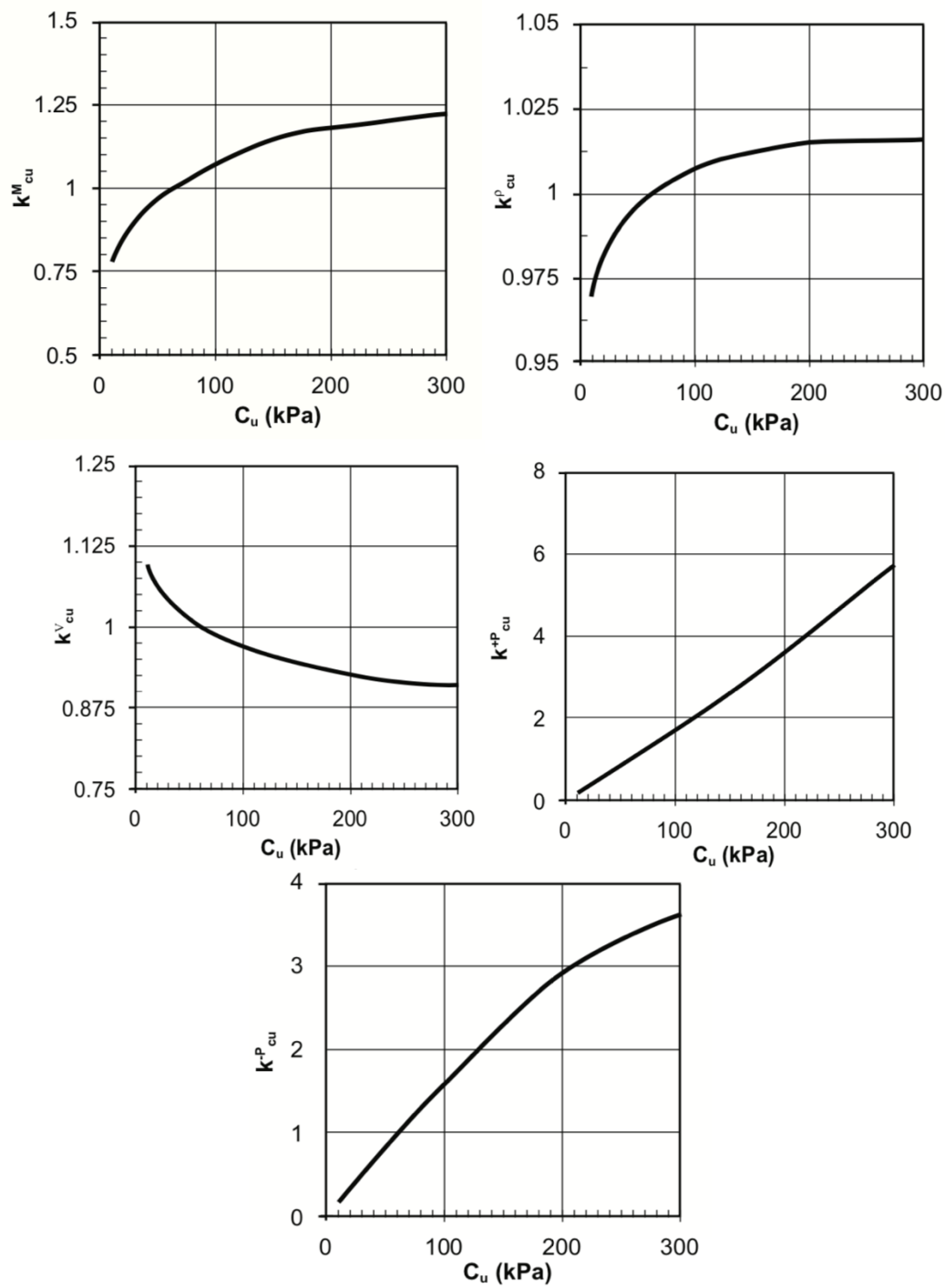

Figure 52.Undrained shear strength correction factor (short pile) (after Loganathan, 2011)

Pile's length to centreline depth correction factor for short piles:

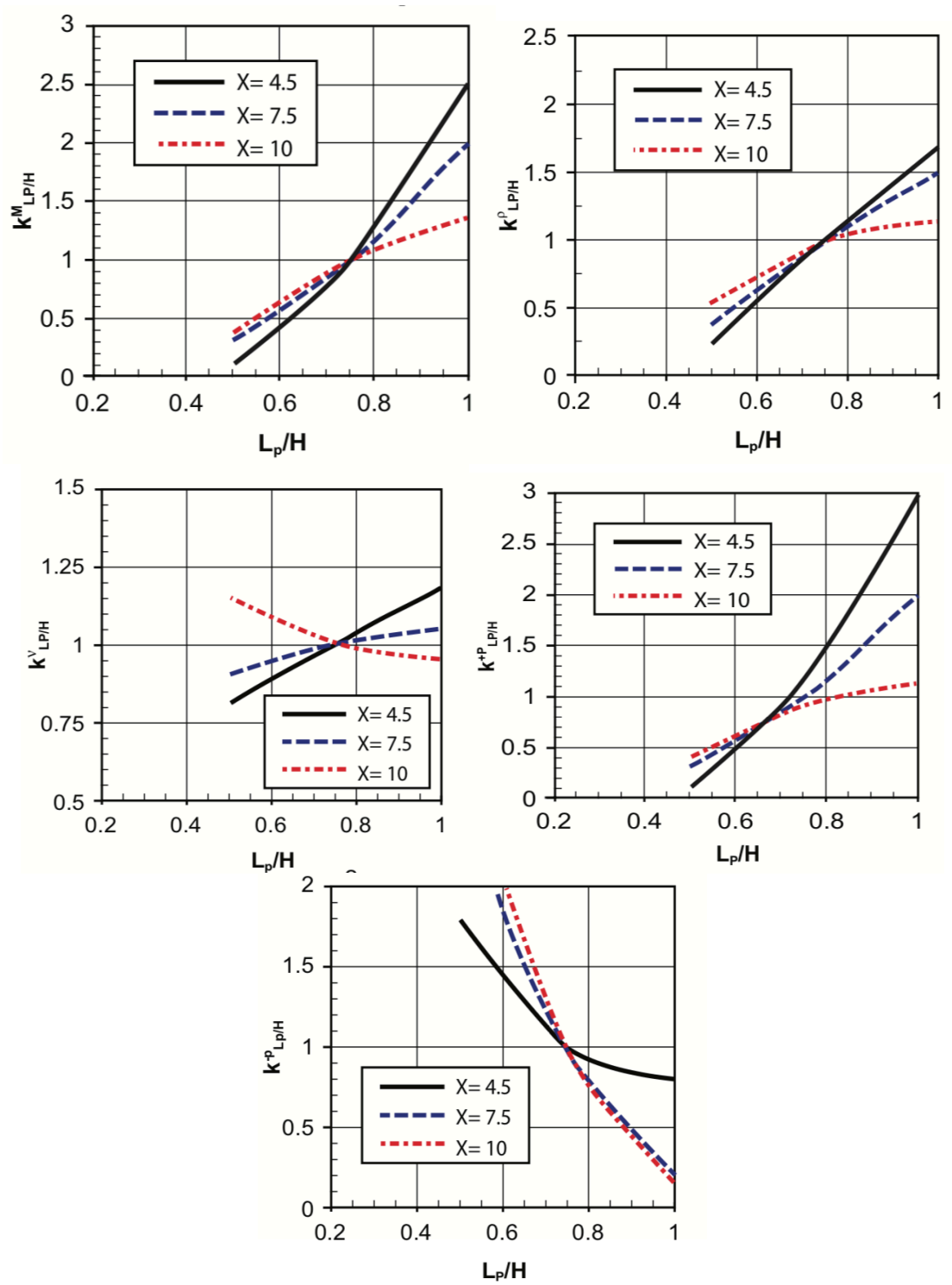

Figure 53. Correction factor for pile length to centreline depth (short pile) (after Loganathan, 2011)

Pile's diameter correction factor for short piles:

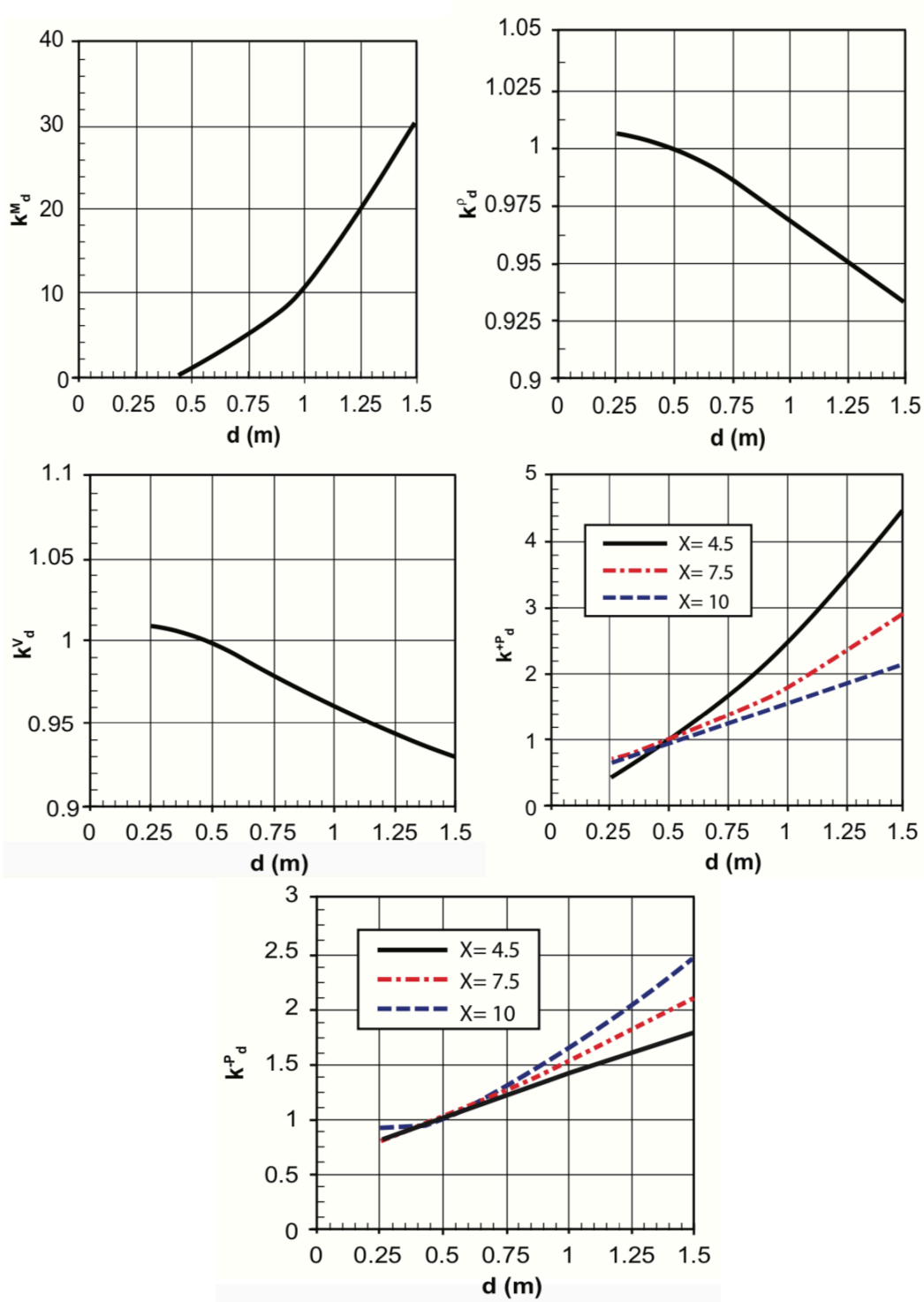

Figure 54. Pile's diameter correction factor (short pile) (after Loganathan, 2011)

Design charts for long piles:

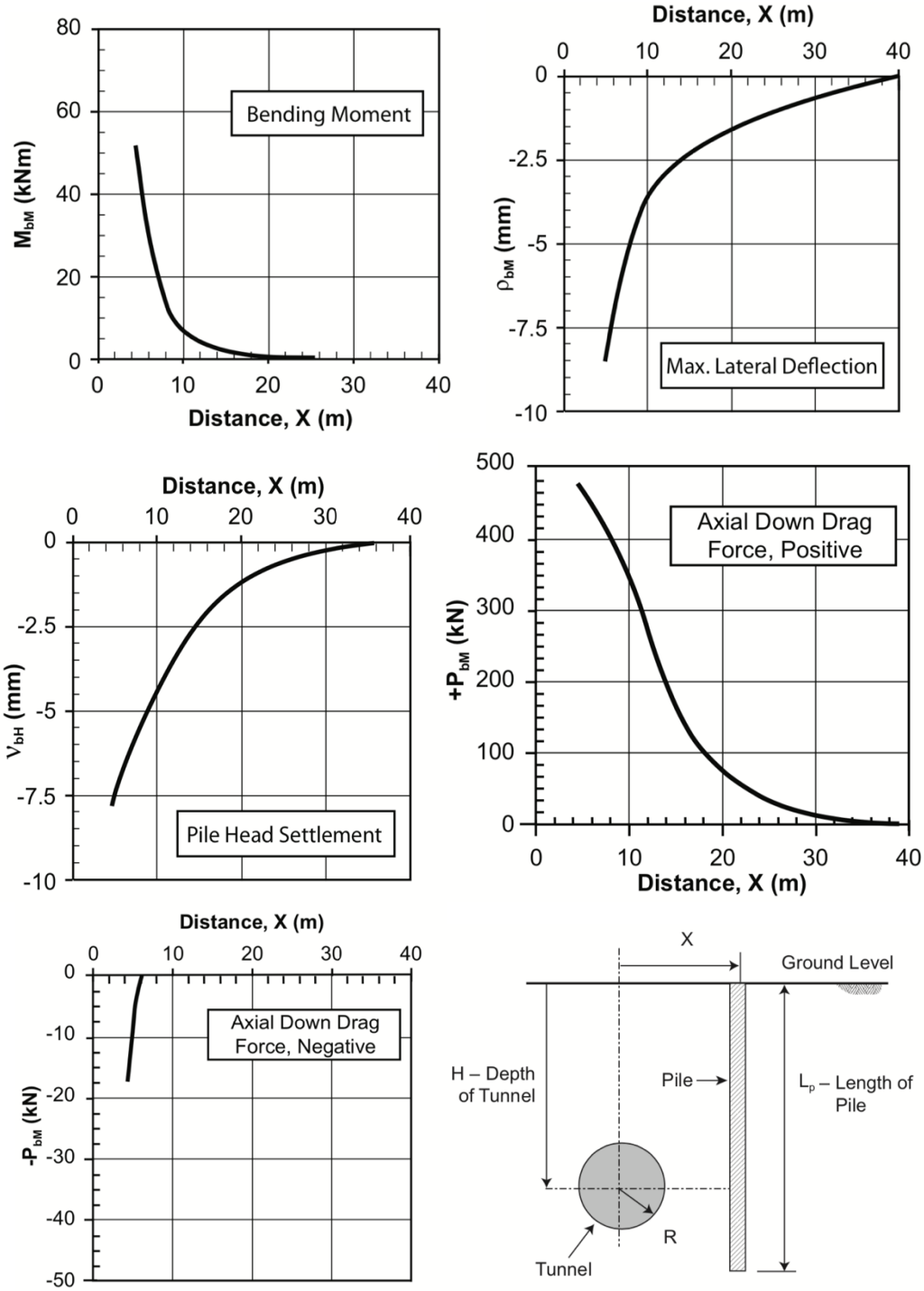

Figure 55. Design charts (long pile) (after Loganathan, 2011)

Undrained shear strength correction factor for long piles:

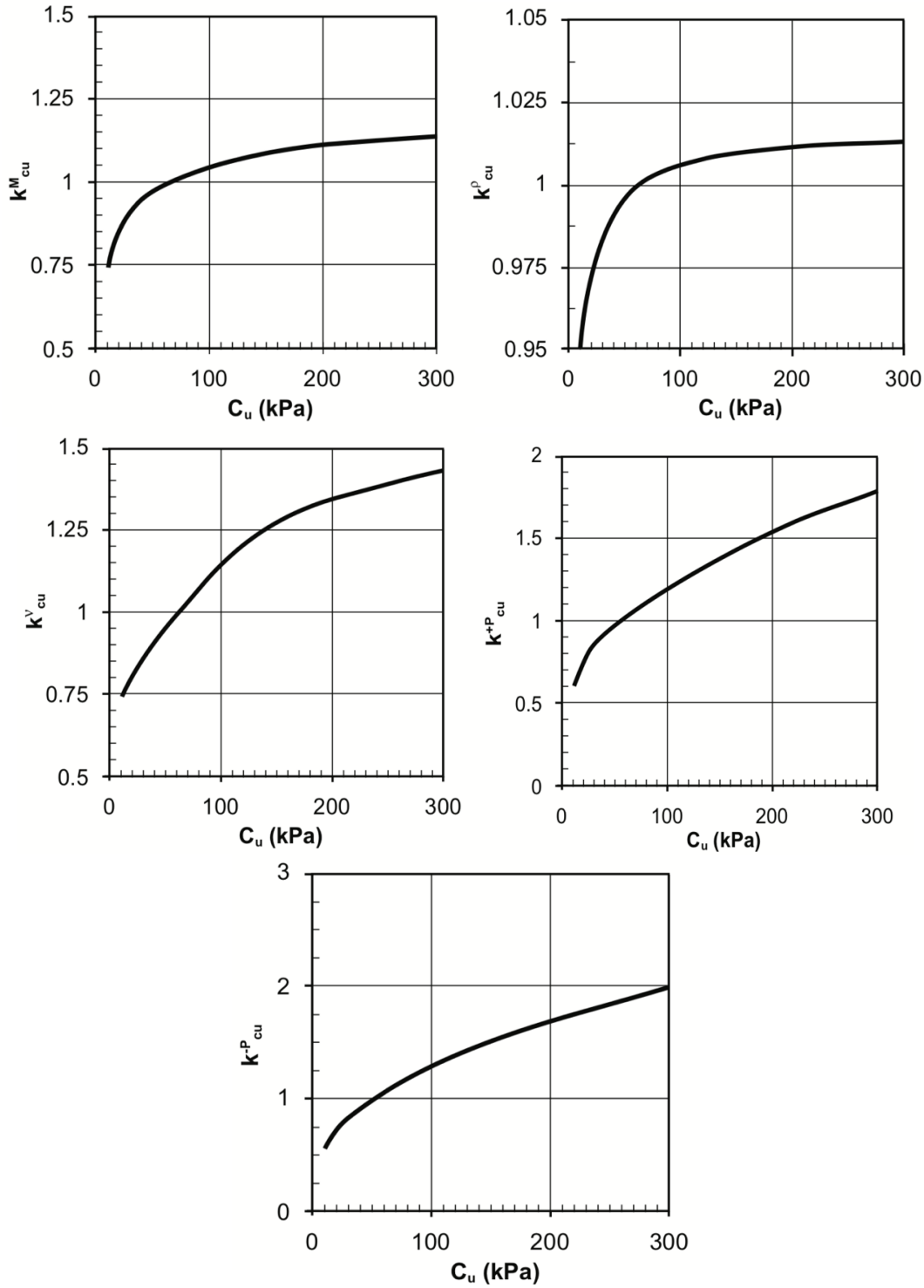

Figure 56. Undrained shear strength correction factor (long pile) (after Loganathan, 2011)

Pile's length to centreline depth correction factor for long piles:

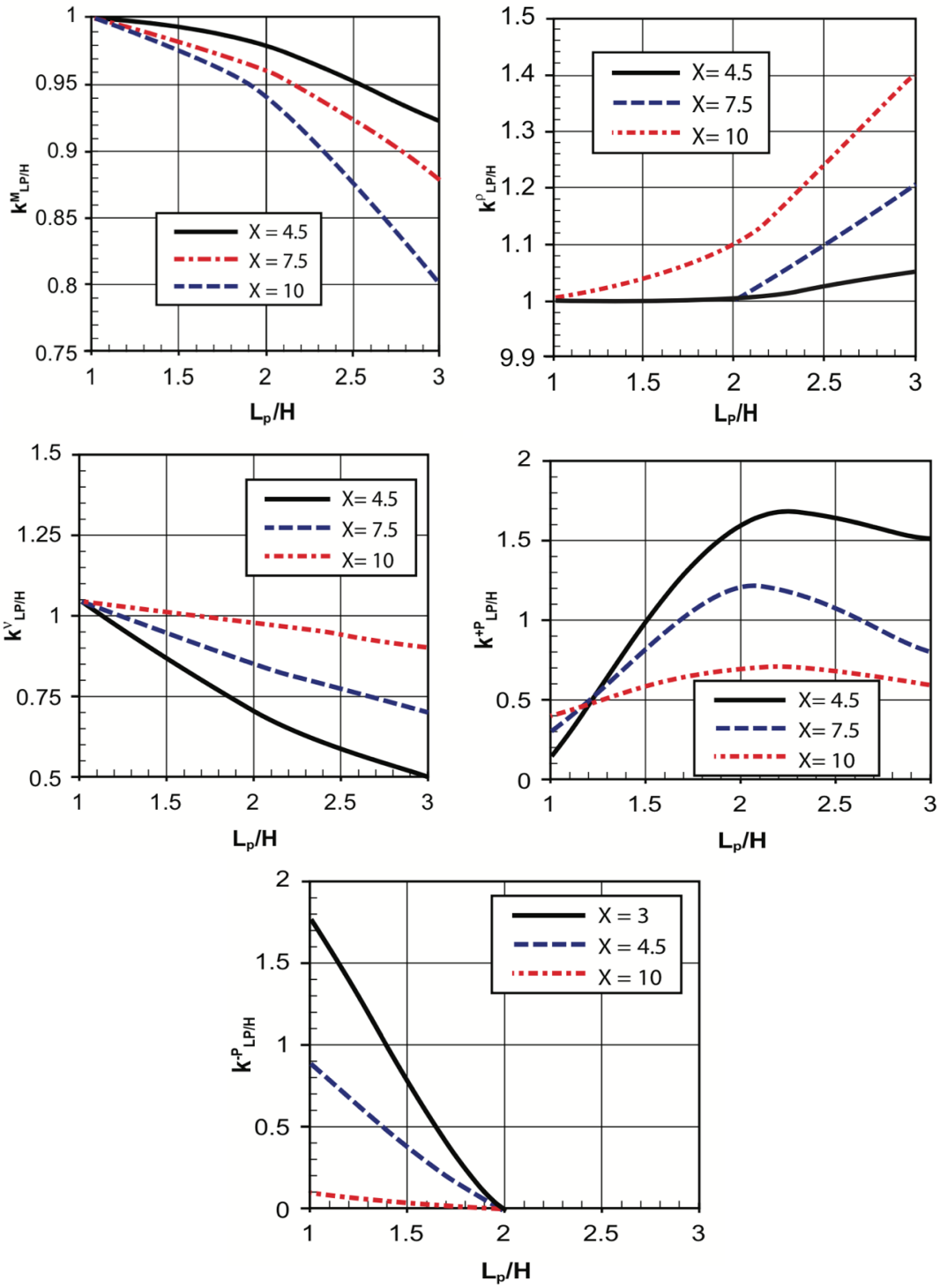

Figure 57. Correction factor for pile length to centreline depth (long pile) (after Loganathan, 2011)

Pile's diameter correction factor for long piles:

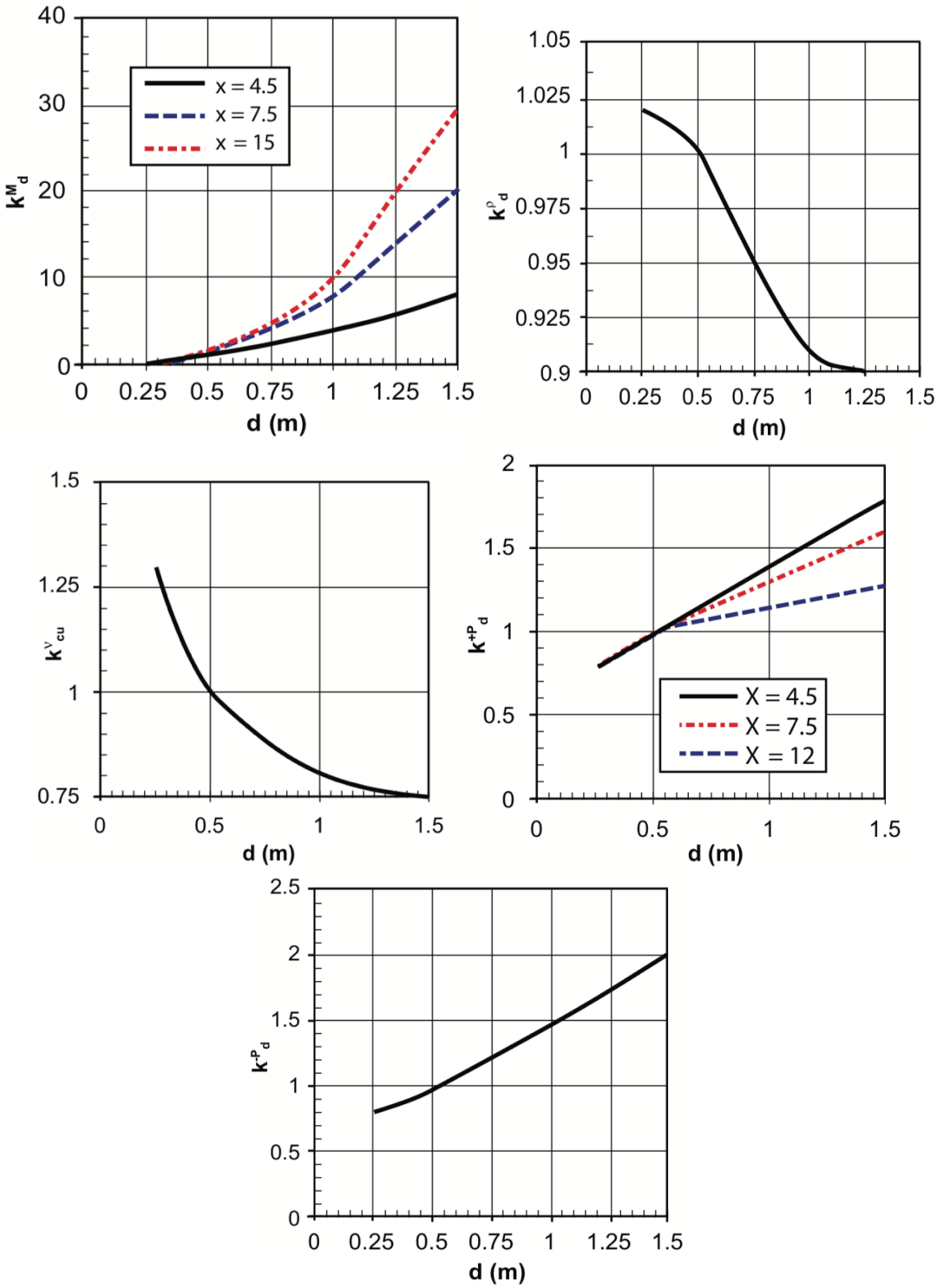

Figure 58. Pile's diameter correction factor (long pile) (after Loganathan, 2011)